
Wayne State University Dissertations

January 2020

Stochastic Programming Models For Electric Vehicles' Operation: Network Design And Routing Strategies

Seyed Sajjad Fazeli
Wayne State University

Follow this and additional works at: https://digitalcommons.wayne.edu/oa_dissertations

 Part of the [Engineering Commons](#), and the [Urban Studies and Planning Commons](#)

Recommended Citation

Fazeli, Seyed Sajjad, "Stochastic Programming Models For Electric Vehicles' Operation: Network Design And Routing Strategies" (2020). *Wayne State University Dissertations*. 2466.
https://digitalcommons.wayne.edu/oa_dissertations/2466

This Open Access Dissertation is brought to you for free and open access by DigitalCommons@WayneState. It has been accepted for inclusion in Wayne State University Dissertations by an authorized administrator of DigitalCommons@WayneState.

**STOCHASTIC PROGRAMMING MODELS FOR ELECTRIC VEHICLES' OPERATION:
NETWORK DESIGN AND ROUTING STRATEGIES**

by

SEYED SAJJAD FAZELI

DISSERTATION

Submitted to the Graduate School,

of Wayne State University,

Detroit, Michigan

in partial fulfillment of the requirements

for the degree of

DOCTOR OF PHILOSOPHY

2020

MAJOR: INDUSTRIAL ENGINEERING

Approved By:

Advisor

Date

© COPYRIGHT BY

SEYED SAJJAD FAZELI

2020

All Rights Reserved

DEDICATION

To Farnaz Fallahi, Nosrat Fazeli, Fatemeh Kia, and Rasool Fazeli.

ACKNOWLEDGEMENTS

Firstly, I would like to express my sincere gratitude to my advisor Dr. Venkatachalam for his support during my Ph.D., for his patience, encouragement, and knowledge. His mentorship helped me in learning the fundamentals of conducting scientific research. Besides my advisor, my special thanks goes to Prof. Chinnam for his continuous support, insightful comments, and immense knowledge. Also, I would like to thank the rest of my thesis committee: Dr. Alper Murat and Mr. Tom Bruff for their insightful comments and encouragement, but also for the hard question which incited me to widen my research from various perspectives. Last but not the least, I would like to thank my family: my wife, my parents and my brother for supporting me spiritually throughout writing this dissertation and my life in general.

TABLE OF CONTENTS

Dedication	ii
Acknowledgements	iii
List of Tables	viii
List of Figures	ix
Chapter 1	INTRODUCTION	1
Chapter 2	TWO-STAGE STOCHASTIC CHOICE MODELLING APPROACH FOR ELECTRIC VEHICLE CHARGING STATION NETWORK DESIGN IN URBAN COMMUNITIES: INTRODUCTION AND PREPROCESSING	8
2.1	Introduction	8
2.2	Literature Review	12
2.3	Preprocessing	16
2.3.1	Dwell Time	16
2.3.2	Arrival Time	17
2.3.3	State of Charge	18
2.3.4	Willingness to Walk	18
2.3.5	EV Market Penetration	20
2.4	Utility Construction	21
Chapter 3	MODEL FORMULATION AND DECOMPOSITION ALGORITHM	23
3.1	Notation and Model Formulation	23
3.1.1	Two-stage Non-linear Stochastic Model	26
3.2	Methodology and Algorithm Development	29
3.2.1	Sample Average Approximation	29
3.2.2	L-shaped Decomposition	32

3.2.3	Value of the Stochastic Solution	37
Chapter 4	CASE STUDY, COMPUTATIONAL EXPERIMENTS, AND CONCLUSION	40
4.1	Case Study and Computational Experiments	40
4.1.1	Scenario Generation	41
4.1.2	Experiments and Results	41
4.1.3	Data-driven Simulation	45
4.2	Conclusion	50
Chapter 5	EFFICIENT ALGORITHMS FOR AUTONOMOUS ELECTRIC VEHICLE MIN-MAX ROUTING PROBLEM: INTRODUCTION AND MODEL FOR- MULATION	52
5.1	Introduction	52
5.2	Model Formulation	56
5.2.1	Notation	57
5.2.2	Min-max AEVRP Model	59
Chapter 6	METHODOLOGY AND ALGORITHM DEVELOPMENT	62
6.1	Branch and Cut Algorithm	62
6.2	GA-based Heuristic Method	63
6.3	Construction Phase	65
6.3.1	Path Representation	65
6.3.2	Modified Cost Matrix	66
6.3.3	Target Assignment	67
6.3.4	Routing	68
6.3.5	Feasibility Check	68
6.3.6	Variable Neighborhood Search (VNS)	69

6.4	Improvement Phase	74
6.4.1	Chromosome Selection	74
6.4.2	Crossover	75
6.4.3	Mutation	75
6.4.4	Post Improvement	76
Chapter 8	COMPUTATIONAL EXPERIMENTS AND CONCLUSION	79
8.1	Instance Generation	79
8.1.1	Parameter Setting	80
8.1.2	Benchmark Instances	80
8.1.3	Large-scale Instances	83
8.2	Sensitivity Analysis	84
8.2.1	Min-max Vs Min-sum	84
8.2.2	Effect of the Number of AEVs	86
8.2.3	Effect of the Number of Charging Stations	87
8.2.4	Data-driven Simulation	88
8.3	Conclusion	90
Chapter 9	CONCLUSION AND FUTURE RESEARCH	92
9.1	Two-stage Stochastic Choice Modeling Approach for Electric Vehicle Charging Station Network Design in Urban Communities	92
9.2	Efficient Algorithms for Autonomous Electric Vehicle Min-max Routing Problem	93
Appendix A	95
Appendix B	98
References	102

Abstract 119

Autobiographical Statement 121

LIST OF TABLES

Table 1	Estimated distance decay function parameters	20
Table 2	Estimated parameters using mixed logit model; Source:[116]	22
Table 3	SAA performance	30
Table 4	Model data specifications	36
Table 5	Computational results for L-shaped method	36
Table 6	Weibull distribution parameters for drivers' dwell time; Source:[27] . .	41
Table 7	All the sub-routes generated in the first step of CS insertion heuristic .	77
Table 8	Final feasible routes resulted from CS insertion in the post improve- ment heuristic	77
Table 9	The characteristic of the large-scale instances for different data sets . .	80
Table 10	Comparison of the performances of GAH and B&C procedure for large- scale instances	84
Table 11	Computational results of benchmark instances; set Random	98
Table 12	Computational results of benchmark instances; set A	99
Table 13	Computational results of benchmark instances; set B	100
Table 14	Computational results of benchmark instances; set P	101

LIST OF FIGURES

Figure 1	The relationship between the charging location decisions and routing strategies for autonomous electric vehicle’s operation	4
Figure 2	Average dwell times for activity types; Sources: [13] and [58].	17
Figure 3	The expected percentage breakdown for various activities by vehicle arrival times on A) weekdays and B) weekends; Sources: [13] and [58].	18
Figure 4	Initial state-of-charge distribution for arriving electric vehicles; Source: [26].	19
Figure 5	Distance decay function for walking trips to different types of destination; Source: [125].	20
Figure 6	Valuating the effect of each source of uncertainty and comparing with the value of stochastic solution	39
Figure 7	Heat map of the demand flow and location of parking lots in the study area.	43
Figure 8	Percentages of accessibility and charging utilization for different budget amounts	43
Figure 9	Number of installed level 1 and level 2 chargers for different budget amounts, labeled by accessibility percentages.	44
Figure 10	a) Average walking distance per person and b) total walking distance for people who have access to a public EV charging station in both optimistic and pessimistic cases.	46
Figure 11	Percentage of average utilization of a) Level 1, and b) Level 2 chargers during each time slot in five parking lots	47
Figure 12	Percentage of average utilization of a) level 1, and b) level 2 chargers in all parking lots during each time slot for different budgets	48
Figure 13	Aggregated EV drivers’ utility of using different charger levels in different parking lots when the level 3 charging price is 9(\$/h), 6(\$/h), 4(\$/h) and 3(\$/h)	49
Figure 14	Percentage of accessibility and level 2 utilization for the proposed approach and two defined configurations	49

Figure 15	A feasible tour for two AEVs which visit all the targets while visiting some charging stations for recharging: AEVRP using min-sum (left) vs AEVRP using min-max (right).	55
Figure 16	The flowchart of GAH including three main phase : construction, improvement and post improvement	65
Figure 17	An example for charging station selection approach	71
Figure 18	The order crossover operation	75
Figure 19	Four different data sets generated based on the study in [8]	81
Figure 20	The performance of the GAH compared to the B&C procedure for benchmark instances with 15 targets	83
Figure 21	The AEV routes in the AEVRP in the Min-max (left) vs Min-sum (right) versions	85
Figure 22	Effect of increase in the number of AEVs on the min-max and the total distance traveled by the AEVs	86
Figure 23	Effect of increase in the number of charging stations on sets A,B,P, and Random	87
Figure 24	Rviz navigation environment illustrated using Turtlebot package	89
Figure 25	Comparison among four different instances for distance, total travel, and workload balance among turtlebots using min-max and min-sum approaches.	90

CHAPTER 1 INTRODUCTION

Logistic and transportation (L&T) activities become a significant contributor to social and economic advances throughout the modern world [78, 101, 102]. Road L&T activities are responsible for a large percentage of CO₂ emissions, with more than 24% of the total emission, which mostly caused by fossil fuel vehicles [80]. Researchers, governments, and automotive companies put extensive effort to incorporate new solutions and innovations into the L&T system. As a result, Electric Vehicles (EVs) are introduced and universally accepted as one of the solutions to environmental issues [80]. Subsequently, L&T companies are encouraged to adopt fleets of EVs. Various factors promote the use of these vehicles, such as: receiving incentives to reduce the carbon footprint; less dependency on the oil-based energy sources; immense government support such as purchasing subsidies, public charging stations, carpool lane access, etc.; and lower maintenance cost [48]. Although the use of EVs should be the first priority to mitigate the environmental issues and improve the energy efficiency, the EV technology suffers from several deficiencies such as limited battery capacity, longer refueling time compared to the conventional vehicles, and the scarcity of electric charging stations. Therefore, integrating the EVs into the logistic and transportation systems introduces new challenges from strategic, planning, and operational perspectives. For example, electric charging station network design in smart cities is dependent on the investment decisions regarding the location, number, capacity, and types of chargers. Likewise, the limited driving range of EVs and scarcity of the charging sites impose new restrictions when L&T companies make efficient routing decisions.

The cumulative global EV sales exceeded 3 million units in 2017, and it is expected to reach 230 million units by the end of 2030. It is estimated that there should be at least 300

public charging locations per million people. At the same time, half of the U.S. population lives in the markets with 70% below the estimated benchmarks for number of charging stations. It is also suggested that there should be a 20% annual growth in the deployment of charging infrastructures to support the current trend of EV sales [92]. Several studies concluded that the workplace and public charging stations are strongly correlated with the adoption of EVs. Therefore, designing a cost-efficient charging network with wide-ranging access is crucial to keep up the current growing trend in the EV market. One of the main challenges to be addressed to expand the EV charging infrastructures is the location of charging stations [35]. Due to the longer charging time in EVs compared to the conventional vehicles, the parking locations can be considered as the candidate locations for installing charging stations. Another essential factor that should be considered in designing the Electric Vehicle Charging Station (EVCS) network is the size or capacity of charging stations. EV drivers' arrival times in a community vary depending on various factors such as the purpose of the trip, time of the day, and day of the week. In the specified time in which EVs stop at a station, if the station is occupied, the vehicles should leave the station or wait in the queue. So, the capacity of stations and the number of chargers significantly affect the accessibility and utilization of charging stations. Also, the EVCSs can be equipped by distinct types of chargers, which are different in terms of installation cost, charging time, and charging price. City planners and EVCS owners can make low-risk and high-utilization investment decisions by considering EV users charging pattern and their willingness to pay for different charger types. Many of the existing studies on the charging facility location problem are based on the assumption that charging service demands are deterministic. However, the real demand is affected by various sources of uncertainty, such

as the day of the week, the time of day, the purpose of the trip, the location of the final destination, a driver's willingness to walk, distance from home, and weather condition. Thus, there may be significant differences between the optimal solutions for deterministic and stochastic models [6, 5, 74, 120, 51]. Stochastic programming is a modeling approach for making decisions under uncertainty. The most well-known method in stochastic programming is two-stage stochastic programming, where the decisions in the first stage are made before the realization of uncertainties, and the second-stage the decisions are made after revealing the uncertainties [4].

Therefore, effective electric vehicle management requires intelligent charging station location decisions at the strategical level and efficient routing strategies at the operational level. These two decisions are inter-related since the location of chargers can significantly affect the routing strategies. Figure 1 illustrates the effect of location decisions on routing policies. At the operational level, managing a fleet of electric vehicles can offer several incentives to the L&T companies. EVs can be equipped with autonomous driving technologies to facilitate online decision making, on-board computation, and connectivity. Energy-efficient routing decisions for a fleet of autonomous electric vehicles (AEV) can significantly improve the asset utilization and vehicles' battery life. However, employing AEVs also comes with new challenges. Two of the main operational challenges for AEVs in transport applications is their limited range and the availability of charging stations. Effective routing strategies for an AEV fleet require solving the vehicle routing problem (VRP) while considering additional constraints related to the limited range and number of charging stations. Autonomous Electric Vehicle Routing Problem (AEVRP) is an extension of multi-charging stations vehicle routing problem, and it is NP-hard. To solve the AEVRP, we face three

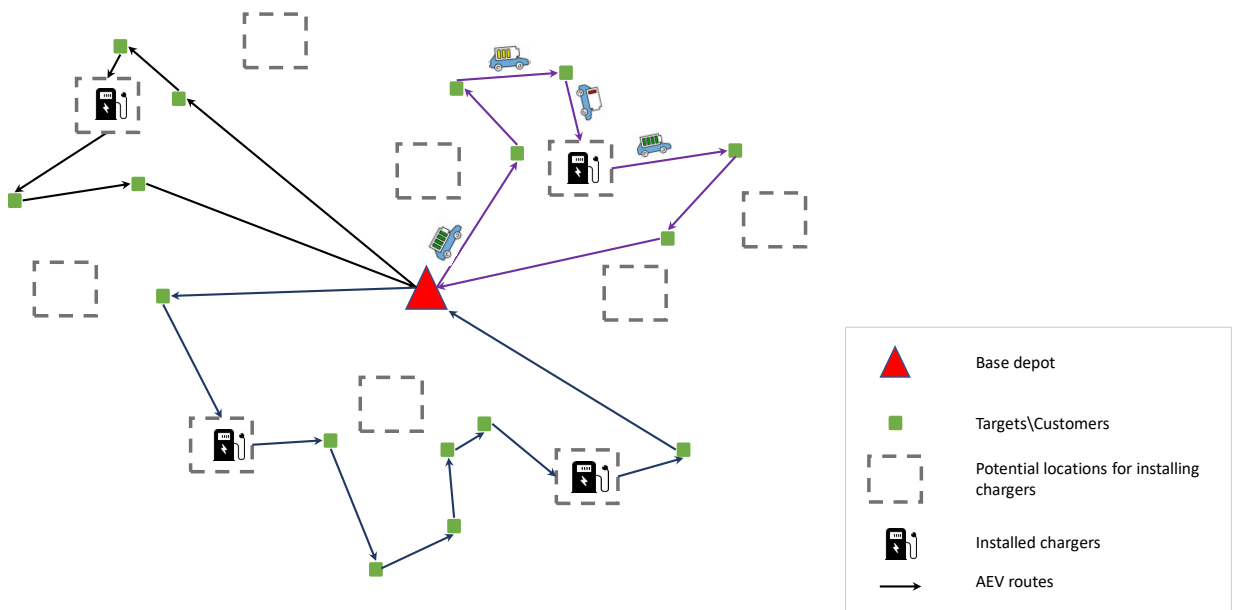


Figure 1: The relationship between the charging location decisions and routing strategies for autonomous electric vehicle's operation

major challenges: 1) assigning targets to the AEVs, 2) finding the best route for each AEV, and 3) maintaining feasibility such that each AEV does not run out of fuel. Each of these is complex and difficult to solve. Hence, simple algorithms do not work well for this problem even for the small size instances.

In this dissertation, we develop models and algorithms to address the challenges in integrating the EVs into the logistic and transportation systems. In the chapter 2, from the strategical point of view, we propose a choice modeling approach embedded in a two-stage stochastic programming model to determine the optimal layout and types of EV supply equipment for a community while considering randomness in demand and drivers' behaviors. Some of the key random data parameters considered in this study are: EV's dwell time at parking location, battery's state of charge, distance from home, willingness to walk, drivers' arrival patterns, and traffic on weekdays and weekends. The two-stage model uses the sample average approximation method, which asymptotically converges to an optimal solution. To address the computational challenges for large-scale instances, we propose an outer approximation decomposition algorithm. We conduct extensive computational experiments to quantify the efficacy of the proposed approach. In addition, we present the results and a sensitivity analysis for a case study based on publicly available data sources. In the chapter three, we address the challenges that arise at the operational level by developing sophisticated algorithms to make efficient routing decisions for the fleet of autonomous electric vehicles. We proposed a mixed-integer programming formulation and computational results are presented for small scale instances using branch and cut procedure. To circumvent the computational challenges for large-scale instances, a Genetic algorithm-based heuristic is developed. Extensive computational results and sen-

sitivity analysis are performed to corroborate the efficiency of the proposed approach, both quantitatively and qualitatively. From the methodological point of view, we implement an exact method for the strategical planning and a hybrid meta-heuristic for operational planning decisions in the electric vehicle operation network. The contribution of this research are summarized as follows:

- Formulated a two-stage stochastic programming model with an embedded choice model for locating charging facilities, and determined the types of chargers to be installed in these facilities based on EV drivers' choices, behaviors, and other random parameters
- Included various uncertainties in the model, such as EV demand flows, EV drivers' charging patterns, state of charge, arrival and departure times, the purpose of arrivals in the community, and preferred walking distances
- Developed an outer-linearization-based decomposition algorithm and performed extensive computational experiments with multiple variations to demonstrate the efficacy of our algorithm
- Conducted a case study using data representing the midtown area of Detroit, Michigan, in the U.S. and provide post-analysis insights for improving accessibility and transportation choices based on our proposed framework.
- Conducted a data-driven simulation where the proposed method is compared to two other configurations from the literature

- Developed an efficient mixed integer formulation for the min-max autonomous electric vehicle routing problem to efficiently solve small-scale instances
- Designed a GA-based heuristic for large-scale instances and performed extensive computational experiments to quantify the efficacy of the proposed approach
- Performed a sensitivity analysis to investigate the aspects of solutions from min-sum and min-max AEVRP
- Conducted a data-driven simulation study using robot operating system (ROS) to showcase the application of the AEVRP for robots

CHAPTER 2 TWO-STAGE STOCHASTIC CHOICE MODELLING APPROACH FOR ELECTRIC VEHICLE CHARGING STATION NETWORK DESIGN IN URBAN COMMUNITIES: INTRODUCTION AND PREPROCESSING

2.1 Introduction

One of the most promising approaches to alleviating vehicle emissions and satisfying climate targets is the deployment of electric vehicles [118]. Lower maintenance costs, lower ownership costs, noise reduction, and charging at home and work and around the community are some of the additional advantages of using EVs. Vehicle purchasing subsidies, public electric charging availability, and carpool lane access are the three most substantial benefits offered to EV consumers [66]. In response to the government's promotion of vehicle electrification objectives, the world's major automobile companies are striving to produce affordable EVs for environmentally conscious consumers [54]. Every year, automotive companies around the world introduce various new models of EVs (e.g., hybrid vehicles, plug-in hybrid vehicles, and pure battery electric vehicles (BEVs)). The U.S. is one of the growing markets for EVs. However, half of the U.S. population live in areas with fewer than 90 charging infrastructures per million people, which is 70% below the estimated benchmarks[92]. By the end of 2025, there should be about a 20% growth in deployment of charging infrastructures per year to support more than three million expected EVs [77]. Therefore, designing a cost-efficient charging network with broad access is critical for supporting the current flourishing trend in the EV market.

Installation of a public charging station costs at least \$5,000 to \$15,000 [107]. Electric vehicle charging stations (EVCSs) can be equipped with different types of chargers that differ in power, installation cost, and charging price. Broadly, EV supply equipment

(EVSE) can be classified into level 1, level 2, and level 3, based on the power supply. Level 1, which is known as home charging, has a 1.9kW electric power supply and requires between 8 and 30 hours to fully charge an EV's battery, depending on its size. Level 2, known as semi-rapid charging, has a 6.6 kW power supply and a charging time between 4 and 8 hours. Level 3, known as fast charging EVSE, has a 50kW power supply and a charging time of less than 30 minutes; this is considered to be the most expensive charger. Given the availability of chargers with different capabilities and prices, it is worth considering EV users' choices of charger levels when establishing an optimal EVCS network.

A study of EV users' charging behaviors, especially their preferences in charging levels and locations, can help increase the accessibility of charging stations for EV users, and this can lead to widespread EV adoption. Also, since establishing an EVCS network is a strategic decision, considering the randomness in demand and analyzing EV users' travel patterns, charging behaviors, and infrastructure utilization will help in designing a charging station network that provides better access [124]. Increasing the overall utilization of charging stations can potentially increase investment opportunities for EVCS providers and automobile makers. The analysis in [77] indicates that EVCS providers can make low-risk and high-utilization investment decisions by expanding charging infrastructures in such a way that the designs of charging outlet networks are matched to the complex driver charging patterns. Different types of users (residential, visitors, employees, fleet users) have different charging needs, as well as different dwell times, frequencies of charging and states of charge (SOCs). Since an EV can be recharged at home, at public charging stations, or at private working places, a wide range of consumers demand several different power supply options. Furthermore, charging prices can significantly affect EV owners'

choices. The importance of this last factor can vary depending on people's socioeconomic characteristics. The authors of [116] showed that EV owners are less likely to use charging stations when the charging costs are higher or when their battery has a sufficient driving range for reaching the next charging opportunity.

Many of the existing studies on the charging facility location problem are based on the assumption that charging service demands are deterministic. However, the real demand is affected by various sources of uncertainty, such as the day of the week, the time of day, the purpose of the trip, the location of the final destination, and the driver's willingness to walk. Thus, there may be significant differences between the optimal solutions for deterministic and stochastic models. Stochastic programming is a modelling approach for making decisions under uncertainty. Discrete choice analysis has also proven to be a useful strategy for analyzing and predicting EV drivers' decisions regarding their choices of location and chargers. In this study, considering the uncertainties in EV users' demand, we propose a two-stage stochastic programming model with an embedded choice model representing EV drivers' choices of chargers for designing an optimal network of charging stations for a community. Since two-stage stochastic programming models often require a large number of scenarios for good approximations of the expectation function, we use the sample average approximation (SAA) method, a Monte Carlo simulation-based sampling technique. Another challenge for the two-stage stochastic programming approach is the computational burden arising from second-stage scenarios, so we use a L-shaped decomposition algorithm with single- and multi-cut variants to solve the model efficiently. Finally, we evaluate our proposed two-stage model and our approach to its solution with a case study based on data representing the midtown area of Detroit, Michigan, in the U.S.

The contributions of this study include the following: (1) we formulate a two-stage stochastic programming model with an embedded choice model for locating charging facilities, and we determine the types of chargers to be installed in these facilities based on EV drivers' choices and behaviors and other random parameters; (2) we include various uncertainties in the model, such as EV demand flows, EV drivers' charging patterns, SOCs, arrival and departure times, the purpose of arrivals in the community, and preferred walking distances; (3) we develop an outer-linearization-based decomposition algorithm and conduct extensive computational experiments with multiple variations to demonstrate the efficacy of our algorithm; and (4) we conduct a case study using data representing the midtown area of Detroit, Michigan, in the U.S. and provide post-analysis insights for improving accessibility and transportation choices based on our proposed framework. In addition, we conducted a data-driven simulation where the proposed method is compared to two other configurations from the literature.

The remainder of this research is organized as follows: Section 2.2 reviews the related literature. Section 2.3 describes the various sources of uncertainty that we consider in the demand generation process as well as our construction of the utility function for the choice model. Section 3.1 provides a mathematical formulation of the problem along with a subsequent reformulation. Section 6 introduces the solution methodologies that we implemented to solve large-scale instances. Section 4.1 presents the case study, computational experiments, data-driven simulation and various insights from our sensitivity analysis. Finally, Section 8.3 provides concluding remarks.

2.2 Literature Review

In this section, we first review the literature related to deterministic and stochastic approaches for the EV charging location problem. Then we provide details about choice models for the behaviors of the EV drivers.

A majority of the studies in the literature on the EV charging location problem consider deterministic models. A capacitated refueling location model with limited traffic flow was introduced in [109] to maximize the vehicle miles traveled by alternative-fuel vehicles. A reformulation of the flow-refueling location model was proposed in [73] to decrease the computational effort needed to solve large-scale set covering and the maximum coverage problem. The research in [38] explored the allocation of public charging stations to increase the social welfare associated with transportation and power networks. Considering users' daily travel, [136] introduced a novel model to determine EVCS locations while minimizing the charging station installation and management costs. The authors of [121] developed a simulation-optimization model for EVCSs to maximize the service level for EV drivers. The results show that a combination of level 1 and level 2 chargers is more desirable than installing only level 1 chargers. The research in [17] addressed the EVCS problem in an urban area. The authors proposed a mixed integer programming (MIP) model for locating slow-charging stations. They considered travelers' parking locations as well as their daily activities to aggregate the demand. An optimization model based on travel behavior to optimally install charging stations was developed in [90]. The research in [115] used an MIP model to determine the locations for multiple types of charging stations. The results indicated that an increase in EV ranges allows installing fewer charging

stations. The authors of [59] formulated a charging station location problem with a focus on human factors. To support recent developments in the electrification of public transportation, the authors of [14, 61], and [114] developed models to optimally determine the locations of charging stations for electric taxis and buses. The impact of different types of EVs [29, 108] , locations and sizes of charging infrastructures [65, 87, 91, 123] on power networks has also been investigated by various studies. Furthermore, various concerns from both the traffic system and power system perspectives are addressed by few studies [113, 126, 130].

Even though it is important to consider uncertainties for strategic and tactical planning, as decisions made using deterministic parameters can under- or over-estimate the reality [12], only a few research studies consider uncertainties for EV infrastructure planning. The research in [27] developed a decision support system consisting of a modeling framework using a stochastic model and the Monte Carlo sampling method to optimally design an EV charging network. The researchers considered uncertainties in SOCs, dwell times, demand distribution, driver preferences regarding charging, the market penetration of EVs, and also drivers' willingness to walk. They used SAA and a heuristic to tackle the computational intractability of the stochastic model. The present research extends this work by considering different types of chargers and their associated preferences by the EV drivers. The authors of [82] developed a two-stage stochastic model for locating charging stations to support both the transportation system and the power grid. They considered uncertainty in the demand for batteries, loads, and generation of renewable power sources. The research in [46] incorporated uncertainty regarding the traffic flow into both capacitated and uncapacitated versions of a two-stage stochastic model to locate EVCSs.

With the objective of maximizing both the miles traveled by EVs and environmental benefits, the research in [7] presented the EVCS problem as an extension of the flow refueling location problem. The authors considered both hybrid and single-fueled vehicles, and they proposed using Benders' decomposition approach for solving large-scale instances. Accounting for EV drivers' route choice behavior, [84] suggested a flow-capturing model with a stochastic user equilibrium to locate wireless charging infrastructures.

Charging behavior has been studied by numerous authors from different perspectives, which are multifarious amongst drivers [137, 31]. To develop models that evaluate EV drivers' preferences for charging services, it is necessary to understand individuals' behaviors [21, 122]. The authors of [124] developed a mixed logit model to explore the factors that affect BEV users in Japan. They considered fast and normal types of chargers along with specific locations such as home, company, and public stations for installing chargers. They identified battery capacities and initial states of charge as the main predictors for drivers' charging and location choices. The research in [63] implemented a tri-level design that considers consumers' charging and routing choices to locate multiple levels of charging facilities, including wireless charging. Findings from a national survey showed that recharging times have a considerable influence on consumers' preferences [42]. The effects of policies on charging behavior and EV adoption were studied in [117]. The authors used a large data set to investigate the influence of daytime and free parking policies on EV drivers' charging behaviors. The research in [95] focused on charging time behavior using a mixed logit model, and the predictors related to charging or not charging were SOC_s, number of days between charging, and kilometers of travel. The results show that fast charging is preferred to normal charging. The authors of [39] suggested a tour-based

BEV network equilibrium model to evaluate drivers' behaviors. Recently, the authors of [37] published a literature review on consumers' preferences for plug-in vehicle charging stations. They focused on approaches related to the expansion of charging infrastructures based on users' interactions with EV charging stations.

Choice models have recently been proposed for various purposes. The authors of [10] proposed integrating a choice model within an optimization framework for locating new facilities in a competitive market. They used a random utility model to model customers' behavior with the aim of predicting the market shares of the locations. In [57], the authors considered clients' utility functions, with waiting time for an appointment and the quality of care used as variables for determining health-care facility locations. Similarly, the authors of [32] applied a robust approach to selecting new housing programs. They incorporated a utility function with a linear combination of the features of locations and their values for potential buyers in a mathematical model with the aim of maximizing customers' satisfaction.

Only a few studies have included multiple types of charging stations in their mathematical models [115, 20, 129], and none of these have considered EV drivers' charging behavior in locating multiple types of charging stations. To the best of the authors' knowledge, the present study is the first attempt to embed a choice model within a two-stage stochastic programming approach. Also, although many studies have considered the EVCS location problem for state-wide networks [129, 84, 19, 67, 9, 70], only a few [27, 132] have investigated the problem for an urban area.

2.3 Preprocessing

In this study, we consider parking facilities as potential candidates for installing chargers. Drivers select parking locations based on their preferences regarding walking distances to their final destinations. We assume that if chargers are installed in any of the parking lots that are within a driver’s preferred walking distance, the driver will be attracted to one of these, depending on the availability of that station at the time of arrival. If there are no charging stations within a driver’s preferred walking distance, we do not consider that driver as contributing to the demand in our model. In the two-stage stochastic model, demand is a multi-variate random variable whose realizations are represented as scenarios. The randomness in the demand comes from many different sources, such as drivers’ arrival time and their purpose in driving to the community, the duration of drivers’ activities, the SOCs of EV batteries at the time of arrival, and the distances the drivers are willing to walk, based on demographics, community size, and weather conditions. The following subsection describes the uncertainties that affect the demand for public EV charging stations, based on previous work in [27].

2.3.1 Dwell Time

Based on National Household Travel Survey (NHTS) data, we selected work, study, social, family, shopping, and meals as six different final destination categories for the EV drivers. The average dwell time reported for each category is shown in Fig. 2. We used a Weibull distribution, as suggested in [135], to represent the duration of weekday and weekend activities.

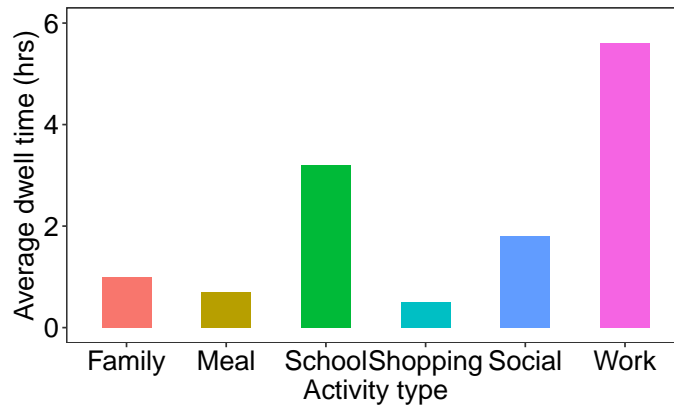


Figure 2: Average dwell times for activity types; Sources: [13] and [58].

2.3.2 Arrival Time

EV drivers' arrival times in a community depend on the time of day, the day of the week, and the commuters' type of activity. On weekends, people tend to participate in social activities and visit shopping malls and their families more than on weekdays. On weekdays, most of the demand for chargers comes from people who are traveling to work or school. Hence, a different demand pattern for charging stations arises on different days of the week. Fig. 3 shows how the demand for charging stations depends on the time and the type of day. On weekdays, the maximum demand occurs during the morning when people are arriving at work or school; in contrast, the maximum demand on weekends usually occurs around noon, when people are traveling to shopping malls and social places. The study in [81] concluded that the Weibull distribution is the best-fitting distribution for arrival times at parking lots. Therefore, we use two Weibull distributions to estimate these arrival times for weekends and weekdays.

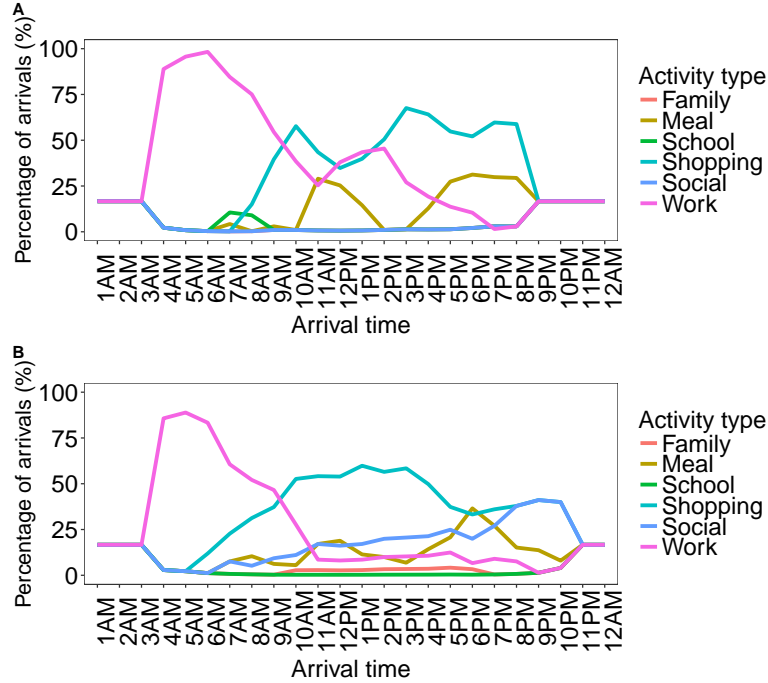


Figure 3: The expected percentage breakdown for various activities by vehicle arrival times on A) weekdays and B) weekends; Sources: [13] and [58].

2.3.3 State of Charge

While the demand for EVs is increasing due to environment- and economy-related concerns, EVs have a limited battery capacity for charging and use. Many factors, such as commuting distance, the driver's behavior, traffic congestion, and weather conditions, can affect an EV's SOC at the time of its arrival at a final destination [128, 104]. Similar to [26], we consider a normal distribution with a mean of 0.3 and a standard variance of 0.1 for the SOC of EVs when they arrive at charging locations. Fig. 4 shows the initial SOC distribution for arriving EVs.

2.3.4 Willingness to Walk

Sociodemographic characteristics such as age, gender, education level, and occupation affect drivers' willingness to walk [79]. Walking distances are typically shorter for children

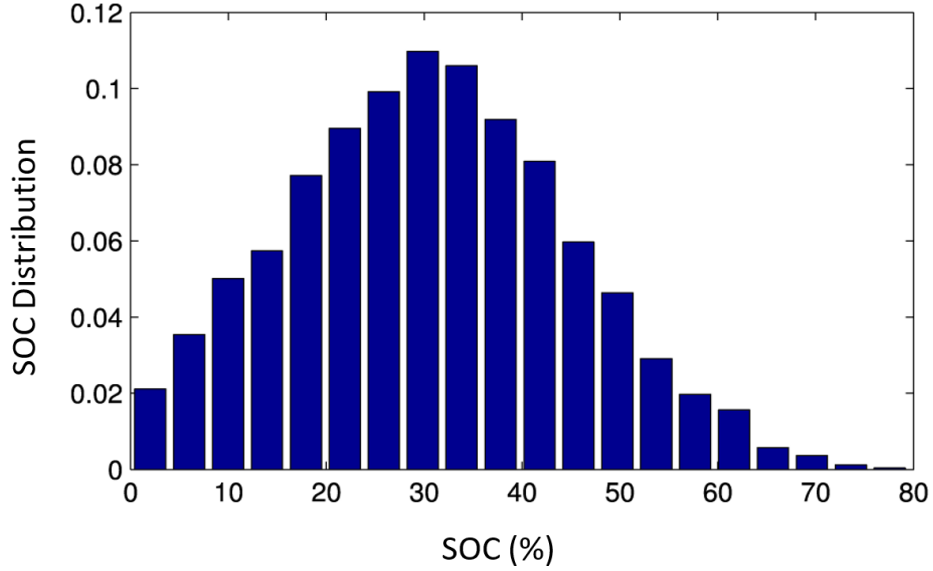


Figure 4: Initial state-of-charge distribution for arriving electric vehicles; Source: [26].

and the elderly than for the young and middle-age groups. Studies have also indicated that walking preferences are associated with many design factors, such as street connectivity, pedestrian infrastructure, and mixed land uses [30]. Many authors have implemented a distance decay function to illustrate individuals' willingness to walk or bicycle. The decay function parameter depends on the type of the final destination, and research using distance decay functions has also revealed different behaviors for people that live in different areas. A negative exponential distribution was used in [125] to estimate walking trips over short distances. The authors defined the distance decay function as $P(d) = e^{-\beta \times d}$, which reflects the total percentage of walking trips for which the distance is greater than or equal to d given in miles; here β is the decay parameter. The authors used 2009 NHTS data to approximate the decay parameter β for different groups and trip purposes. In our study, we consider the effects of the destination activity type, the season, the community size, and the region of the U.S. on drivers' walking preferences. The variation for each of these factors on the walking distance preferences estimated by [125] is shown in Fig. 10, and

details are provided in Table 1.

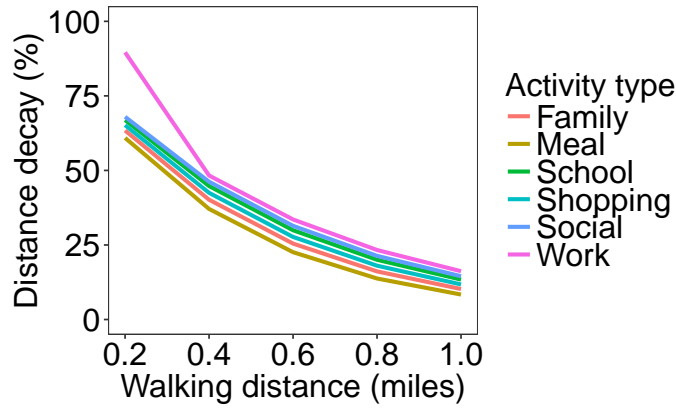


Figure 5: Distance decay function for walking trips to different types of destination;
Source: [125].

Table 1: Estimated distance decay function parameters

Factor	Category	β
Season	Winter	1.88
	Spring	1.68
	Summer	1.64
	Autumn	1.7
Region	Northeast	1.85
	Midwest	1.65
	South	1.76
	West	1.65
Community	Town and country	1.68
	Suburban	1.63
	Urban and second city	1.78

2.3.5 EV Market Penetration

Various social, environmental and economic factors can significantly contribute to the increasing market share of different types of EVs [27]. The research in [111] showed that the presence of charging infrastructure contributes to the adoption of battery EVs but does not have any significant effect on adoption of Plug-in hybrid vehicles. The authors of [62] considered many sources of uncertainty in their sampling process, such as charging infrastructure availability, energy prices, and consumers' preferences. Their results project

that BEV share distributions in 2030 and 2050 will have mean values of 11% and 28%, respectively.

2.4 Utility Construction

Discrete choice models are utilized to help decision makers select the best choice among different options in a choice set. These models are designed to maximize the utility of a decision maker's behaviors [106]. When an EV driver j reaches a charging station, he/she can choose between n different charging types that differ in terms of prices and charging duration. A given choice among the n charging types will provide an EV driver with a certain level of utility. We denote the utility that EV driver j obtains from charging type n as $U_{n,j}$, $n = 1, \dots, N$. The behavioral model will then choose charging type n if and only if $U_{n,j} \geq U_{n',j}, \forall n, n' \in N; n \neq n'$. Thus, a "utility function" can be defined as $U_{n,j} = V_{n,j} + \epsilon_{n,j}$, where $V_{n,j} = V(X_{n,j})$ captures the deterministic part of the utility and $\epsilon_{n,j}$ is the random part capturing the non-observable variables [75]. Some of the variables in V are unknown to us, so we need to estimate them statistically.

We consider $U_{n,j}$ to be the utility of an EV driver who is willing to charge at station j using charging type n . Let K be the set of predictor variables. Then the utility function can be represented as

$$U_{n,j} = \sum_{k \in K} \beta^k X_{n,j}^k + \epsilon_{n,j}^k,$$

where β^k are the coefficients of the corresponding variables representing the decision maker's taste. The research in [116] analyzed drivers' charging choices through a web-based preference survey, using a mixed logit model with various predictor variables. Table 2 shows the estimated fixed and random effects of variables provided in [116].

Table 2: Estimated parameters using mixed logit model; Source:[116]

Variable	Fixed Effects	Random Effects
	Estimate	Standard Deviation
Intercept	4.756	0.022
Price	- 0.607	0.089
Charging cost	-0.062	0.004
Cost at home	0.009	0.489
Dwell time \geq 30 min	0.335	0.188
Chargers power (Reference: Level 1)		
Level 2	1.229	0.253
Level 3	1.609	0.264
Range charged	0.014	0.003
Remaining range	-0.130	0.006
Enough to Next Charging Opportunity	-4.401	0.078

Using the estimated parameters, we calculate EV drivers' utility from charging at each type of charger and also the utility of not charging at that station. As mentioned earlier, when an EV driver arrives in the community to reach his/her final destination, a set of available parking lots is selected based on the driver's walking preferences. Then the driver's utility for each parking lot in the selected set is calculated. This process is repeated for each driver. Finally, we aggregate the utilities of the individuals to obtain the aggregated utility for each charger type in each parking lot. The details about the utility construction phase is provided in APPENDIX A.

CHAPTER 3 MODEL FORMULATION AND DECOMPOSITION ALGORITHM

3.1 Notation and Model Formulation

One of the common approaches to modeling a problem under uncertainty is two-stage stochastic programming. We formulate the EVCS network design problem as a scenario-based, two-stage non-linear stochastic programming model that considers the randomness arising from dwell times, drivers' willingness to walk, the EV market penetration, the demand patterns on weekdays and weekends, and SOCs. The first-stage decision variables represent “here-and-now” decisions that are determined based on deterministic parameters in the first-stage constraints before the uncertainty is revealed. Subsequently, second-stage decisions are determined based on the first-stage decisions and the realizations of the random variable.

We define J as the set of potential parking lots for installing a set of charger types, denoted as N . We define B as the set of buildings that are considered to be the final destinations for EV drivers. Given $b \in B$, we define $m \in S^M(b)$ to be collection of subsets of available parking lots within the walking preference ranges of drivers whose final destination is building b . We consider a collection of subsets since the EV drivers have commonality among the parking lots in reaching their final destinations. This is due to that the drivers have different walking distance preferences and hence have different parking lot subsets. We define T to be the set of time slots within a day, indexed by $t \in T$. We use Γ to denote a set of arrival and departure times, where $\gamma(a)$ and $\gamma(d)$ indicate a combination of arrival and departure times for $\gamma \in \Gamma$. We define $\tilde{\omega}$ to be a multi-variate random variable representing the demand, where each scenario ω is a realization of $\tilde{\omega}$. In the first-stage of the model, the locations and types of chargers are determined by binary variables, and the

numbers of charger types in the selected parking lots are represented by integer variables. In the second-stage, based on EV drivers' walking preference ranges and the aggregated utilities for each parking lot and charger type, EV drivers are allocated to parking lots in a way that maximizes their expected access. For the mathematical formulation, we first define the model sets, parameters, and variables:

- Sets

- J : Set of parking lots, with $j \in J$.
- T : Set of time slots, with $t \in T$.
- N : Set of charger types, with $n \in N$.
- B : Set of buildings, with $b \in B$.
- $S^M(b)$: Collections of subsets of possible parking lots based on the walking preferences of drivers who are going to building b . There are M subsets and M depends upon building b , with $m \in S^M(b)$.
- Γ : Set of arrival and departure times, with $\gamma \in \Gamma$.
- Ω : Set of scenarios, with $\omega \in \Omega$.

- Model parameters

- c_n : Cost of installing charger of type n .
- k_j : Capacity of parking lot j for installing chargers.
- F : Total amount of the budget for installing chargers.
- $d_{\gamma,b}(\omega)$: Total demand for building b between the arrival and departure times $\gamma \in \Gamma$ for a given $t \in T$ in scenario $\omega \in \Omega$.

- $u_{n,j}(\omega)$: The aggregated utility of EV drivers who are willing to use charger type n in parking lot j in scenario $\omega \in \Omega$.
 - $u_{nc,j}(\omega)$: The aggregated utility of EV drivers who are not willing to charge their EVs in parking lot j in scenario $\omega \in \Omega$.
 - $d'_{\gamma,b,m}(\omega)$: The demand for building b among drivers who are willing to use parking lots $m \in S^M(b)$ between the arrival and departure times $\gamma \in \Gamma$ in scenario $\omega \in \Omega$.
- First-stage decision variables
 - $x_{n,j}$: 1 if parking lot j is chosen for installing charger type n ; 0 otherwise.
 - $z_{n,j}$: Number of charger of type n in parking lot j .
 - Second-stage decision variables
 - $y^m_{\gamma,b,j,n}(\omega)$: The proportion of the demand for building b in the subsets of parking lots $S^M(b)$ between the arrival and departure times $\gamma \in \Gamma$ for a given $t \in T$ that is satisfied by parking lot $j \in S^m(b)$, where $m \in S^M(b)$, using charger of type n in scenario $\omega \in \Omega$.

3.1.1 Two-stage Non-linear Stochastic Model

The two-stage non-linear stochastic programming model is defined as follows:

First-Stage Model:

$$\text{Max } E_{\Omega}[\varphi(x, z, \tilde{\omega})] \quad (3.1)$$

s.t.

$$\sum_{n \in N} z_{n,j} \leq k_j \quad \forall j \in J, \quad (3.2)$$

$$z_{n,j} \leq k_j x_{n,j} \quad \forall n \in N, j \in J, \quad (3.3)$$

$$\sum_{n \in N} \sum_{j \in J} c_n z_{n,j} \leq F \quad (3.4)$$

$$x_{n,j} \in \{0, 1\}, z_{n,j} \in \mathbb{Z}^+ \quad \forall n \in N, j \in J. \quad (3.5)$$

The second-stage recourse function based on the first-stage decisions x and z and a scenario ω is given by the following non-linear programming model:

$$\varphi(x, z, \omega) = \text{Max} \sum_{\gamma \in \Gamma} \sum_{b \in B} \sum_{m \in S^M(b)} \sum_{j \in S^m(b)} \sum_{n \in N} d_{\gamma,b}(\omega) y_{\gamma,b,j,n}^m(\omega) \quad (3.6)$$

s.t.

$$\sum_{\substack{\gamma \in \Gamma: \\ \gamma(a) \leq t \leq \gamma(d)}} \sum_{b \in B} \sum_{\substack{m \in S^M(b): \\ j \in S^m(b)}} d_{\gamma,b}(\omega) y_{\gamma,b,j,n}^m(\omega) \leq z_{n,j} \quad \forall t \in T, j \in J, n \in N, \quad (3.7)$$

$$\sum_{\substack{m \in S^M(b): \\ j \in S^m(b)}} y_{\gamma,b,j,n}^m(\omega) \leq \frac{e^{u_{n,j}(\omega)} x_{n,j}}{e^{u_{nc,j}(\omega)} + \sum_{l \in N} e^{u_{l,j}(\omega)} x_{l,j}} \quad \forall \gamma \in \Gamma, b \in B, j \in J, n \in N, \quad (3.8)$$

$$\sum_{n \in N} \sum_{m \in S^M(b)} \sum_{j \in S^m(b)} y_{\gamma,b,j,n}^m(\omega) \leq 1 \quad \forall \gamma \in \Gamma, b \in B, \quad (3.9)$$

$$d_{\gamma,b}(\omega) \sum_{n \in N} \sum_{j \in S^m(b)} y_{\gamma,b,j,n}^m(\omega) \leq d'_{\gamma,b,m}(\omega) \quad \forall \gamma \in \Gamma, b \in B, m \in S^M(b), \quad (3.10)$$

$$0 \leq y_{\gamma,b,j,n}^m(\omega) \leq 1 \quad \forall \gamma \in \Gamma, b \in B, m \in S^M(b), j \in S^m(b), n \in N. \quad (3.11)$$

The first-stage objective function (3.1) maximizes the expected EV drivers' access to the charging stations. Constraints (3.2) represent capacity restrictions for each type of charger in a parking lot based on its capacity, and constraints (3.3) state that a parking lot must be selected before selecting the charger type. Constraints (3.4) give the budgetary constraints. Constraints (3.5) define the binary and integer restrictions for the first-stage variables. For a realization of $\omega \in \Omega$, the second-stage objective function (3.6) maximizes the EV traffic flows based on the network decisions made in the first-stage. For each time slot in the planning horizon $t \in T$, the constraints (3.7) limit access based on the capacity decided upon

in the first-stage. Constraints (3.8) limit EV drivers' choice of different levels of chargers based on the utility function estimated by the mixed logit model described in the previous section. Constraints (3.9) ensure that the allocation of flow to the charging stations for each building does not exceed the building's demand in any time slot. Constraints (3.10) guarantee that drivers are assigned to only one of the parking lots within their walking distance range. Finally, constraints (3.11) define the restrictions for the second-stage variables. Due to the constraints (3.8), the two-stage model is non-linear in nature and is in general difficult to solve. In the next section, we provide details for linearizing the model so that it is viable for computational efficiency.

Proposition 1. *First, we restate constraints (3.8) as:*

$$\sum_{\substack{m \in S^M(b): \\ j \in S^m(b)}} y_{\gamma,b,j,n}^m (e^{u_{nc,a}} + \sum_{l \in N} e^{u_{l,j}} x_{l,j}) \leq e^{u_{n,a}} x_{n,j}.$$

Then for bounded continuous and binary variables y and x , respectively, we define a non-negative bi-linear variable as follows:

$$o_{\gamma,b,j,n,l}^m = x_{l,j} y_{\gamma,b,j,n}^m$$

$$\forall \gamma \in \Gamma, n \in N, l \in N, b \in B, m \in S^M(b), j \in S^m(b).$$

Using the variables o , a standard approach that has been adopted for linearizing the bi-linear terms is to replace each term by its convex and concave envelopes, also called the ‘‘McCormick

envelopes" [71]. The constraints (3.8) can then be rewritten as:

$$\begin{aligned}
& e^{u_{nc,j}} \sum_{\substack{m \in S^M(b): \\ j \in S^m(b)}} y_{\gamma,b,j,n}^m + \sum_{\substack{m \in S^M(b): \\ j \in S^m(b)}} \sum_{l \in N} e^{u_{l,j}} o_{\gamma,b,j,n,l}^m \\
& \leq e^{u_{n,j}} x_{n,j} \quad \forall \gamma \in \Gamma, b \in B, j \in J, n \in N,
\end{aligned} \tag{3.12}$$

$$\begin{aligned}
& o_{\gamma,b,j,n,l}^m \leq x_{n,j} \\
& \forall \gamma \in \Gamma, n \in N, l \in N, b \in B, m \in S^M(b), j \in S^m(b),
\end{aligned} \tag{3.13}$$

$$\begin{aligned}
& o_{\gamma,b,j,n,l}^m \leq y_{\gamma,b,j,n}^m \\
& \forall \gamma \in \Gamma, n \in N, l \in N, b \in B, m \in S^M(b), j \in S^m(b),
\end{aligned} \tag{3.14}$$

$$\begin{aligned}
& o_{\gamma,b,j,n,l}^m \geq x_{n,j} + y_{\gamma,b,j,n}^m - 1 \\
& \forall \gamma \in \Gamma, n \in N, l \in N, b \in B, m \in S^M(b), j \in S^m(b).
\end{aligned} \tag{3.15}$$

Proof. For the proof, see [71]. \square

This reformulation helps represent the second-stage problem as a linear programming model, thus allowing us to use the L-shaped method as a decomposition algorithm. It is worth to mention that since the two-stage model is an extension of capacitated facility location problem, it is a NP-hard problem [72].

3.2 Methodology and Algorithm Development

3.2.1 Sample Average Approximation

The SAA method is an approach to solving two-stage stochastic programming problems that uses Monte Carlo simulation. It is a sampling technique for approximating the

expectation function in a two-stage model. SAA approximates the second-stage expected recourse function of the two-stage stochastic programming model by a sample average estimate derived from a random sample. Then the sample average approximating the two-stage model is solved using a decomposition algorithm or a direct solver. The SAA model is solved multiple times with different samples to obtain candidate solutions along with statistical estimates of their optimality gaps. The SAA procedure is specified in Algorithm 1.

The SAA procedure for statistical evaluation of a candidate solution was suggested in [68], while convergence properties for the SAA method were studied in [55].

Table 3: SAA performance

S	P	UB	LB	Gap	SD
10	5	230.78	224.40	6.38	5.57
	10	246.89	242.83	4.06	4.98
	15	277.43	272.72	4.71	3.55
	20	300.76	295.42	5.34	3.76
20	5	227.90	224.90	3.00	6.11
	10	268.78	264.95	3.83	5.20
	15	296.59	291.80	4.79	3.65
	20	310.49	306.78	3.71	4.76
30	5	229.75	226.23	3.52	2.03
	10	265.20	261.82	3.38	2.98
	15	286.43	285.11	1.32	3.81
	20	273.18	272.28	0.90	2.48
40	5	227.29	226.40	0.89	2.75
	10	278.13	277.00	1.13	2.21
	15	304.46	302.31	2.15	1.17
	20	323.39	322.85	0.54	1.88
50	5	220.10	219.70	0.40	2.90
	10	289.42	288.21	1.21	3.12
	15	308.24	307.90	0.34	2.26
	20	322.00	321.85	0.15	2.59

Table 3 presents the computational results for the two-stage model using the SAA procedure. In the table, ‘S’ and ‘P’ represent the numbers of scenarios and parking lots, respectively. The upper and lower bounds are represented as ‘LB’ and ‘UB’, respectively. The

Algorithm 1 : SAA

Estimate the upper bound:

Generate K independent sample sets of scenarios, each of size L , i.e., $(\omega_j^1, \omega_j^2, \dots, \omega_j^L)$ for $j = 1, 2, \dots, K$.
For each sample set $j = 1, 2, \dots, K$, find the optimal solution:

$$v_L^j = \frac{1}{L} \sum_{i=1}^L \varphi(x, z, \omega_j^i).$$

Calculate:

$$\bar{v}_{L,K} = \frac{1}{K} \sum_{j=1}^K v_L^j,$$

$$\sigma_{\bar{v}_{L,K}}^2 = \frac{1}{K(K-1)} \sum_{j=1}^K (v_L^j - \bar{v}_{L,K})^2.$$

Estimate the lower bound:

Choose any feasible solution (\bar{x}, \bar{z}) from the first-stage problem, which provides a lower bound for the optimal value $f(\bar{x}, \bar{z}) \leq v^*$.

Choose a sample of scenarios of a size L' that is much larger than L and independent of the samples, i.e., $(\omega^1, \omega^2, \dots, \omega^{L'})$.

Estimate the objective function f :

$$f(\bar{x}, \bar{z}) = \frac{1}{L'} \sum_{i=1}^{L'} \varphi(x, z, \omega^i).$$

Calculate the variance of this estimation:

$$\sigma_{L'}^2(\bar{x}, \bar{z}) = \frac{1}{L'(L'-1)} \sum_{i=1}^{L'} (\varphi(x, z, \omega^i) - f(\bar{x}, \bar{z}))^2.$$

Estimate the optimality gap and variance:

Based on the computed upper and lower bounds, the optimality gap is estimated as follows:

$$Gap_{K,L,L'}(\bar{x}, \bar{z}) = \bar{v}_{L,K} - f(\bar{x}, \bar{z}).$$

Similarly, the variance is calculated as follows:

$$\sigma_{gap}^2 = \sigma_{\bar{v}_{L,K}}^2 + \sigma_{L'}^2(\bar{x}, \bar{z}).$$

upper bound for the expected accessibility of the charging station is estimated by a batch size of 20 ($K=20$). An independent sample of scenarios ($L'=1,000$) were used to estimate a lower bound for the optimal solution. The gap and standard deviation are represented in the columns ‘Gap’ and ‘SD’, respectively.

3.2.2 L-shaped Decomposition

SAA was adopted for the model presented in section 5.2.2, and two-stage sample average stochastic programs are commonly solved by decomposition algorithms such as Benders’ method and the L-shaped method. Realistic problems are continuously growing in size and complexity; for this reason, decomposition techniques are more attractive. Decomposition methods break a problem down into smaller problems that are easier to solve. The L-shaped method has been applied to the class of mixed-integer linear stochastic programming problems with only continuous variables in the second-stage. The L-shaped method works by approximating the expected second-stage recourse function through construction of optimality cuts in the first-stage based on the dual solutions of the second-stage problems. The procedure alternates between a master problem (MP), as represented in (3.16), and sub-problems (SPs), trading information to obtain the optimal solution. The SPs are the second-stage formulation (3.6), subject to constraints (3.7)-(3.11).

Master Problem (MP):

$$\text{Max } \eta \tag{3.16}$$

s.t.

$$(3.2) - (3.5), \eta \text{ free.}$$

In the problem, constraints (3.7), (3.12), (3.13), and (3.15) are referred to as the linking constraints because of the presence of the first-stage variables x and z in the second-stage, which links the two stages. Let A be the coefficient matrix for variables $z_{n,j}$ in the linking constraints (3.7), where $a_{i,q}$ is the entry of matrix A at indices i and q , and $a_{i,q} \in R^{|\mathcal{N}||\mathcal{J}||\mathcal{T}||\mathcal{N}||\mathcal{J}|}$. In addition, let F and G be the coefficient matrices for variables $x_{n,j}$ in the linking constraints ((3.12) and ((3.13), (3.15))), respectively, where $f_{i,q}$ and $g_{i,q}$ are the entries of the matrices F and G at indices i and q , and $f_{i,q} \in R^{|\mathcal{N}||\mathcal{J}||\mathcal{T}||\mathcal{B}||\mathcal{N}||\mathcal{J}|}$, $g_{i,q} \in R^{2|\mathcal{T}||\mathcal{N}||\mathcal{B}||\mathcal{J}||\mathcal{S}||\mathcal{N}||\mathcal{J}|}$. We use π_ω as the notation for a vector for the dual values of the second-stage constraints ((3.7), (3.9), (3.10), (3.11) (3.12), (3.13), (3.14), (3.15)), and π_ω^1 , π_ω^2 , and π_ω^3 as dual values corresponding to the constraints (3.7), (3.12) and ((3.13), (3.15)) in each scenario. We use Δ_ω to refer to the right-hand sides of the SPs in each scenario. The L-shaped method is initialized by solving the first-stage EVCS problem to obtain the initial solutions x^0 and z^0 . These solutions are then used as fixed parameters in the second-stage problem. For each scenario $\omega \in \Omega$, a sub-problem is defined based on the second-stage problem. In the next step, the SPs are solved to obtain the dual values and the corresponding objective functions. The optimality cut(s) is (are) then generated using matrix multiplication. For each scenario, an optimality cut can be defined as follows:

$$\sum_{n \in \mathcal{N}} \sum_{j \in \mathcal{J}} \left(((\pi^1)^T A) \cdot z_{n,j} + (((\pi^2)^T F)((\pi^3)^T G)) \cdot x_{n,j} \right) + \eta \leq \pi^T \cdot \Delta \quad ,$$

where η is a free variable. We use Θ_ω^k to denote the optimality cut corresponding to scenario ω at iteration k . It should be noted that because the second-stage is feasible for every

solution of the first-stage (complete recourse), we do not need to add any feasibility cuts in (3.16). In the next step, the generated cut(s) are added to the MP (3.16) with the objective function to maximize η for the single-cut and $\sum_{\omega \in \Omega} p_{\omega} \eta_{\omega}$ for the multi-cut L-shaped decomposition where p_{ω} is the probability of occurrence for each scenario ω . Then the MP is solved to obtain a new solution for the variables x and z , and the updated solution is then added to the sub-problems. In each iteration, upper and lower bounds are updated based on the new solutions obtained from the sub-problems and the MP. This process is repeated until the difference between the upper and lower bounds reaches a pre-determined threshold.

To evaluate the efficacy of the L-shaped algorithm, we conducted computational experiments with various instances. We implemented single- and multi-cut L-shaped decomposition methods to solve the large-scale sample average two-stage stochastic programming models. We compared the performance of these two methods to the deterministic equivalent problem (DEP). The DEP is the entire representation of formulation (3.1)-(3.11) without any decomposition for the problem. Table 4 indicates the complexity of instances in terms of the number of variables and constraints in the first-stage and the second-stage, along with the number of non-zeros. The columns labelled ‘ S ’, ‘ P ’, ‘Cons’, and ‘Vars’ represent the number of scenarios, parking lots, constraints, and variables, respectively. Table 5 shows the numerical results. The first two columns indicate the performance of the DEP in terms of runtime in seconds and the MIP gap (%). The next three columns specify the performance of single-cut L-shaped decomposition, with ‘time(s),’ ‘gap(%)’ and ‘# of cuts’ indicating runtime (seconds), the gap percentage, and the total number of cuts within the stipulated time limit, respectively. Similarly the last three columns indicate the per-

Algorithm 2 : L-shaped decomposition

Initialization:

Obtain an initial solution z^0 and x^0 by solving the first-stage problem.

Set $UB \leftarrow \infty$, $LB \leftarrow -\infty$, $k \leftarrow 0$.

Define the free variable η for single-cut and η_ω for multi-cut decomposition.

While $UB - LB > \epsilon$:

Sub-problems:

For $\forall \omega \in \Omega$:

Solve $\varphi(x, z, \omega)$.

Calculate the dual solution for $\varphi(x, z, \omega)$ and store it as π^k .

Extract $\pi^{1,k}$, $\pi^{2,k}$, and $\pi^{3,k}$ from π^k .

Calculate the objective function value for $\varphi(x, z, \omega)$ and store it as f_ω^k .

Update upper bound:

Set $v^k = \sum_{\omega \in \Omega} p_\omega f_\omega^k$, where p_ω is the probability of the occurrence of scenario $\omega \in \Omega$.

Set $UB \leftarrow \min(UB, v^k)$.

Cut generation:**Single-cut:**

Add $\sum_{\omega \in \Omega} p_\omega \Theta_\omega^k$ to the first-stage problem.

Multi-cut:

$\forall \omega \in \Omega$:

Add Θ_ω^k to the first-stage problem.

Master problem:

Set $v^{k+1} \leftarrow \eta$ as the objective function for single-cut.

Set $v^{k+1} \leftarrow \sum_{\omega \in \Omega} \eta_\omega$ as the objective function for multi-cut.

Solve the MP and update $z^* \leftarrow z^k$ and $x^* \leftarrow x^k$.

Update lower bound:

Set $LB \leftarrow \max(LB, v^{k+1})$.

Set $k \leftarrow k + 1$.

Table 4: Model data specifications

S	P	Cons	Vars	First-Stage Vars	First-Stage Cons	Second-Stage Vars	Second-Stage Cons	# of Non-zeros
10	5	477,970	178,770	15	21	447,955	178,749	2,886,750
	10	951,240	357,540	30	41	951,210	357,499	7,987,222
	15	1,424,510	536,310	45	61	1,424,465	536,249	12,342,786
	20	1,897,780	1,715,080	60	81	1,897,720	714,999	18,967,552
20	5	1,043,334	390,210	15	21	1,043,319	390,189	4,245,768
	10	2,076,404	780,360	30	41	2,076,374	780,319	11,879,054
	15	3,109,474	1,170,630	45	61	3,109,429	1,170,569	17,652,320
	20	4,142,544	1,560,840	60	81	4,142,484	1,560,759	25,657,932
25	5	1,244,946	465,090	15	21	1,244,931	465,069	6,676,510
	10	2,477,576	930,180	30	41	2,477,546	930,139	15,777,890
	15	3,710,206	1,395,270	45	61	3,710,161	1,395,209	21,876,112
	20	4,942,836	1,860,360	60	81	4,942,776	1,860,279	33,132,981
30	5	1,456,852	543,450	15	21	1,456,837	543,429	8,352,947
	10	2,899,182	1,086,900	30	41	2,899,152	1,086,859	20,301,290
	15	4,341,512	1,630,350	45	61	4,341,467	1,630,289	37,392,389
	20	5,783,842	2,173,800	60	81	5,783,782	2,173,719	75,390,221
35	5	1,750,951	653,910	15	21	1,750,936	653,889	10,893,269
	10	3,484,551	1,307,820	30	41	3,484,521	1,307,779	21,290,765
	15	5,218,151	1,961,730	45	61	5,218,106	1,961,669	45,888,242
	20	6,951,751	2,615,640	60	81	6,951,691	2,615,559	80,561,107
40	5	2,093,635	781,590	15	21	2,093,620	781,569	15,896,110
	10	4,166,475	1,563,180	30	41	4,166,445	1,563,139	30,290,137
	15	6,239,315	2,344,770	45	61	6,239,270	2,344,709	59,876,208
	20	8,312,155	3,126,360	60	81	8,312,095	3,126,279	101,965,108

Table 5: Computational results for L-shaped method

S	P	DEP		Single-cut			Multi-cut		
		time(s)	gap(%)	time(s)	gap(%)	# of cuts	time(s)	gap(%)	# of cuts
10	5	303	0.00	1,234	0.00	453	204	0.00	570
	10	2,263	0.00	3,600	0.30	598	539	0.00	780
	15	2,779	0.00	3,600	0.20	438	321	0.00	510
	20	3,600	0.10	3,600	3.00	253	3,600	2.00	1,750
20	5	1,845	0.00	2,747	0.00	349	432	0.00	1,060
	10	3,200	0.00	3,600	0.70	366	1,036	0.00	1,420
	15	3,600	10.80	3,600	3.90	272	737	0.00	1,180
	20	3,600	0.20	3,600	33.00	162	3,600	0.70	1,360
25	5	2,575	0.00	3,600	0.04	508	921	0.00	1,675
	10	3,600	-	3,600	4.10	301	3,600	0.20	3,300
	15	3,600	-	3,600	5.20	251	3,600	0.30	3,125
	20	3,600	0.20	3,600	12.80	153	3,600	0.50	2,775
30	5	3,057	0.00	3,600	0.00	467	661	0.00	1,530
	10	3,600	-	3,600	62.40	499	1,086	0.00	1,710
	15	3,600	-	3,600	5.80	201	1,198	0.00	1,860
	20	3,600	2.40	3,600	46.25	116	3,600	6.00	2,130
35	5	3,200	0.00	3,600	0.20	207	1,401	0.00	1,610
	10	3,600	-	3,600	11.60	177	3,600	0.02	2,380
	15	3,600	-	3,600	5.10	152	3,600	0.01	2,205
	20	3,600	-	3,600	11.80	98	3,600	0.15	1,575
40	5	3,600	-	3,600	0.15	203	3,600	0.11	2,240
	10	3,600	-	3,600	2.40	148	3,600	0.22	1,680
	15	3,600	-	3,600	9.00	137	1,414	0.00	840
	20	3,600	-	3,600	37.00	76	3,600	4.00	400

formance metrics related to multi-cut L-shaped. The gap percentage is calculated as the difference between the upper bound and the lower bound divided by the lower bound. Similarly, the last three columns specify the performance of multi-cut L-shaped decomposition. All of the optimization models were implemented in Python 3.6 using Gurobi 8.1.1, with a one-hour time limit. The computational experiments were performed on a computer with an Intel [®] Xeon [®] CPU E5-2640, 2.60 GHz, and 80GB RAM. As shown in Table 5, the runtime for most instances increased with an increase in the number of parking lots and scenarios, as expected. When the number of scenarios was less than 20, DEP performed better than the single-cut method. However, for the rest of the 16 instances, DEP could obtain a feasible solution within the one-hour time limit in only four instances, while single-cut decomposition performed better in most of these instances. Especially for the large-scale instances, multi-cut decomposition outperformed DEP with a much better runtime and gap. Also, multi-cut decomposition outperformed single-cut decomposition in all instances. Given the relatively simple and fewer constraints in the first-stage model, the multi-cut variant was able to perform better than single-cut. The single-cut L-shaped method mostly had difficulties in accelerating the convergence of the upper and lower bounds. Hence, for any given data set, multi-cut decomposition outperformed the other methods, and especially when there were a larger number of parking lots and scenarios.

3.2.3 Value of the Stochastic Solution

The utility of the stochastic programming approach can be evaluated by estimating the value of the stochastic solution (VSS) introduced by [11]. The objective value of the recourse problem (RP) can be stated as $RP = E_{\Omega}[\varphi(x, z, \tilde{\omega})]$; then we take the expected value of the random variable and solve the *expected value problem*, $EV = \varphi(x, z, \bar{\omega})$, where $\bar{\omega}$ for

the demand parameter is $\sum_{\omega \in \Omega} p_{\omega} d_{\gamma, b}(\omega)$, with p_{ω} indicating a scenario ω 's probability of occurrence and $\sum_{\omega \in \Omega} p_{\omega} = 1$. Considering \bar{x}, \bar{z} as the solutions for the EV problem, the expected result of using the expected value solutions (\bar{x}, \bar{z}) is $EEV = E_{\Omega}[\varphi(\bar{x}, \bar{z}, \tilde{\omega})]$. Then the VSS can be defined as the difference between the objective values of the recourse problem and the EEV, i.e, $VSS = RP - EEV$. In Fig. 6, value of the stochastic solution is calculated as $\frac{RP - EEV}{EEV} * 100$, 'VSS' represents the series while considering uncertainties in all the parameters, and each of the other series represent the value of stochastic solution for each uncertain parameter while other parameters are replaced by their mean values. Five replications and 40 scenarios were used to obtain value of stochastic solutions. Within the parameters, dwell time has the highest impact on the accessibility to charging stations. Due to the limited capacity of charging locations, and an EV is plugged-in till the end of a driver's activity, dwell time significantly affects the accessibility to the charging stations. For the same reason, SOC's impact is minimum and contributes to a driver's decision on whether to charge or not. At lower budgets, arrival time of an EV to the community has more impact due to lesser availability of charging stations. Also, as the budget increases, due to the availability of more charging stations within the drivers' walking distance, the stochastic influence of walking has decreased. By adopting the stochastic programming approach, the overall improvement in accessibility to charging stations is 11.37 %.

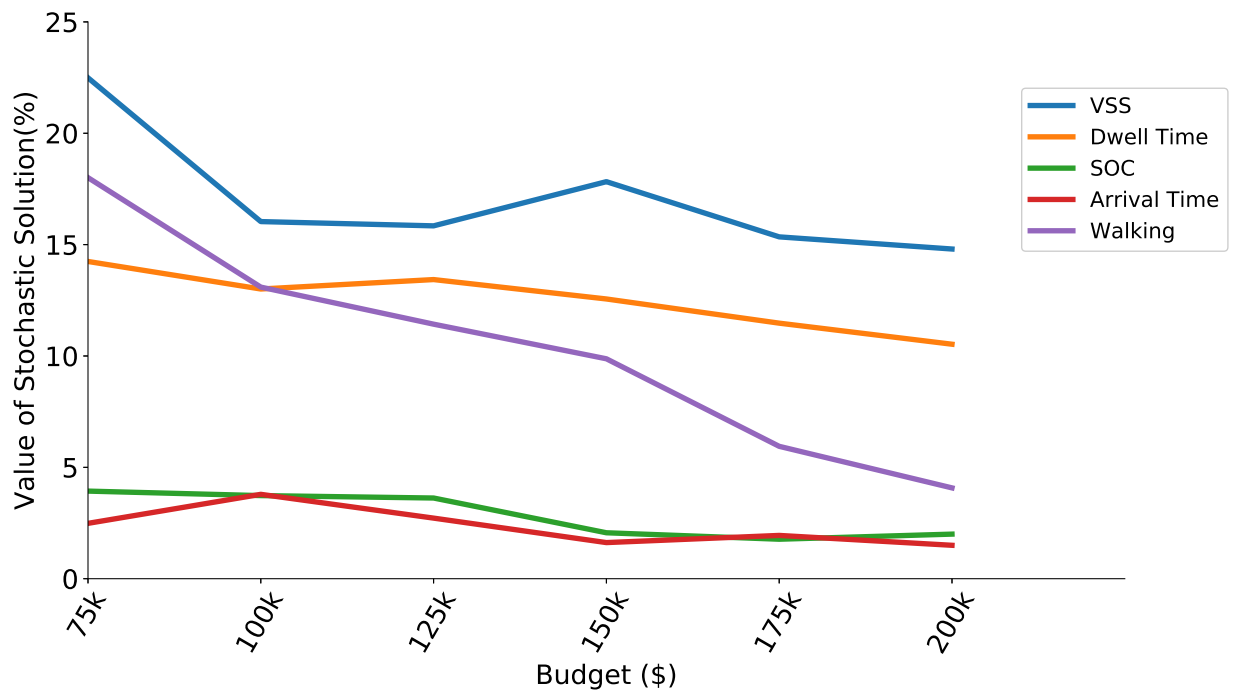


Figure 6: Valuating the effect of each source of uncertainty and comparing with the value of stochastic solution

CHAPTER 4 CASE STUDY, COMPUTATIONAL EXPERIMENTS, AND CONCLUSION

4.1 Case Study and Computational Experiments

We conducted a case study using data obtained from the Southeast Michigan Council of Governments (SEMCOG) and literature sources for the midtown area of Detroit, Michigan, in the US. This area includes different types of destinations, which attracts lots of traffic. There are 67 offices, 44 school-related buildings, 12 social places, 5 family-related buildings, 4 restaurants, and 3 shopping places in this area. We selected 10 parking lots as potential locations for installing chargers and assumed that the parking lots are available for use from 6:00a.m to 6:00p.m and that the capacity of each of the parking lots is based on its size. We estimated the EV demand for the case study through a two-step process. The data from SEMCOG shows that the average annual daily traffic for the Detroit midtown area is between approximately 10,000 and 14,000 vehicles and follows a uniform probability distribution. Furthermore, we calculated the EV demand for the final destination based on drivers' different activity types during the time of day and the day of the week. According to the U.S. Environmental Protection Agency's analysis, 3% and 5% of the light-duty vehicle fleet comprise EVs, and BEVs' market share can be affected by cold-temperature weather conditions [82]. Since our case study is in a cold area, we considered a 2% market share for BEVs in each case. Following a suggestion in [125], we used a negative exponential distribution function to capture EV drivers' willingness-to-walk patterns based on the activity type, season, and community size. On average, given our parameter settings, 13% of the total demand is lost because there is no parking available within drivers' preferred walking distances.

Table 6: Weibull distribution parameters for drivers' dwell time; Source:[27]

Type of day	Work	Social	Family	Meal	School	Shopping
Weekday	(5.89, 10)	(1.89, 10)	(1.05, 10)	(0.79, 2)	(3.61, 2)	(0.56, 2)
Weekend	(6.04, 6)	(2.03, 2)	(1.13, 2)	(0.79, 2)	(3.36, 10)	(0.25, 0.5)

4.1.1 Scenario Generation

We modeled uncertainties using case scenarios in the two-stage model. Each scenario represents a single day and is affected by the total number of EV drivers arriving in the community on a weekday or weekend in specific seasons of the year. Following the uniform probability distribution, each scenario occurs in each season of the year with the same probability. The arrival times of BEV drivers were estimated by Weibull distributions with parameters (8, 3) and (13, 4) for a weekend and a weekday, respectively [135]. Based on a driver's activity, the dwell time was calculated using a Weibull distribution. The scale and shape parameters for each type of activity and type of day are provided in Table 6. When a driver arrives in the community, a building or final destination is randomly assigned to the driver based on his/her activity type, using a uniform distribution. As mentioned in the previous section, we use a truncated normal distribution $N(0.3, 0.1)$ with limits of 0 and 1 to estimate the SOC for an EV upon its arrival at a parking lot. This process was repeated multiple times to generate a set of scenarios.

4.1.2 Experiments and Results

The availability of an EVCS can offer a greater driving range for an EV and make it unnecessary to use other vehicles for longer trips. To examine the effects of different parameters and their impact on the accessibility of EVCSs in the proposed model, we studied different cases and evaluated the model with a sensitivity analysis. We considered 6:00

am – 9:00 am, 9:00 am – 12:00 pm, 12:00 pm – 2:00 pm, and 2:00 pm – 6:00 pm to be the four time slots in a day. Also, we considered \$900, \$3,450, and \$25,000 to be the average installation costs for level 1, level 2, and level 3 chargers, respectively [93]. Forty scenarios were generated for the two-stage model, and 10 parking lots were used in all cases. Fig. 7 shows the heat map for the demand distribution and the locations of parking lots. Parking lots 1 through 8 are the parking structure facilities that have the highest capacity in the area in terms of parking spots. The other two parking lots are smaller parking facilities. A darker color indicates a higher demand for a parking lot. Parking structures are considered to have a capacity for 20 stations, while the parking lots are considered to have a capacity for 5. A set of available parking lots was generated for each EV driver based on the driver's preferred walking distance. Four different metrics were used to assess the performance of the EVCS network design, including EVCS accessibility, charger utilization, total walking distance, and average walking distance per driver. Accessibility is defined as the percentage of EV drivers who could charge their vehicles in the charging locations proposed by the two-stage model. Utilization is defined as the percentage of the total time that a charger is used by EVs. Because the installation of public charging stations can change travelers' walking patterns, especially in an urban community, we measured the walking distance trend before and after installing charging stations. Fig. 8 compares the accessibility of charging stations with the utilization of each level of chargers as the budget increases. As expected, the results indicate that, with a budget increase, the accessibility of the charging levels also increases. In addition, level 1 utilization decreases faster than level 2 utilization with a budget increase. This is because more level 2 chargers than level 1 chargers are installed as the budget increases, since level 2 chargers have a higher

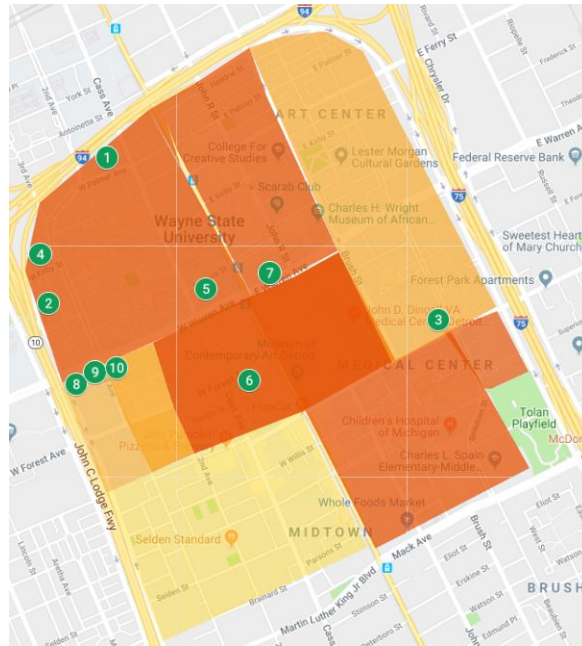


Figure 7: Heat map of the demand flow and location of parking lots in the study area.

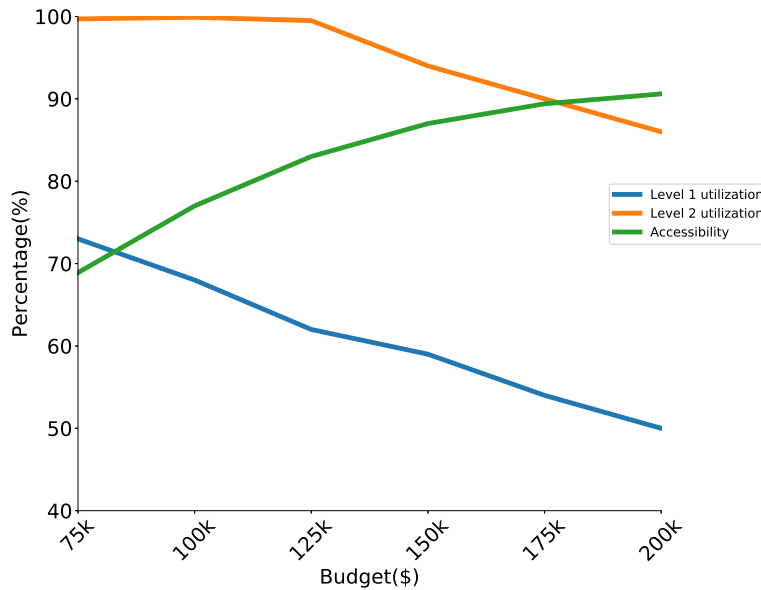


Figure 8: Percentages of accessibility and charging utilization for different budget amounts

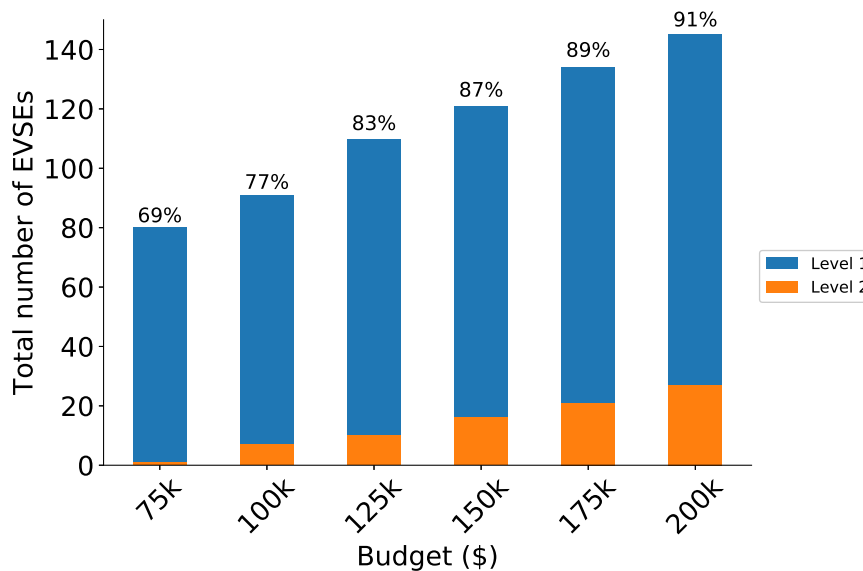


Figure 9: Number of installed level 1 and level 2 chargers for different budget amounts, labeled by accessibility percentages.

utility for commuters. Fig. 9 compares the total number of level 1 and level 2 chargers that are installed in parking lots based on different budgets, and these are labeled with accessibility percentages. In Fig. 11, the average utilization percentages for level 1 and level 2 chargers in the ten parking lots are compared for different time slots. The maximum utilization occurs between 9:00 am and 12:00 pm, and this matches the activity types of the case community, which are mostly school and work. In addition, Fig. 12 illustrates the trade-off between the budget size and the utilization percentage in different time slots for level 1 and level 2 chargers. Figs. 11 and 12 present the utilization of chargers, which is a major factor in estimating the financial rate of return for investors.

Although this was not the focus of the study, increases in travel options enable commuters to dedicate a part of their trip to walking or biking in order to improve their health. Thus, an optimal design of public charging infrastructures can provide opportunities for

people in a community to increase their levels of physical activity [78]. This can also improve the livability metrics within a city. Based on walking preferences, two cases were generated; pessimistic and optimistic cases. Both cases generated from a distribution given by [125]; however, in the pessimistic case the distribution is truncated for value over 0.2 mile. Fig. 10 compares the total walking distance and the walking distance per person among EV drivers who access public charging stations for the two cases.

As the results indicate, level 3 chargers are not installed in the parking locations. This is due to the limited budget size, since the level 3 installation cost is relatively high compared to the cost for the other levels of chargers. Based on our data sources, Fig. 13 indicates that within the urban community, people are unwilling to use level 3 chargers when the price is about 35 cents per minute. However, the utility of level 3 increases as the charging price decreases. When the charging price is finally lowered to \$3 per hour, the preference for using fast chargers is higher than for level 1 and level 2 chargers.

4.1.3 Data-driven Simulation

A data driven simulation study was performed to evaluate the efficacy of the proposed work with the approach presented in [27] which ignores choice modeling. Two configurations were considered to establish the baseline for [27]: configuration 1 - where all the chargers are considered to be level 2; configuration 2 - 80% of the parking lots' capacity is allocated for installing level 2 chargers and the remaining capacity is assigned to level 1. Based on the network designs proposed by each of the approaches, a simulation experiment was performed to measure the 'accessibility' for each driver based on the availability and choice during their arrival. If an EV driver could not find his/her first-choice of charger, the driver will search for the next best alternative. We used two performance

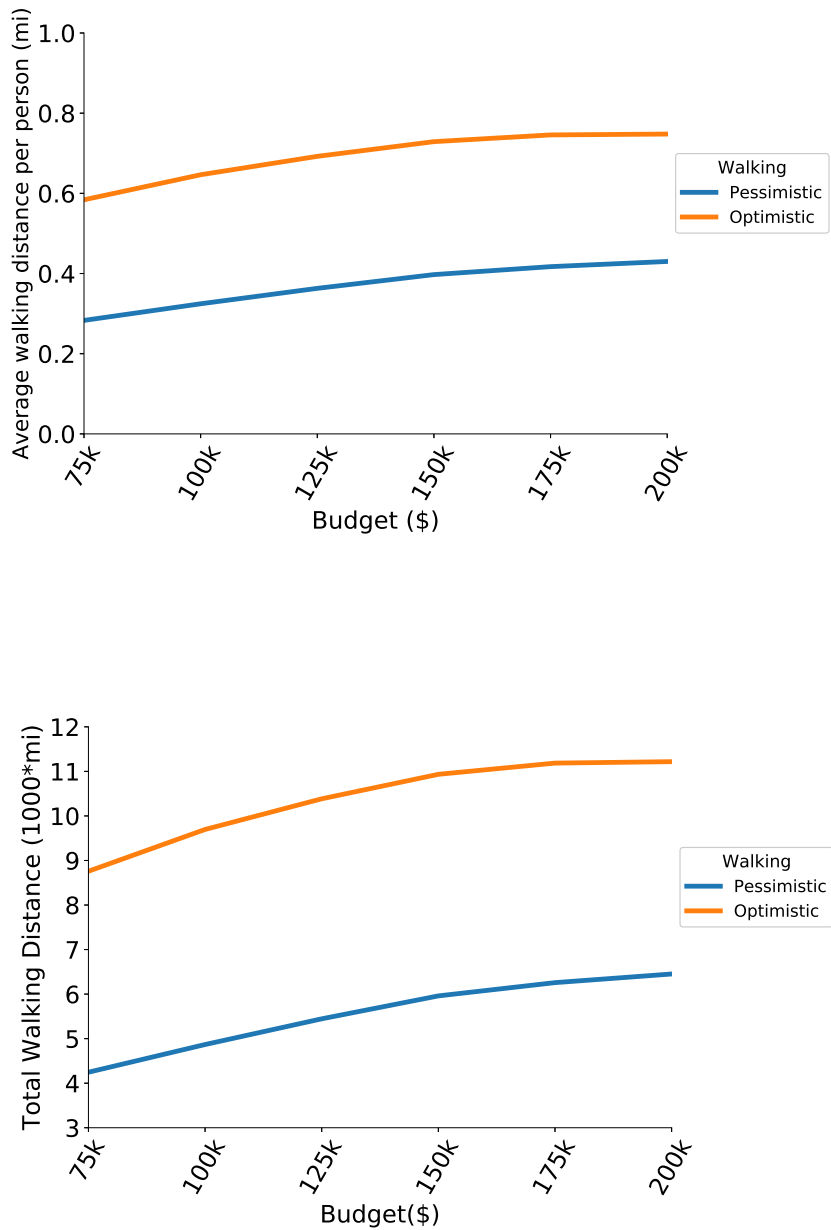


Figure 10: a) Average walking distance per person and b) total walking distance for people who have access to a public EV charging station in both optimistic and pessimistic cases.

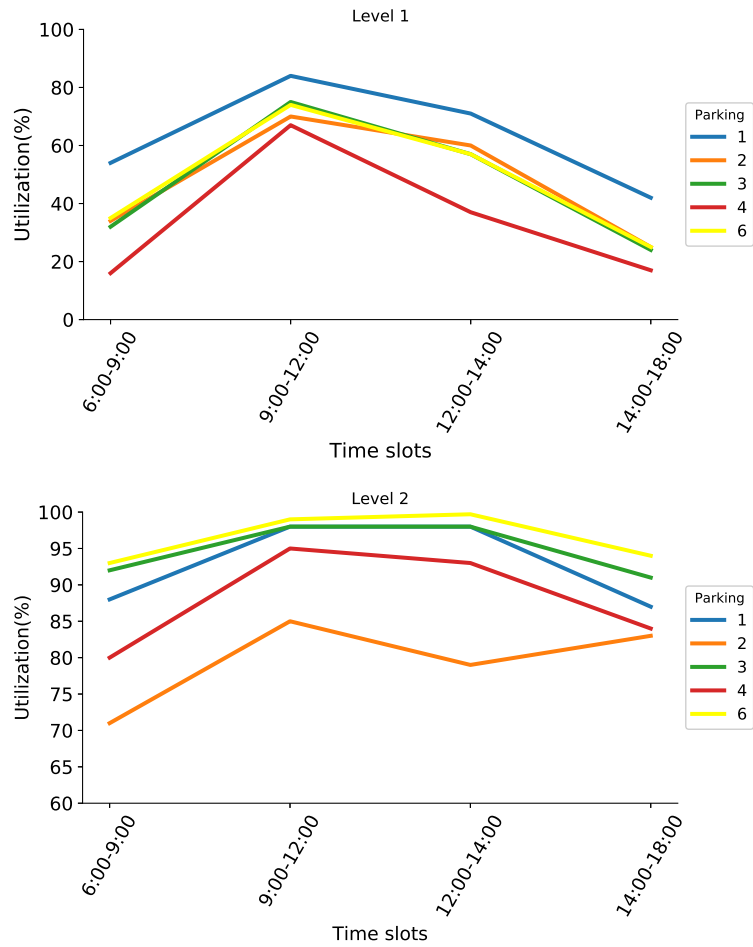


Figure 11: Percentage of average utilization of a) Level 1, and b) Level 2 chargers during each time slot in five parking lots

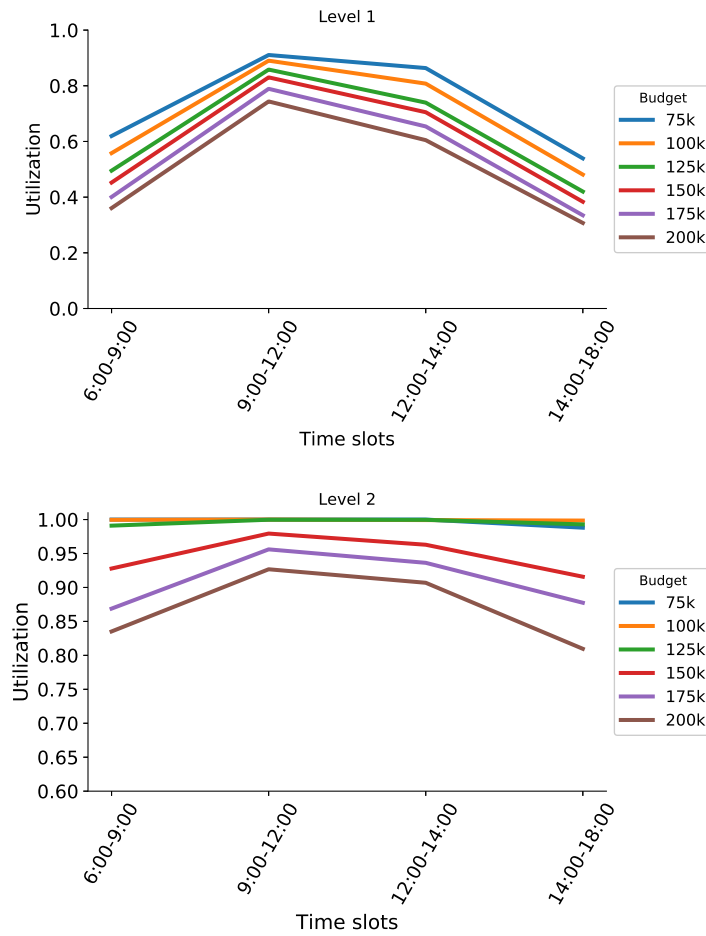


Figure 12: Percentage of average utilization of a) level 1, and b) level 2 chargers in all parking lots during each time slot for different budgets

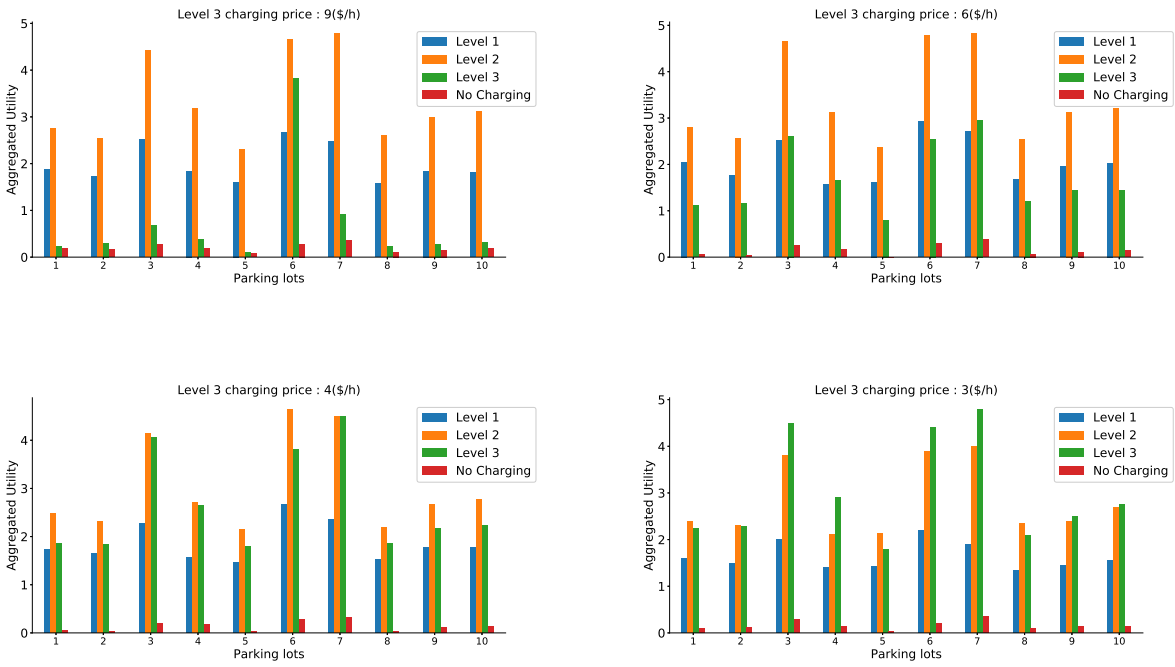


Figure 13: Aggregated EV drivers' utility of using different charger levels in different parking lots when the level 3 charging price is 9(\$/h), 6(\$/h), 4(\$/h) and 3(\$/h)

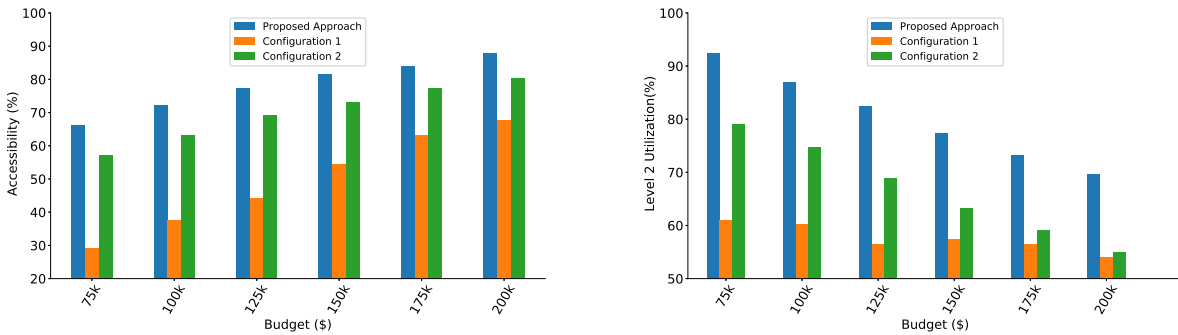


Figure 14: Percentage of accessibility and level 2 utilization for the proposed approach and two defined configurations

metrics: "accessibility" is the percentage of EV drivers who could use the chargers at their arrival; "utilization" is calculated as the total number of hours that a charger is used by drivers over the total number of hours within the simulation period. Fig. 14 shows that the proposed approach considering choice modelling has better accessibility and utilization at each of the budget levels compared to other two configurations using the model proposed in [27]. For each budget, we used 200 replications for simulation, and on average, the proposed approach could increase the accessibility by 29% and 10%, and level 2 utilization by 23% and 14% compared to using configurations 1 and 2 without choice modelling, respectively.

4.2 Conclusion

In this research, we propose a choice modeling approach embedded in a two-stage stochastic programming model for EV charging station network design within a community. Various factors, such as the total EV flow, arrival and dwell times, batteries' SOCs upon arrival, and the distances that EV drivers are willing to walk, are considered in the model as sources of uncertainty. Factors such as charging prices, the cost of charging at home, driving range charges, total trip distances, and dwell times are used to capture BEV drivers' charging choice behaviors. The framework suggests relationships among the budget size and the capacity and accessibility of the charging stations for EVs. A choice model utility function was helpful in determining preferences for different charger types among the EV drivers. The proposed model presents a robust charging station network solution to any future changes in the community's pattern of willingness to walk. The computational results indicate that the optimal layout of charging stations should include a mix of different chargers. For the given data, accessibility improved with an increase in the budget, and

more level 2 chargers are installed compared to the level 1. Also, with increase in budget, utilization of chargers decreased. Based on current pricing policy and utility function, level 3 is not preferred in urban communities. The simulation study in post optimization helps to study the influence of price on utility function and subsequent improvement in preferences for level 3 chargers. We ran experiments to quantify the influence of stochastic data parameters, and dwell time had the highest impact on accessibility to charging stations. Furthermore, a data-driven simulation study was conducted to evaluate the benefits of using choice modelling approach. We solve the proposed two-stage stochastic programming models using sample average approximation and the L-shaped decomposition method. We compare the computational results with single- and multi-cut variants of the L-shaped method for a deterministic equivalent problem formulation. We present a case study using the model's results along with various insights, including (among others) a demarcation in the utility function for different charger types and the sensitivity of the optimal network to the budget.

CHAPTER 5 EFFICIENT ALGORITHMS FOR AUTONOMOUS ELECTRIC VEHICLE MIN-MAX ROUTING PROBLEM: INTRODUCTION AND MODEL FORMULATION

5.1 Introduction

Global warming has been primarily linked to human activities which release greenhouse gases [76]. Among those activities, the transportation sector causes the largest share (about 24%) of greenhouse gas emissions, which mainly originate from fossil fuel burner vehicles [94]. Given this, a lot of efforts are made to transform the transportation systems by driving new technological innovations in vehicles [119]. One of the outcomes is electric vehicles (EVs) which are becoming rapidly important for many automotive companies. Many countries have offered incentives to accelerate the adoption of EVs to increase the EV share in future vehicle fleets [127]. Meanwhile, autonomous driving technologies are evolving and considerable efforts are been made to advance the real-world applications for self-driving [119].

Due to natural synergies between the autonomous and EVs, automotive companies are striving to equip the EVs with autonomous driving technologies [18]. Autonomous electric vehicles (AEV) have capabilities for decision making, on-board computation, and connectivity. It is important for AEVs to choose energy-efficient routes and find the best locations for recharging during their itineraries. Transportation network companies (e.g., Lyft and Uber), and logistic companies (e.g., FedEx and UPS) seek to operate a fleet of AEVs in their business in the future [133]. Adopting AEVs also brings new challenges. One of the main operational challenges for AEVs in transport applications is their limited range and the availability of charging stations (CS) [98, 88, 44]. It is estimated that half of the US population lives in areas with fewer than 90 charging infrastructures per million

people, which is 70% below the benchmarks [92, 28]. To successfully employ AEVs, we need strategies that can alleviate the range and recharging limitations. Effective routing strategies for an AEV fleet ask for solving the vehicle routing problem (VRP) with the limited range and number of CSs. Hence, the autonomous electric vehicle routing problem (AEVRP) naturally appears in order to operate a team of AEVs efficiently. AEVRP falls into the category of green vehicle routing problem (GVRP). The GVRP embraces a broad and extensive class of problems considering environmental issues as well as finding the best possible routes for vehicles. The GVRP research flow can be divided into two categories: 1) minimize the fuel consumption while considering loading weights [56]; and 2) replace the conventional vehicles with Alternative Fuel Vehicles (AFV) [88, 96, 23, 112, 47, 56]. This research focuses on AFVs, hence we briefly review the related literature on routing strategies for AFVs. An initial work was done by [25], where they developed a mixed integer programming (MIP) formulation and a heuristics to overcome the range limitation of AFVs and shortage of refueling locations. Authors in [88] introduced the EV routing problem with time windows and charging stations with the limited freight capacity for the vehicles. They developed a hybrid meta-heuristic by integrating variable neighborhood and tabu search. The research work in [43] considered a mixed fleet of conventional, plug-in hybrid, and EVs. They proposed a hybrid genetic algorithm integrated with a neighborhood search approach. Also, to include CSs in each trip and determining the fuel type, they applied a layered optimization algorithm by combining labeling technique and a greedy algorithm. For single unmanned aerial vehicles' routing problem, authors in [96] proposed a novel approach based on an approximation algorithm combined with a heuristic method. Later, the authors extended their work to multiple vehicles by applying

the Voronoi algorithm as the construction phase, and 2-opt, 3-opt variable neighborhood searches in the improvement phase [60].

In this research, we define the AEVRP as follows: given a set of AEVs which are initially stationed at a depot, a set of targets and a set of CSs, the goal is to visit each target exactly once by any AEV and return to the depot while no AEV runs out of charge as they travel in their routes. We assume that all AEVs get fully charged at charging stations, and the fuel consumption rate is linearly proportioned with traveled distance. This research considers a variant of the AEVRP, which we refer to as min-max AEVRP. The objective of this problem is to minimize the maximum distance traveled by any AEV instead of the total distance (min-sum), that is the conventional case in VRP. The min-max AEVRP is fundamentally different from min-sum AEVRP. An optimal solution in min-max AEVRP assigns routes to all AEVs such that none of the AEVs has a longer route. This will result in a more balanced distribution of loads and fair and equitable utilization of the AEVs, which can decrease the rates of battery degradation in AEVs [64]. Refer to Figure 15 for an illustration for min-max and min-sum routes for AEVs. In Figure 15, AEV1 visits most of the targets while AEV2 visits only a few targets with min-sum. However, using min-max, the two AEVs visit almost the same number of targets.

The min-max AEVRP is also of interest when minimizing time to visit targets is more important than the total traveled distance. This situation arises mainly in emergency management situations such as providing relief after a disaster [15, 3]. Other applications of min-max AEVRP are in intelligence, surveillance, and reconnaissance by unmanned ground or aerial vehicles [2, 105, 131, 69, 52], and multi-robot coverage path planning. For example, in time-critical scenarios, a group of unmanned aerial vehicles can be engaged in

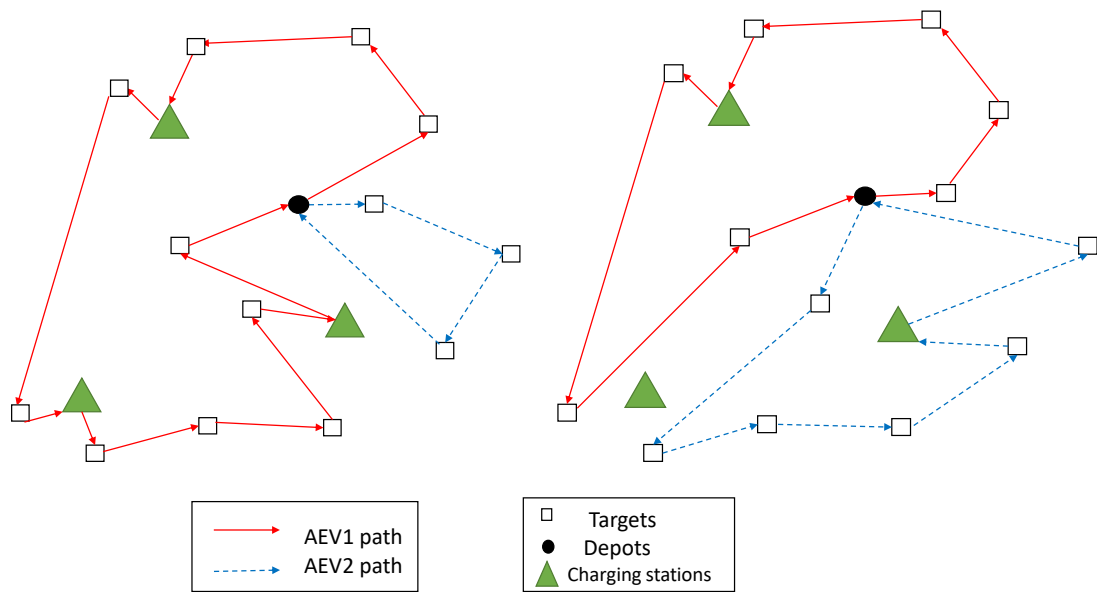


Figure 15: A feasible tour for two AEVs which visit all the targets while visiting some charging stations for recharging: AEVRP using min-sum (left) vs AEVRP using min-max (right).

large scale surveillance operations to minimize the maximum time needed to visit particular targets. In the energy-efficient multi-robot coverage path planning, the goal is to obtain an optimal path considering all targets within the area of interest, and avoiding sub-areas with unique characteristics such as obstacles, not-flight zones in the presence of recharging points [49]. Additionally, the min-max provides a fair and equitable utilization for the resources, and maximum wait time of the targets will be less compared to a solution from min-sum. Especially, this is very vital if the AEVs are used to transport people, and the targets are considered as stops in the AEVs' routes.

To the best of our knowledge, this study is the first attempt to formulate and solve the min-max version of AEVRP. We propose an efficient mixed-integer programming formulation that is adaptable for branch and cut algorithm to obtain optimal solutions for smaller

instances. For the large-scale instances, we developed a Genetic Algorithm-based Heuristic (GAH) with three phases. We then evaluate the performance of the exact and heuristic methods through extensive numerical studies on a variety of benchmark instances. Also, we conducted a data-driven simulation using robot operating system (ROS) to showcase the application of the AEVRP in a multi-robot environment.

The contributions of this study include the following: an efficient MIP formulation for the AEVRP; a GA-based heuristic for large-scale instances and perform extensive computational experiments to quantify the efficacy of the proposed approach; computational experiments for MIP formulation using branch and cut algorithm; a sensitivity analysis to investigate the aspects of solutions from min-sum and min-max AEVRP, and a data-driven simulation study using ROS.

The remainder of this research is organized as follows: Section 3.1 provides a mathematical formulation of the problem along with a subsequent reformulation. Section 6 introduces the solution methodologies where we present exact and heuristic methods to solve small and large-scale instances, respectively. Section 8 presents extensive computational experiments and sensitivity analysis. Finally, Section 8.3 provides concluding remarks.

5.2 Model Formulation

We define T as a set of targets, and \bar{D} as a set of CSs. Define $D = \bar{D} \cup d_0$, be a set of CSs, including a depot d_0 where m AEVs are initially stationed, and each AEV is charged to its battery capacity. The AEVRP is defined on a directed graph with a set of vertices V and a set of edges E as $G = (V, E)$ where $V = T \cap D$. We assume that the graph G does not contain any self-loop. Each edge $(i, j) \in E$ is associated with a distance c_{ij} between

vertices i and j , and f_{ij}^m is the charge consumed by traveling from i to j by an AEV m . The f_{ij}^m is calculated by multiplying the energy consumption rate of AEV m and $c_{i,j}$. It is also assumed that both the distances and the charge costs satisfy the triangle inequality, e.g., $\forall i, j, k \in V, f_{ij}^m + f_{jk}^m \geq f_{ik}^m$. Also, let F_m denote the maximum charging capacity of any AEV m . The objective of the model is to find a route for each AEV starting and ending at the base depot such that: each target is visited at least once by an AEV; no AEV runs out of charge during the trip; and maximum distance traveled by an AEV is minimized.

5.2.1 Notation

- Sets

- T : Set of targets, indexed as $t \in T$.
- \bar{D} : Set of charging stations, indexed as $d \in \bar{D}$.
- D : Set of charging stations and base depot, $D = \bar{D} \cup \{d_0\}$.
- V : Set of all vertices in the graph, including all targets, CSs and base depot,
 $V = T \cup D$.
- E : Set of all edges connecting any two vertices without any self-loop, $(i, j) \in E$
and $i, j \in V$.
- S : Subset of targets and a depot in V , $S \subset V$, $\sigma^+(S) = \{(i, j) \in E : i \in S, j \notin S\}$
- M : Set of AEVs which are initially stationed at base depot d_0 , indexed by
 $m \in M$.

- Model parameters

- c_{ij} : Distance associated with edge $(i, j) \in E$.
 - f_{ij}^m : Amount of charge spent by an AEV $m \in M$ while traversing from i to j with $i, j \in V$.
 - F_m : Battery capacity of AEV m , with $m \in M$.
 - Q : A big number
- Decision variables
 - x_{ij}^m : 1 if the edge (i, j) is traversed by an AEV m , and 0 otherwise;
 - z_{ij}^m : The total battery charge spent by any AEV m since the start from base depot or a CS and reaches the vertex $j \in V$ while the predecessor of j is $i \in V$.
 - y_d^m : 1 if the CS $d \in D$ is visited by any AEV m , and 0 otherwise.

5.2.2 Min-max AEVRP Model

$$\text{Min} \left(\text{Max}_{\forall m \in M} \sum_{(i,j) \in E} c_{ij} x_{ij}^m \right) \quad (5.1)$$

s.t.

$$\sum_{i \in V} x_{di}^m = \sum_{i \in V} x_{id}^m \quad \forall d \in \bar{D}, m \in M, \quad (5.2)$$

$$\sum_{i \in V} x_{di}^m \leq Q y_d^m \quad \forall d \in \bar{D}, m \in M, \quad (5.3)$$

$$\sum_{i \in V} x_{id_0}^m = 1, \quad \forall m \in M, \quad (5.4)$$

$$\sum_{i \in V} x_{d_0 i}^m = 1, \quad \forall m \in M, \quad (5.5)$$

$$\sum_{i \in V} \sum_{m \in M} x_{ij}^m = 1 \quad \forall j \in T, \quad (5.6)$$

$$\sum_{i \in V} \sum_{m \in M} x_{ji}^m = 1 \quad \forall j \in T, \quad (5.7)$$

$$x(\sigma^+(S)) \geq y_d$$

$$\forall d \in S \cap \bar{D}, S \subset V \setminus \{d_0\} : S \cap \bar{D} \neq \emptyset, \quad (5.8)$$

$$\sum_{j \in V} z_{ij}^m - \sum_{j \in V} z_{ji}^m = \sum_{j \in V} f_{ij}^m x_{ij}^m \quad \forall i \in T, m \in M, \quad (5.9)$$

$$z_{ij}^m \leq F_m x_{ij}^m \quad \forall (i, j) \in E, m \in M, \quad (5.10)$$

$$z_{di}^m = f_{di}^m x_{di}^m \quad \forall i \in T, d \in D, m \in M, \quad (5.11)$$

$$x_{ij}^m \in \{0, 1\}, z_{ij}^m \geq 0 \quad \forall (i, j) \in E, m \in M, \quad (5.12)$$

$$y_d^m \in \{0, 1\} \quad \forall d \in \bar{D}, m \in M, \quad (5.13)$$

The objective function (5.1) minimizes the maximum distance traveled by any AEV. Constraints (5.2) and (5.3) impose the in-degree and out-degree of any AEV using a CS d to be equal. Additionally, the constraints (5.3) force the variable y_d^m to be one if CS d is visited. Constraints (5.4) and (5.5) ensure that AEVs start and end their trip from the base depot d_0 . Constraints (5.6) and (5.7) force the in-degree and out-degree of each target to be equal, and each target should be visited by exactly one AEV. Connectivity of any feasible solution is guaranteed by constraints (5.8). Constraints (5.9) introduce the flow variable z_{ij}^m for each edge $(i, j) \in E$ and also removes the sub-tours. Constraints (5.10) and (5.11) ensure that no AEV runs out of charge during its trip. Finally, constraints (5.12) and (5.13) define the restrictions for the decision variables.

Proposition 2. *Relax the binary restrictions on constraints (5.13) and replace them by the following constraints:*

$$x_{id}^m \leq y_d^m \quad \forall i \in T \cup \{d_0\} \quad d \in \bar{D}, m \in M, \quad (5.14)$$

$$0 \leq y_d^m \leq 1 \quad \forall d \in \bar{D}, m \in M. \quad (5.15)$$

Proof. See [98] for the proof. \square

The model is non-linear due to the min-max term in the objective function (5.1). To improve computational efficiency, the model is linearized using the following proposition.

Proposition 3. *Define a non-negative continuous variable w and restate the objective function as follows:*

$$\text{Min } w \quad (5.16)$$

Then, we add the following constraint:

$$w \geq \sum_{(i,j) \in E} c_{ij} x_{ij}^m \quad \forall m \in M. \quad (5.17)$$

Proof. See [83] for the proof. \square

CHAPTER 6 METHODOLOGY AND ALGORITHM DEVELOPMENT

The chapter presents a summary and directions of future research.

6.1 Branch and Cut Algorithm

In this section, we describe the main components of a branch-and-cut algorithm used to optimally solve the formulation presented in the previous section. To solve the formulation developed in section 3.1, off-the-shelf commercial branch-and-cut solvers could be used. The formulation contains constraints (5.8) to guarantee the connectivity of any feasible solution. However, the number of such constraints is exponential, and it may not be computationally efficient to consider all these constraints in advance while using an off-the-shelf solver. To address this issue, we relax the constraints (5.8) from the formulation. Whenever the solver obtains a feasible integer solution, we check if any of the constraints (5.8) are violated by the feasible integer solution. If so, we add the corresponding constraint and continue solving the problem. It has been observed that this process is computationally efficient for a variety of the VRP problems [97, 110]. Now, we describe the details about the algorithm used to find a constraint (5.8) that is violated for a given integer feasible solution to the relaxed problem. For every AEV $m \in M$, a violated constraint (5.8) can be denoted by a subset of vertices $S \subset V \setminus \{d_0\}$ such that $S \cap \bar{D} \neq \emptyset$; and $x(\sigma^+(S)) < y_d^m$ for every $d \in S \cap \bar{D}$. We construct an auxiliary graph $G' = (V', E')$ for any feasible solution where $V' = T \cup d_0 \cup \{d \in \bar{D} : y_d^m = 1\}$, and $E' = \{(i, j) \in E : x_{ij}^m = 1\}$. We then find Strongly Connected Components (SCC) of this graph. Every SCC which does not contain base depot d_0 violates the constraint (5.8). Hence, we add all these cuts for any feasible integer solution until we reach optimality. To implement this algorithm within the branch and cut framework, we use *Callback* feature provided by most of the commercial

solvers like Gurobi [34]. Although the branch-and-cut can find an optimal solution, the AEVRP is an extension of VRP problem and it is NP-hard [25]. Thus, to circumvent computational challenges for large-scale instances, we develop a heuristic method in the next section.

6.2 GA-based Heuristic Method

The genetic algorithm (GA) is a stochastic optimization technique inspired by the process of natural selection, which is widely applied to solve different classes of NP-Hard problems [45, 89, 103]. GA maintains a population of candidates solution through the selective procedure. GA is initialized by a set of solutions called population. Each solution in the population is called chromosome. Chromosomes progress through successive iterations called generations. Throughout each iteration, the chromosomes are evaluated by a fitness function. The fitter chromosomes have higher chances of being selected for GA operations such as mutation and crossover. The GA operations choose some parents and produce some off-springs as the new solutions. The new solutions are then accepted or rejected based on their fitness values as well as the solutions from the previous iterations to keep the population size fixed. The GA may converge to the best solution after a certain number of iterations. To solve the AEVRP using the GA algorithm, we have three major challenges: 1) assigning targets to the AEVs; 2) finding the best route for each AEV; and 3) maintaining feasibility such that each AEV does not run out of fuel. Each of these is complex and difficult to solve. Hence, a naive GA may not perform well for this problem. Therefore, to overcome the complexity, we implement several heuristics to improve the solution further.

The flowchart of GAH for the AEVRP is shown in Figure 16. We describe the procedure

of the GAH as follows: the algorithm starts by computing a modified traveling cost matrix for each AEV to consider the charging limitation of AEVs. Subsequently, a LP relaxation of an assignment problem is solved to assign the targets to the AEVs. Then, an optimal or a sub-optimal TSP tour for the AEVs is determined by the Lin-Kernigan-Helgaun heuristic [40]. In the next step, the feasibility of each route in terms of charge limitation is checked. On every infeasible route, a heuristic is applied to find CSs for recharging and the distance traveled by each AEV is calculated. To provide a pool of high-quality solutions, an iterative Variable Neighborhood Search (VNS) is implemented. The VNS starts with the initial solution obtained in the previous step. Three different insertions are used to improve the current solution. At each iteration, a new solution is generated and compared to the current solution. If the new solution is better than the current solution, it is considered as an incumbent and added to the GA pool. Also, if a new solution is not better but has a cost relatively closer compared to the current solution, it is considered as a potentially good solution and added to the GA pool. This process is repeated until either no improvement is found or the maximum number of iterations is reached. Once the GA pool is filled with high-quality solutions from VNS, the GA parameters such as the iteration number, population size, crossover rate, mutation rate, stopping criteria are initialized. The solutions in the pool represent GA chromosomes, and the fitness value of chromosomes is considered as the maximum distance traveled by any AEV. The chromosomes are sorted based on their fitness value and the ones with the higher fitness values are eliminated based on fixed population size. During the improvement phase, through a roulette wheel selection operation, some chromosomes are selected for the GA operations. The GA operations such as crossover and mutation are performed to generate new solutions (offsprings). The routing

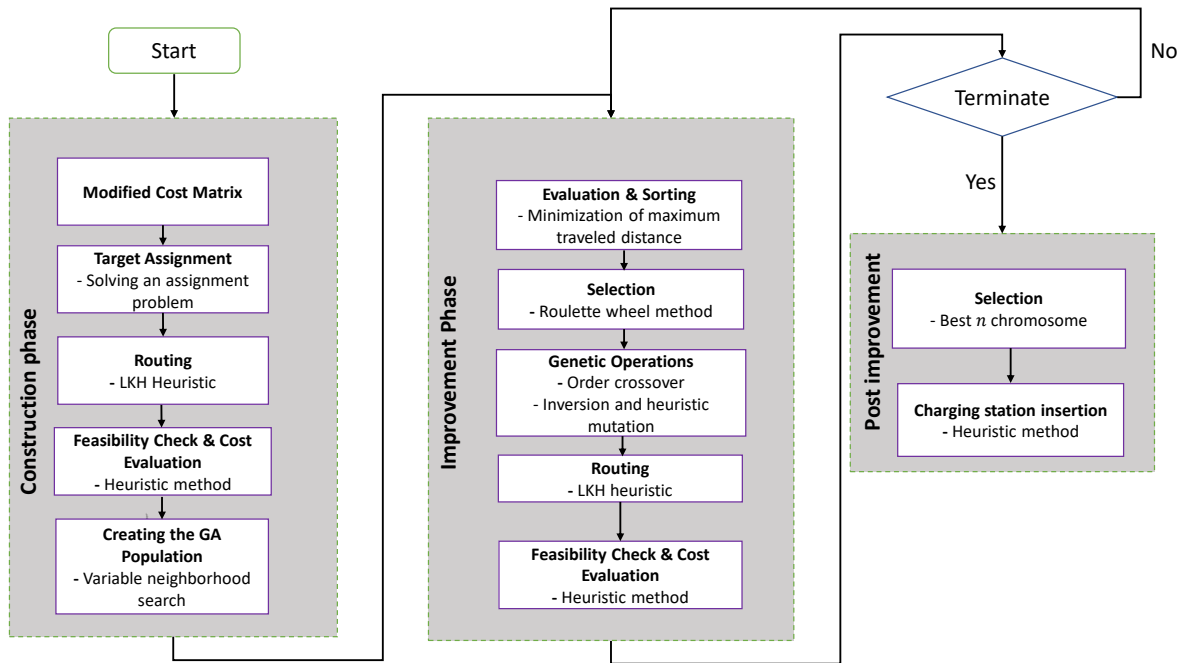


Figure 16: The flowchart of GAH including three main phase : construction, improvement and post improvement

and feasibility check are performed again on the offsprings. The fitness value of the feasible offsprings is measured and compared to other chromosomes. These steps constitute an iteration, and then the roulette wheel selection is applied again to begin the next iteration. The GAH is terminated whenever a stopping criterion is met. In the post improvement, a heuristic is performed on some of the best chromosomes to further improve the solution from the improvement phase. Steps of GAH are explained in the subsequent sections.

6.3 Construction Phase

6.3.1 Path Representation

To encode the solution of the AEVRP problem, we use path representation in a way that targets are listed based on the order in which they are visited. Suppose that there are 10 targets and numbered from t_5 to t_{14} . In order to form a chromosome, we generate a path where targets are randomly placed in each gene of the chromosome. A sample

chromosome of AEVRP problem is as follows:

t_{10}	t_7	t_{11}	t_{12}	t_9	t_5	t_6	t_8	t_{13}	t_{14}
----------	-------	----------	----------	-------	-------	-------	-------	----------	----------

Note that each chromosome contains $|M|$ string, each related to an AEV.

6.3.2 Modified Cost Matrix

In this step, considering the range limitation of AEVs, we compute a new traveling cost based on [50]. The new cost matrix considers the additional charge that an AEV may need to visit the available CSs as it traverses between two targets. The maximum charge remained at the AEV's battery when it visits a target i is denoted as $F - f_{d_i}^{min}$ where $f_{d_i}^{min}$ denotes the amount of fuel an AEV requires to reach a CS with the minimum distance from target i . This ensures that in any feasible tour, an AEV must have an option of recharging at the nearest CS to continue visiting other targets when it reaches a target i . So, we say that an AEV can directly travel from target i to target j if and only if $f_{ij} \leq F - f_{d_i}^{min} - f_{d_j}^{min}$. If the AEV is unable to directly travel from target i to j , we create an auxiliary graph $G^* = (V^*, E^*)$ where $V^* = \bar{D} \cup \{i, j\}$. Any edge that can satisfy the fuel constraint, will be added to the auxiliary graph. So, we add the following three sets of edges to the graph:

$$E^* =: \begin{cases} (i, d) : & \text{if } f_{i,d} \leq F - f_{d_i}^{min}, \forall d \in \bar{D}, \\ \cup(d, j) : & \text{if } f_{d,j} \leq F - f_{d_j}^{min}, \forall d \in \bar{D}, \\ \cup(d_k, d_{k'}) : & \text{if } f_{d_k, d_{k'}} \leq F, \forall d_k, d_{k'} \in \bar{D}. \end{cases}$$

For every AEV, the cost(length) of edges in graph E^* is calculated by finding the shortest path between the any two nodes using Dijkstra Algorithm [24]. The modified cost matrix is created by replacing the new computed costs with old costs in the original cost matrix.

We denote the modified cost matrix as c' .

6.3.3 Target Assignment

To assign targets to the AEVs, we use a LP-based Load Balancing heuristic (LLBH) as suggested in [16] with some modifications. The LLBH assumes that the distance traveled by the AEVs should almost be the same, and designed for multi-depot problems. Hence, in a network where targets are uniformly distributed, AEVs visit nearly the same number of targets. For the sake of compatibility, we perturb the location of AEV in the base depot to create multiple depots. We uniformly place the AEVS on a small circle around the base depot. Given a set of K base depots, indexed by i , with one AEV stationed at each of them, and set of t targets, indexed by j , the LLBH solves the relaxation of the following assignment problem where u_{ij} is 1 if target j is assigned to the depot i , and 0 otherwise. Also, c'_{ij} indicates the modified cost matrix.

$$\text{Min} \sum_{i \in K} \sum_{j \in T} c'_{ij} u_{ij} \quad (6.1)$$

s.t.

$$\sum_{i \in K} u_{ij} = 1 \quad \forall j \in T, \quad (6.2)$$

$$\sum_{j \in T} u_{ij} = \lfloor \frac{|T|}{K} \rfloor \quad \forall i \in K, \quad (6.3)$$

$$u_{ij} \in \{0, 1\} \quad \forall i \in K, j \in T. \quad (6.4)$$

Constraints (6.2) assign targets to the 'K' copies of depots made around the base depot d_0 . Constraints (6.3) determine the number of targets that each AEV should visit. For the cases where $\frac{|T|}{K}$ is fractional, as per [16] we assume that $|T| = pK + q$, with $p, q \in \mathbb{Z}^+$ and

q is residue. The extra q targets are assigned to the AEVs based on a insertion technique which we describe in the next sections. After the initial assignment of targets to AEVs by solving the above assignment problem, the auxiliary depots are removed. Then, we add the base depot (d_0) to the beginning and end of each route. Adding the base depot to the routes would result in a group of strings as follows:

d_0	t_{10}	t_7	t_{11}	d_0	d_0	t_{12}	t_9	d_0	d_0	t_5	t_6	t_8	t_{13}	t_{14}	d_0
-------	----------	-------	----------	-------	-------	----------	-------	-------	-------	-------	-------	-------	----------	----------	-------

Now, we solve a single AEV routing problem for every set of targets assigned to each AEV including the base depot.

6.3.4 Routing

Lin-Kernigan-Helgaun (LKH) heuristic is considered as one of the best algorithms for solving single vehicle routing problem without recharging constraints. After assigning AEVs to targets, the LKH heuristic is used to find the best tour for each AEV.

6.3.5 Feasibility Check

The route found by LKH heuristic for each AEV may be infeasible due to the exclusion of range constraint (5.10). Hence, this step is performed to attain feasibility for the tours. The feasibility procedure is demonstrated using the following example: consider a substring of an AEV including targets 5, 6 and 8 (t_5 , t_6 and t_8). Assume that there are three CSs (d_1 , d_2 and d_3) along this path as shown in Figure 17, and an AEV reaches t_6 , with 20 units of travel distance remaining in the battery. Since the AEV cannot reach the target t_8 due to insufficient charge, recharging is required at one of the available CSs. The algorithm

developed by authors in [134] considers the minimum of $dist(t_6, d_k) \forall k \in \bar{D}$ which is d_2 . However, in this study, we choose the minimum of $dist(t_8, d_k) \forall k \in \bar{D}$ which is d_3 . The advantage of this approach is that the AEV will have more charge to complete the rest of the trip, and also has less necessity for recharging. Consequently, this may lead to shorter distance traveled in overall. However, if the AEV does not have sufficient charge to reach d_3 , then d_2 is selected for recharging. If visiting d_2 is also not possible, then we do a "backward" move and go to the previous edge (t_5, t_6) and travel from t_5 to d_1 for recharging. We call a route is infeasible if one of the following circumstances occurs: 1) backward moves resulted in visiting the base depot; 2) all the available CSs in one edge are visited and yet it is impossible to move to the next edge; or 3) exiting from a target is impossible due to insufficient charge, and also the closet CS to the target is visited in the previous edge. The feasibility check procedure is given in Algorithm 3. In this algorithm, we define AEVRPP route as a sequence of targets $(t_0, t_1, t_2, \dots, t_{i-1}, t_i, t_{i+1}, \dots, t_{n+1})$ where the t_0 and t_{n+1} represent the depot. We also define $m_{(t_i, t_{i+1})} = 1$ if the edge $(i, i + 1)$ is traversed by an AEV. We consider $c_{d_i}^{min}$ for the CS d which has the minimum distance to the target i . We define $d_{(v_i, v_{i+1})}^k = 1$ if the eligible CS $d^k, \forall k \in \bar{D}$ is visited by the AEV, and location of the AEV is referred as loc . The feasibility procedure is applied on every route to create a feasible solution along with its corresponding cost for the min-max AEVRP problem. This solution x is considered as the incumbent solution $x_{inc} = x$.

6.3.6 Variable Neighborhood Search (VNS)

To create a pool of high-quality solutions for the GA, we implement a VNS-based algorithm. The VNS framework is based on a systematic change of neighborhood integrated with a local search [36]. A local search starts with an initial solution x and look for a

Algorithm 3 : Feasibility Check

Initialization:

Set: $Status \leftarrow \text{Feasible}$, $BM \leftarrow \text{False}$, $FM \leftarrow \text{True}$,
 $h \leftarrow \text{Battery Capacity}$, $i \leftarrow 0$, $loc \leftarrow t_i$

while any $m_{(t_i, t_{i+1})} \neq 1$:

if $Status = \text{Infeasible}$

break

else do FM

$i++$

while $FM = \text{False}$

do BM

Forward Move (FM):

if: $z > f_{(t_i, t_{i+1})}$:

$loc \leftarrow t_{i+1}$, $z- = f_{(t_i, t_{i+1})}$, $m_{(t_i, t_{i+1})} = 1$

return True

elif: $z > f_{(t_i, c_{d_{i+1}}^{min})}$ and $F > f_{(c_{d_{i+1}}^{min}, t_{i+1})}$ and

$m_{(t_i, t_{i+1})} \neq 1$:

$loc \leftarrow t_{i+1}$, $z = F - f_{(c_{d_{i+1}}^{min}, j)}$, $m_{(t_i, t_{i+1})} = 1$,

$d_{(t_i, t_{i+1})}^k = 1$

return True

elif: $z > f_{(t_i, c_{d_i}^{min})}$ and $F > f_{(t_i, c_{d_i}^{min})}$ and $m_{(t_i, t_{i+1})} \neq 1$:

$loc \leftarrow t_{i+1}$, $z = F - f_{(c_{d_i}^{min}, t_{i+1})}$, $m_{(t_i, t_{i+1})} = 1$,

$d_{(t_i, t_{i+1})}^k = 1$

return True

else: False

Backward Move:

if: $loc = t_0$ or $d_{(t_i, t_{i+1})}^k = 1, \forall k \in \bar{D}$

$Status \leftarrow \text{Infeasible}$

Stop

else:

$loc \leftarrow t_{i-1}$, $z+ = f_{(t_{i-1}, t_i)}$, $m_{(t_{i-1}, t_i)} = 0$,

$d_{(t_{i-1}, t_i)}^k = 0$,

do FM

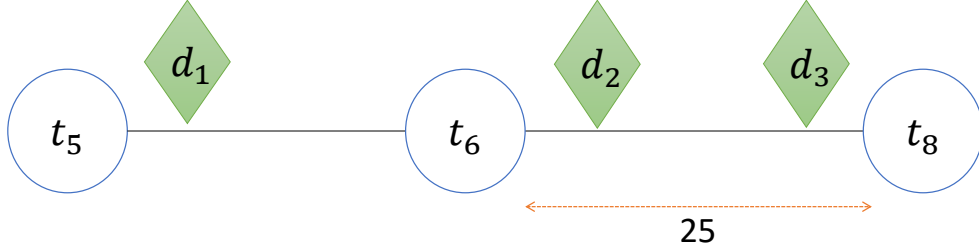


Figure 17: An example for charging station selection approach

descent direction from x within a neighborhood $N(x)$. The algorithm stops if there is no further improvement. In this problem, we consider four neighborhoods including one, two, and three insertions which we refer as $N_1(x)$, $N_2(x)$ and $N_3(x)$, respectively, and swap operation as $N_4(x)$. In the insertion procedure, we try to improve the initial solution by removing the target from the longest route (in terms of distance) and insert it to another route. Considering the initial solution obtained in the previous section, we generate a new solution x' from $N_1(x)$. In order to select the target for removal, we calculate the amount of saving by removing each target from the longest route. The saving of targets i (t_i) is calculated as follows:

$$\text{dist}(t_j, t_i) + \text{dist}(t_i, t_k) - \text{dist}(t_j, t_k), \quad (6.5)$$

where t_j and t_k are the preceding and succeeding targets in the same route.

We select the target with the highest saving from the longest route. In the next step, we

determine the route on which we want to insert the target. We compute the insertion cost of the selected target in all other routes and select the route with the minimum insertion cost. The insertion cost of each route is calculated based on the equation (6.5) where t_i is inserted between any two consecutive targets t_j and t_k from the route. Then, we apply the LKH and feasibility check on the new solution. If x' is better than x_{inc} then $x_{inc} = x'$, and the similar procedure continues with a new solution from $N_1(x')$. Otherwise, we select the next target with the highest saving. If no improvement occurs with removing any target from the longest route and inserting into other route, we create a new solution from $N_2(x)$ as x'' . If x'' is better than x , then $x_{inc} = x''$ and we return to the 1-insertion neighborhood, and select a new solution from $N_1(x'')$. Otherwise, we proceed by selecting another targets. If no improvement found in the 2-insertion neighborhood, we activate the $N_3(x)$ and proceed as before. We also use the swap operation $N_4(x)$ by randomly selecting a target from the longest route and exchanging it with any target from the route with the lowest insertion cost to further improve the solution. The swap operation activated between any insertion operations (e.g. between $N_1(x)$ and $N_2(x)$) and repeated for predetermined number of iterations (l_{max}). We terminate the search if no improvement occurs in the 3-insertion neighborhood or maximum number of iteration is reached. It should be noted that the saving and insertion cost calculations are based on the modified cost matrix. The VNS algorithm procedure is summarized in the Algorithm 4.

During the search process, every new solution is added to the GA pool. Inspired from simulated annealing, 'possibly' good solutions are stored. A solution is potentially good if $\frac{f(x') - f(x_{inc})}{f(x_{inc})} \leq r$, where $f(x')$ and $f(x_{inc})$ are the cost of the potentially good solution and the incumbent solution, and r is a relatively small parameter ($r = 0.15$ in our im-

Algorithm 4 : Variable Neighborhood Search

Initialization:

$k, l \leftarrow 0, x_{inc} \leftarrow x^0, N_1 \leftarrow \text{True}, N_2 \leftarrow \text{False},$
 $N_3 \leftarrow \text{False}$

while $k \leq k_{max}$:**while** $N_1 = \text{True}$

$k \leftarrow k + 1$

select $x' \in N_1(x_{inc})$

if $f(x') \leq f(x_{inc})$:

$x_{inc} = x'$

if $\nexists x \in \{x' | x' \in N_1(x'), f(x') \leq f(x_{inc})\}$:

$N_1 \leftarrow \text{False}, N_2 \leftarrow \text{True}$

while $l < l_{max}$

do swap

while $N_2 = \text{True}$

$k \leftarrow k + 1$

select $x'' \in N_2(x_{inc})$

if $f(x'') \leq f(x_{inc})$:

$x_{inc} = x''$

$N_1 \leftarrow \text{True}, N_2 \leftarrow \text{False},$

if $\nexists x \in \{x'' | x'' \in N_2(x''), f(x'') \leq f(x_{inc})\}$:

$N_2 \leftarrow \text{False}, N_3 \leftarrow \text{True}$

while $l < l_{max}$

do swap

while $N_3 = \text{True}$

$k \leftarrow k + 1$

select $x''' \in N_2(x_{inc})$

select $x''' \in N_2(x_{inc}), k \leftarrow k + 1$

if $f(x''') \leq f(x_{inc})$:

$x_{inc} = x'''$

$N_1 \leftarrow \text{True}, N_3 \leftarrow \text{False},$

if $\nexists x \in \{x''' | x''' \in N_2(x'''), f(x''') \leq f(x_{inc})\}$

Terminate

plementation). In the next step, we apply the GA operations on the pool of high quality solutions.

6.4 Improvement Phase

6.4.1 Chromosome Selection

Chromosome selection significantly affects GA's convergence. The roulette wheel selection was first introduced by [22] to select the chromosomes for GA operations. Each section of the roulette wheel is assigned to a chromosome based on the magnitude of its fitness value. The fitness value of each chromosome is calculated as: $f_c = \min\{\max_{\forall m \in M}\{DT_m\}\}$ where DT_m is the total distance traveled by AEV m . The fitness values of the chromosomes determine their chance of being selected. We summarize the selection procedure in Algorithm 5. In the algorithm, the selection and cumulative probabilities of a chromosome c are referred as p_c and g_c , respectively, and the population size as $psize$.

Algorithm 5 : Selection

Step 1: Calculate the total fitness F :

$$F = \sum_{c=1}^{psize} f_c$$

Step 2: Calculate the selection probability for each chromosome:

$$p_c = \frac{F - f_c}{F \times (psize - 1)}$$

Step 3: Calculate the cumulative probability for each chromosome:

$$g_c = \sum_{i=1}^c p_j \quad c = 1, 2, \dots, psize.$$

Step 4: Select the chromosome c if :

$$g_{c-1} < r \leq g_c$$

where r is a random number in range (0,1].

6.4.2 Crossover

We apply order crossover introduced in [33]. In this approach, two children are generated in each iteration. We summarize the order crossover procedure with an example demonstrated Figure 18 as follows: 1) a sub-string is randomly selected from a parent, 2) Empty offsprings are created, and the sub-string is placed into the corresponding positions in the offsprings, 3) starting from the end-point of the sub-string of parent 1, the sequence of the genes from parent 2 is taken (9, 11, 6, 10, 5, 8, 7) and the genes that already exist in the first sub-string are removed (11, 5, 8, 7), 4) the remaining genes are inserted into the empty positions of the offspring starting from the sub-string end-point, 5) a new offspring is created by exchanging the genes between two parents.

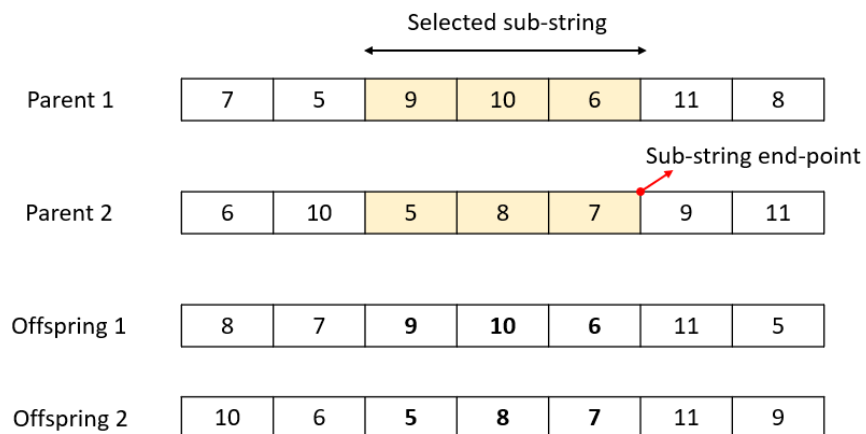


Figure 18: The order crossover operation

6.4.3 Mutation

The mutation operator is a genetic operator that helps to diversify the population. Mutation reorders some of the gene values in a chromosome from their existing state. We apply heuristic and inversion mutation proposed by [33]. The heuristic mutation is a

neighborhood method to generate better offsprings. The chromosomes which are generated from exchanging genes of some parents are considered as the neighborhood. The best chromosome is selected as the offspring. The procedure of the heuristic mutation operation is as follows: 1) three genes are selected from a parent randomly; 2) all the possible combination of the selected genes are generated; 3) the best chromosome is considered as the offspring. The inversion mutation is used to bring diversity into the population instead of increasing the quality. In the inversion mutation, a sub-string of a parent chromosome is selected and turned over to produce an offspring.

6.4.4 Post Improvement

The GA algorithm returns the best set of chromosomes after any of the predefined stopping criteria is met. In the feasibility heuristic, an insertion of CS is performed whenever a recharging is required. A route r for an AEV is defined as a sequence of targets and CSs $(d_0, t_i, t_j, d_n, \dots, t_l, d_m, \dots, d_0)$ where d_0 denotes the base depot and $i, j, l \in V$ and $m, n \in \bar{D}$. In some instances, it is possible to obtain better fitness value by changing the position of the CSs in chromosomes. To further enhance the quality of the GA solution, we propose a heuristic which is described by an example as follows: suppose that there are three CSs (d_1, d_2 , and d_3), and the following string is a feasible path for an AEV (the visited CSs are colored with red):

d_0	t_8	t_{11}	d_3	t_9	t_5	d_2	d_0
-------	-------	----------	-------	-------	-------	-------	-------

Here we define the “sub-string” as a sequence of visits where the last node is a CS. We select the first sub-string and delete the CS from the sub-string. We then insert all the eligible CSs among the targets to generate new sub-routes. A CS is considered eligible if

the AEV starting from a target can reach that CS without visiting other CSs and also reach the next target from the CS after recharging. New sub-routes are checked for feasibility using the 'feasibility check' procedure describe in the earlier section. The total distance traveled and the AEV's remaining battery charge are stored for each feasible route. This considerably decreases the computational effort. Table 7 shows all the new sub-routes generated by CS insertion, where the feasible sub-routes are highlighted. In the next

d_0	d_1	t_8	t_{11}	t_9
d_0	t_8	d_1	t_{11}	t_9
d_0	t_8	t_{11}	d_1	t_9
d_0	d_2	t_8	t_{11}	t_9
d_0	t_8	d_2	t_{11}	t_9
d_0	d_3	t_8	t_{11}	t_9
d_0	t_8	t_{11}	d_3	t_9

Table 7: All the sub-routes generated in the first step of CS insertion heuristic

step, we delete the infeasible sub-routes and add the second sub-string. We repeat the CS insertion procedure for the second sub-string and check the feasibility of the new sub-routes using the information stored in the previous step. The final possible routes are shown in Tabel 7. When we visit the base depot as the last node in a route then the feasible route with the lowest distance is considered as the AEV's total traveled distance. For the cases where the AEVs have to visit two consecutive CSs, we fix the second CS and proceed as before. Once we get the feasible sub-routes, starting from the first CS position, we insert eligible charging stations between the targets and proceed as before. It should

d_0	d_1	t_8	t_{11}	t_9	d_1	t_5	d_0
d_0	t_8	t_{11}	d_1	t_9	t_5	d_1	d_0
d_0	d_3	t_8	t_{11}	t_9	d_2	t_5	d_0
d_0	t_8	t_{11}	d_3	t_9	t_5	d_2	d_0
d_0	t_8	t_{11}	d_3	t_9	d_3	t_5	d_0
d_0	t_8	t_{11}	d_3	t_9	t_5	d_3	d_0

Table 8: Final feasible routes resulted from CS insertion in the post improvement heuristic

be noted that since the heuristic does not change the order of the targets, the chromosome remains the same. So, we use this heuristic only on final n best chromosomes returned by GA algorithm, where n is a predefined user parameter.

CHAPTER 8 COMPUTATIONAL EXPERIMENTS AND CONCLUSION

In this section, we compare the computational performance of the branch-and-cut algorithm and GAH. Both methods were implemented in Python 3.7, and the mixed-integer linear problems were solved using THE branch-and-cut framework and the solver callback functionality of Gurobi 9.0. The computational experiments were performed on a computer with an Intel [®] Xeon [®] CPU E5-2640, 2.60 GHz, and 80GB RAM.

8.1 Instance Generation

For the computational experiments, we selected three data sets (A, B, and P) of the capacitated vehicle routing problem developed by Augerat et al. [8]. We then modified them to adapt for AEVRP by randomly adding CSs. We also generated a random data set to maintain the diversity in our experiments. The details of the data sets are as follows:

- **Random instances:** Random instances were generated in a square grid of size [100,100].

The base depot is considered to be at [50,50]. Also, the number of CSs was set to 5, and the locations of the depot as well as the charging stations were fixed a prior for all the random test instances. The number of targets varies from 10 to 50 in steps of five, while their locations were uniformly distributed in the square grid. For each of the generated instances, the number of AEVs in the base depot is varied from 2 to 8. The battery capacity of AEVs was set to 100, and the Energy Consumption Rate is considered to be 0.8.

- **Augerat et.al instances:** The data sets reported in the study by Augerat et al. [8] are developed for capacitated vehicle routing problems. These instances include three sets which have differences in terms of the distribution of the targets, number

Table 9: The characteristic of the large-scale instances for different data sets

Sets	Target range	Vehicles range	Consumption rate range	Battery Capacity range
A	[31,60]	[5,9]	[0.81,0.99]	100
B	[30,60]	[4,9]	[0.82,1]	100
P	[21,59]	[5,15]	[0.88,0.99]	[70,170]
Random	[20,50]	[4,10]	[0.8,0.8]	100

of targets, vehicle's capacity, demand/capacity tightness, and number of vehicles.

To make the instances compatible to AEVRP, we added five CSs. The coordination of CSs are similar for all instances within each set. Also, the capacity of vehicles is considered as the charging capacity of AEVs and capacity tightness as the fuel consumption rate in our problem. We use the same base depot in the instances.

Figure 19 shows the four different data sets used in AEVRP.

8.1.1 Parameter Setting

For GAH, we set the GA parameters as follows: population size is 100; crossover rate is 0.4; and mutation rate is 0.2. A stopping criterion is chosen based on the trade-off between solution quality and run-time. Based on experiment trails, we chose the stopping criterion as 45 non-improving iterations, and number of best chromosomes for the post improvement phase as ten ($n = 10$). Also, for the branch and cut algorithm, we set a 2-hour time limit for all instances.

8.1.2 Benchmark Instances

To create benchmark instances, we selected a subset of targets, the first 10 and 15 targets with 2 and 3 AEVs from instances within each set, respectively. We solve the benchmark instances with GAH and compare the obtained results to the optimal or near-optimal solution by branch and cut algorithm and Gurobi described in section. 6.1 solved b. Figure 20 represents the differences in the objective function between GAH and B&C(Gurobi) for

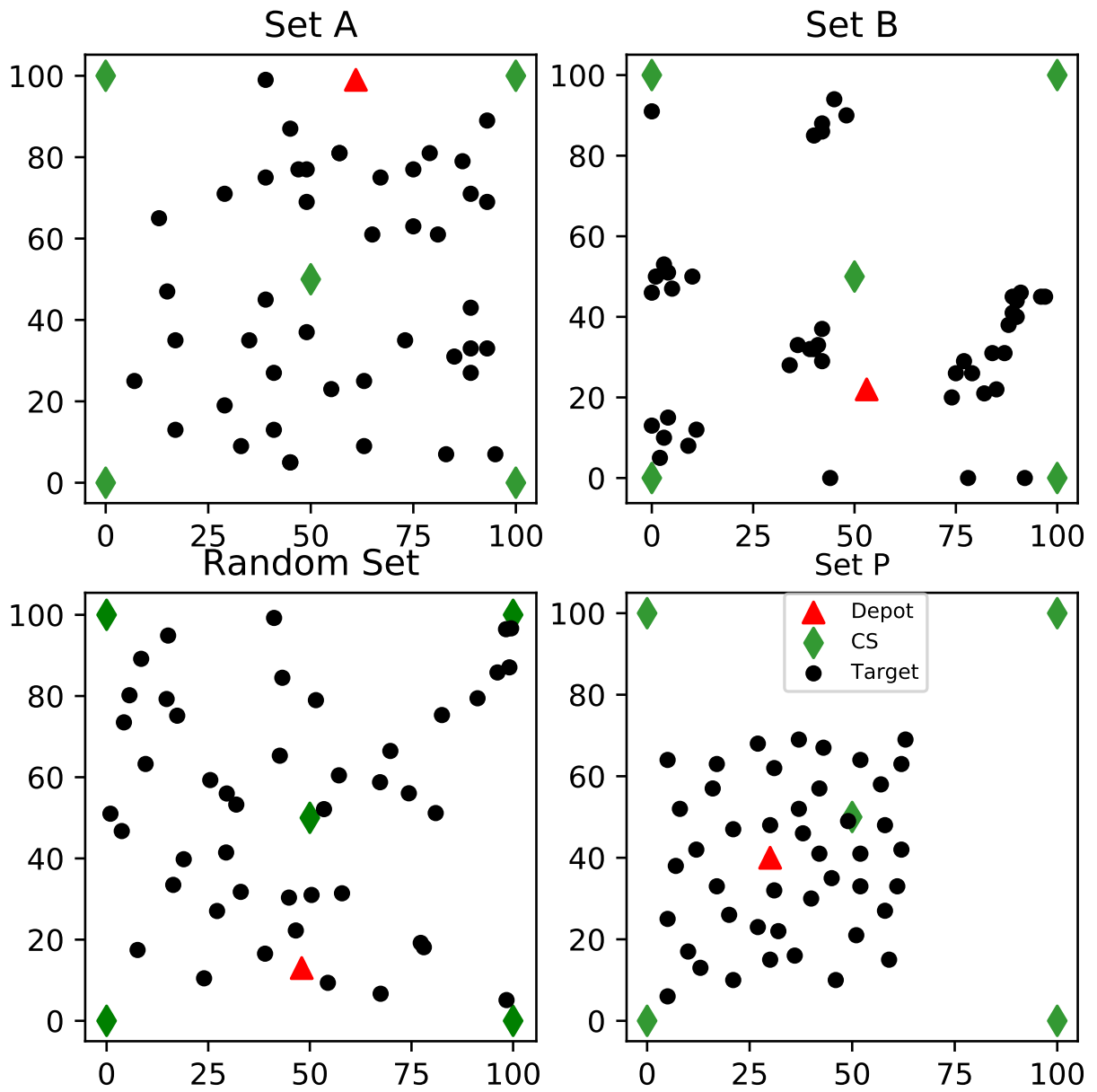


Figure 19: Four different data sets generated based on the study in [8]

the instances with 15 targets. The difference in percentage is calculated as $\frac{B\&C(O)-GAH(O)}{B\&C(O)}$, where $GAH(O)$ and $B\&C(O)$ are objective function values from GAH and B&C, respectively. In total, we solved 71 10-target and 71 15-target benchmark instances. For all the 10-target instances, the B&C algorithm was able to reach solutions within 1% of optimality gap. For many of the 15-target instances from sets A, B, and Random, the B&C algorithm was not able to find the optimal solution within the stipulated time limit. However, the B&C found the optimal solution for most of the 15-target instances from set P. For all the completed runs using B&C; the GAH reached the optimal solution or near-optimal solution with less than 2.5% gap as it is shown in Figure 20. For the instances where B&C was not able to reach optimality, the GAH could find a solution closer or better compared to the upper bound provided by B&C. In terms of run-time, for most of the 10-target instances, the B&C outperformed the GAH with a small margin. However, the GAH outperformed the B&C with a much better run-time. The run-time difference(%) between the two algorithms is provided in Figure 20. The characteristics of the instances and the performance of algorithms are provided in APPENDIX B. Table (11) compares the branch and cut algorithm with the GA-based heuristic for the random benchmark instances. The columns 2 to 5 show the number of targets, number of AEVs, battery capacity (F), and energy consumption rate (α), respectively. The next four columns specify the performance of branch and cut algorithm with 'Obj,' 'Time(s),' 'Gap(%)' and 'Cuts(#)' indicating the objective function, run-time (seconds), the gap percentage, and the total number of connectivity cuts within the stipulated time limit, respectively. The last three columns indicate the performance of GAH algorithm with 'Obj,' 'Time(s)', and 'PI(%)' representing the objective function, run-time (seconds) and the post improvement percentage, respectively.

The PI(%) indicates the improvement obtained by using CS insertion heuristic comparing to the the best results of the GA algorithm ($\frac{GA-Heuristic}{GA} \times 100$). Similarly, tables (12),(13), and (14) compare the two methods over the Augerat instances.

The results from the benchmark instances indicate that GAH approach is capable of providing highly efficient routes for AEVs.

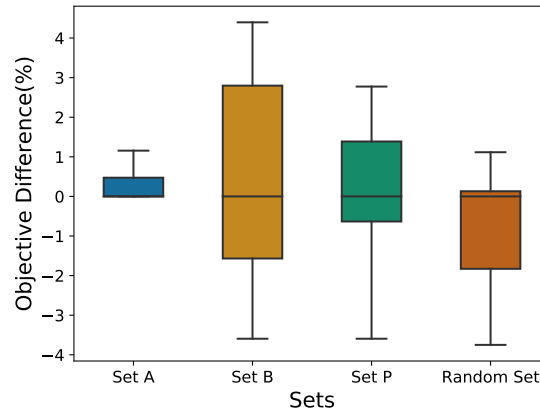


Figure 20: The performance of the GAH compared to the B&C procedure for benchmark instances with 15 targets

8.1.3 Large-scale Instances

To demonstrate the performance of GAH on large scale problem sets, we considered 82 instances with the number of targets and AEVS up to 60 and 15, respectively. Among these instances, 18 instances are from set A, and 17, 12 and 35 instances are from sets B, P, and Random. Similar to the benchmark instances, the number of CSs is five. In 32 instances, B&C procedure was not able to find any feasible solution whereas the GAH was capable of providing a feasible solution for all instances in just a few seconds. For set A, B&C procedure found a feasible solution for six instances with an average gap of 63.7%. Similarly, for sets B, P and Random, B&C procedure found a feasible solution for 5, 10 and 20 instances with an average gap of 51.3%, 35.3%, and 61.1%, respectively.

Table 10: Comparison of the performances of GAH and B&C procedure for large-scale instances

Sets	# of Instances	# of Inf(B&C)	# of Inf(GAH)	AG-B&C(%)	ART-GAH(s)	AOD(%)
A	18	9	0	63.7	290	22.1
B	17	12	0	51.3	246	16.8
P	12	2	0	35.3	128	18.2
Random	35	5	0	61.1	220	24

For all the experiments using large-scale instances, GAH outperformed B&C procedure in terms of computational time and the quality of the solution. Table 10 represents the comparison between the B&C procedure solved by Gurobi and GAH for each set. Column ‘# of Instances’ indicates the total number of instances. The columns ‘# of Inf(B&C)’ and ‘# of Inf(GAH)’ indicate the number of instances in which the B&C procedure and GAH could not find any feasible solution in the stipulated time limit. The next column ‘AG-B&C(%)’ specifies the average gap percentage obtained by B&C procedure, and the average run-time in seconds by GAH is represented by the column ‘ART-GAH(s).’ The last column ‘AOD(%)’ is the average objective difference percentage between B&C procedure and GAH.

8.2 Sensitivity Analysis

8.2.1 Min-max Vs Min-sum

To provide managerial insights for using different objective functions for the AEVRP, we construct an experiment where we compare the solutions of min-max and min-sum AEVRP. We selected an instance from set P with 20 targets and two AEVs. The optimal route for each AEV and the distribution of targets are depicted in Figure 21. In the min-sum version, the AEV 1 traveled 20 units and visited only one target, and did not stop at any CS whereas AEV 2 traveled 178.6 units and visited 19 targets, and visited a CS once. On the other hand, in the min-max version, the AEV 1 traveled 112.7 units, visited eight targets, whereas AEV 2 traveled 112.4 units and visited 12 targets, and none of them

used any CS during their trips. The total distance traveled in min-sum AEVRP and min-max is 198.6 and 225.1 units, respectively. This results from this instance indicate that with a reasonable sacrifice in the total distance, one can greatly decrease the travel time to visit some of the targets. This is an important factor in the context of humanitarian relief where delivering aid supplies to the victims is the first priority or in the on-demand mobility (car-sharing and ride-sharing [100, 99]) when the transportation companies aim at minimizing the customers' wait times in the network. Another aspect is the fair workload among the AEVs in the min-max compared to the min-sum objective. The unfair workload could result in heterogeneous charging/discharging among the AEVs. This may lead to significant battery aging or degradation [64] which can increase the maintenance cost for the ownership of AEVs.

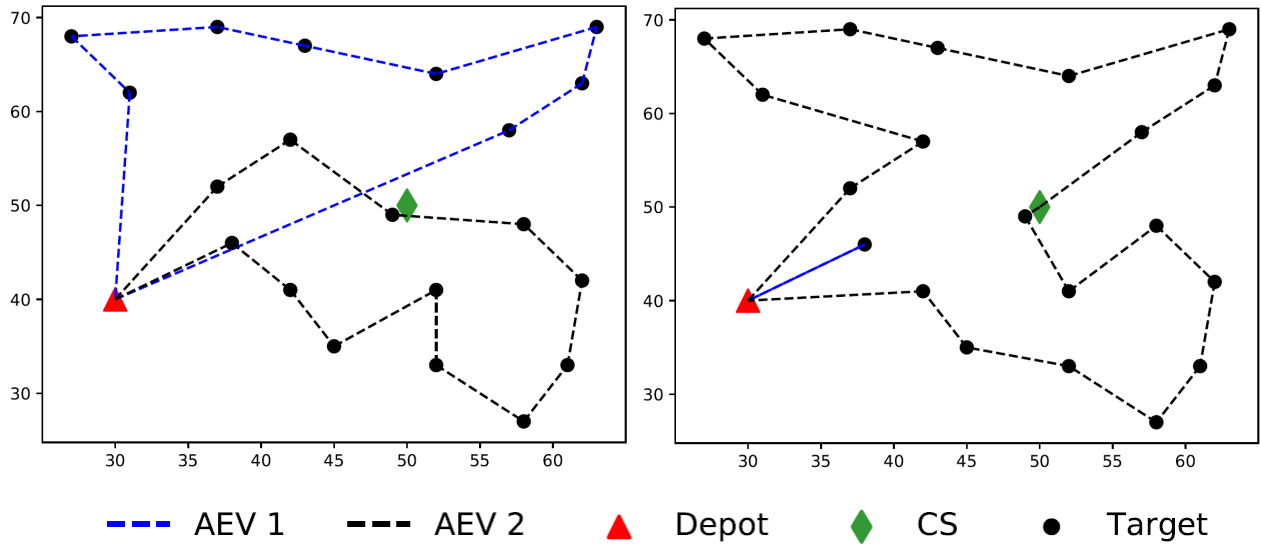


Figure 21: The AEV routes in the AEVRP in the Min-max (left) vs Min-sum (right) versions

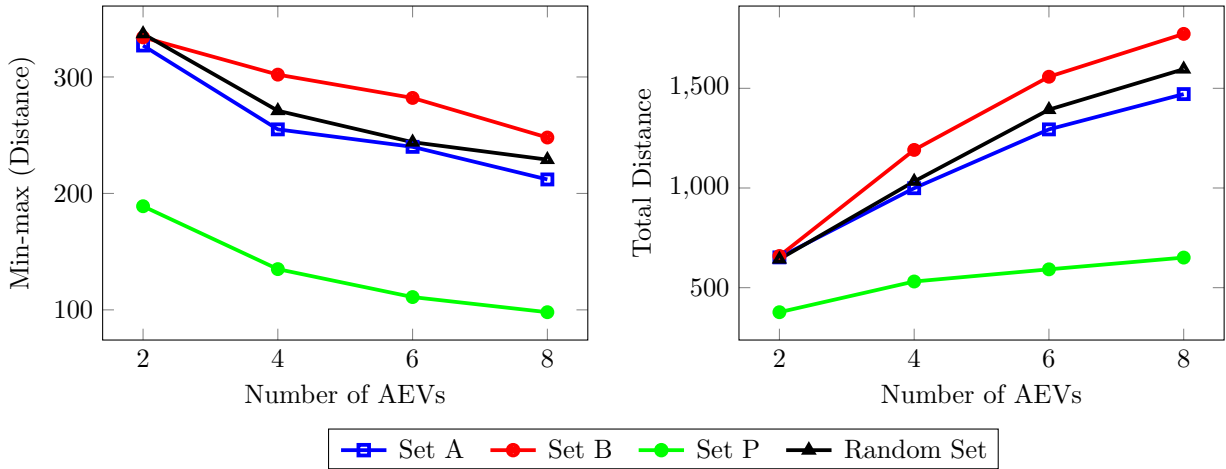


Figure 22: Effect of increase in the number of AEVs on the min-max and the total distance traveled by the AEVs

8.2.2 Effect of the Number of AEVs

We analyze the effect of increase in the number of AEVs on the objective function of min-max AEVRP as well as the total distance traveled by all the AEVs. Instances from each of the four data sets are selected. As shown in Figure 22, it can be observed that when there is an increase in the number of AEVs, the maximum distance traveled by the AEVs decreases. However, the total distance traveled by all the AEVs increases. The instance from set B has the highest increase in the total distance. This can be due to the cluster-like distribution of the targets. When the number of AEVs surpasses the number of clusters, each cluster is assigned to more than one AEV which can increase the total distance. Another factor that may significantly affect the total distance is the position of the depot. In the cases where the depot is far from the targets, dispatching multiple AEVs could result in a longer total distance. Since the targets are closer to each other in set P, an increase in the number of AEVs would not result in a notable decrease or increase in the

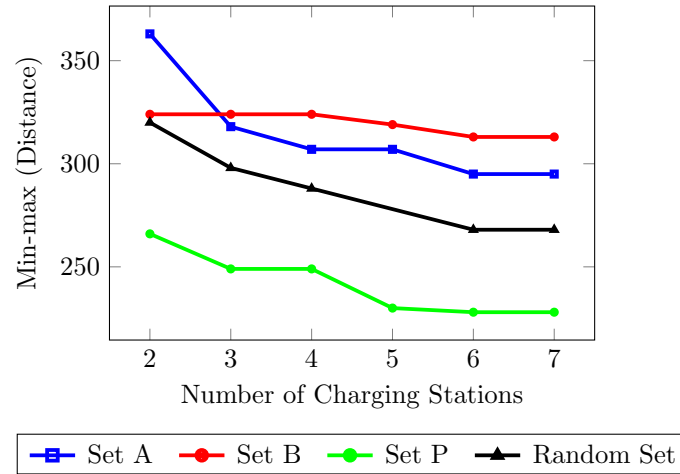


Figure 23: Effect of increase in the number of charging stations on sets A,B,P, and Random min-max or total distance, respectively. In conclusion, decision makers should evaluate the trade-off between the maximum and total distance due to the distribution of the targets and depot.

8.2.3 Effect of the Number of Charging Stations

Another perspective is the impact of increase in the number of CSs on the traveled distance by the AEVs due to min-max objective function. We chose an instance from each of the four data sets, and for each instance, we considered 2 to 7 randomly placed CSs. Figure 23 shows the effect of number of CS on min-max AEVRP for different instances. An increase in the number of charging instances has a lower impact on sets P and B instances where the targets are condensed in a smaller area. Due to the scattered distribution of the targets in the random set and set A, we observe a rapid decrease in the maximum distance as the number of charging stations decreases.

8.2.4 Data-driven Simulation

We performed a data-driven simulation study in rviz [41] 3D-simulation environment for ROS [85] to showcase the application of AEVRP in the robotic operating systems (ROS). We used Turtlebot [53] in the turtlebot_stage package environment as shown in Figure 24. The black oval indicates the base depot where the Turtlebots are stationed. The red rectangles indicate targets, and the blue circles represent the charging locations. The highlighted black lines are walls (obstacles) that prevent Turtlebots to move from one target to another directly. The navigation stack of ROS computes the distance between any pair of targets/depots in the environment. However, it is not possible to use the distance matrix in the AEVRP model since it does not satisfy the triangle inequality. Hence, to preserve the triangle inequality, we convert the distance between each pair of nodes calculated by ROS denoted as f'_{ij} to f_{ij} using Dijkstra algorithm. The Dijkstra algorithm creates a mapping between f'_{ij} to f_{ij} by calculating the shortest path between nodes. We use the new distance matrix as cost to the AEVRP problem, and conducted experiments with four different instances. In each instance, there are two Turtlebots, nine targets, and five charging locations. The experiments performed using ROS Kinetic Kame [86] using a Ubuntu 16.04 (Xenial) release and the ROS publishers were developed using Python programming language. Figure 25 shows the traveled distance by each turtlebot for min-max and min-sum AEVRP. In the instances one and two, observe the total distance traveled by turtlebots are same, however, a significant difference between the traveled distance for each turtlebots in the min-max versus min-sum. In instances 3 and 4, we notice a slight increase in the total traveled distance in min-max but considerable improvement in the

workload balancing between the two turtlebots. In summary, on average, we observed 2% increase in the total traveled distance by the turtlebots using the min-max, however 95% improvement in balancing the traveled distance between the turtlebots comparing to the min-sum AEVRP.

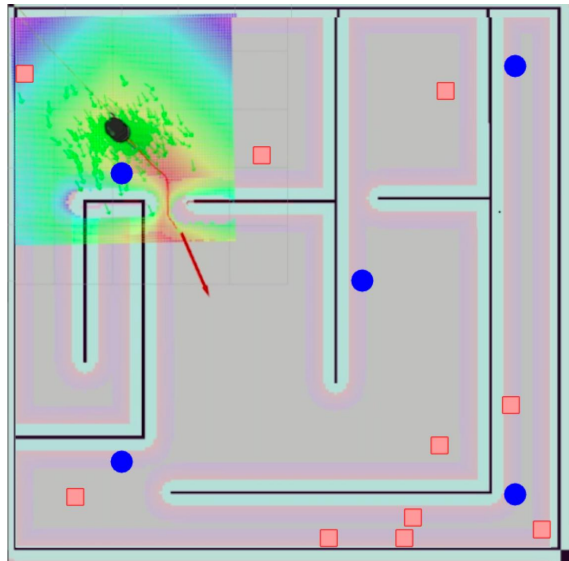


Figure 24: Rviz navigation environment illustrated using Turtlebot package

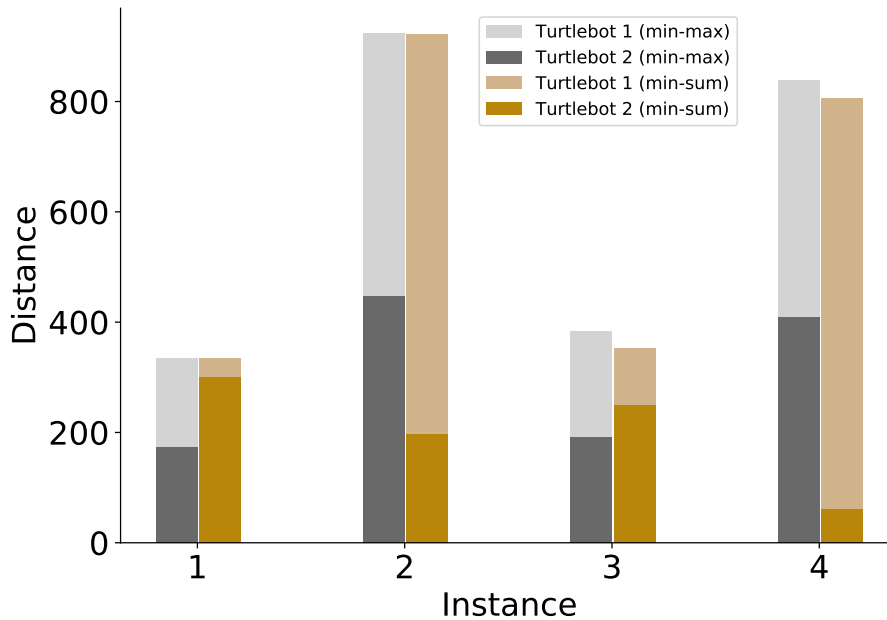


Figure 25: Comparison among four different instances for distance, total travel, and workload balance among turtlebots using min-max and min-sum approaches.

8.3 Conclusion

In this research, we consider a routing problem for a fleet of autonomous electric vehicles in the presence of charging stations with an objective of minimizing the maximum distance traveled by any autonomous electric vehicle (AEV). The goal is to find an efficient tour for each AEV while no AEV runs out of fuel, and all the targets are visited. We proposed an efficient mixed-integer programming formulation and a genetic algorithm based heuristic (GAH) to solve small and large-scale instances, respectively. Numerical studies are performed on randomly generated data sets and capacitated vehicle routing problem data sets from literature. The efficacy of the proposed methods are benchmarked using extensive computational experiments. The results indicate that GAH was able to find so-

lutions within 1% of optimality gap for the 10-target, and equal or better solutions in the 15-target benchmark instances. Also, GA-based heuristic could produce high-quality solutions in large-scale instances whereas the branch-and-cut procedure could not even find a feasible solution for most of the instance within the stipulated time limit. The proposed methods are capable for facilitating routing and charging decisions for a fleet of AEVs employed by logistics and transportation companies. The sensitivity analysis indicates that with a reasonable sacrifice in the total distance, the proposed approach can significantly decrease the travel time to visit some of the targets. In addition, this may decrease the maintenance cost of the AEVs due to fair and equitable distribution of workload among the AEVs fleet. This could potentially decrease the aging or degradation of battery in AEVs. In addition, we conducted a data-driven simulation using the ROS package to investigate the application of the AEVRP in the robot environment.

CHAPTER 9 CONCLUSION AND FUTURE RESEARCH

The chapter presents a summary and directions of future research.

9.1 Two-stage Stochastic Choice Modeling Approach for Electric Vehicle Charging Station Network Design in Urban Communities

We studied the problem of designing an effective network of charging stations for electric vehicles. We integrated behavioral aspects which take account for drivers' preference toward their different charging options into the charging location decisions. Since there are many factors such as EV's dwell time at parking location, battery's state of charge, distance from home, willingness to walk, drivers' arrival patterns, and traffic on weekdays and weekends, that affect the demand of charging station, we formulated the problem as a two-stage stochastic programming model. The framework provides opportunities for a planning agencies and stakeholders to evaluate the trade-off between accessibility, budget, and utilization. We present a case study using the model's results along with various insights, including (among others) a demarcation in the utility function for different charger types and the sensitivity of the optimal network to the budget. The computational results indicate that the optimal layout of charging stations should include a mix of different chargers. Also, we provide pricing insights toward installing different types of chargers. In addition, we investigated the effect of different sources of uncertainty to give more insights into this problem. To overcome the complexity of the problem, we implemented a decomposition method integrated with scenario sampling techniques.

A potential research extension might be to add multi-modal transportation options to the existing framework to consider the interactions between various transportation modes and EV drivers' choices. Another extension could be a study on impact of EV charging station

loads on the electricity distribution network within the current framework. From modelling perspective, other appropriate risk measures can be added to the recourse function, and the subsequent analysis can help us understand the implications of dispersion statistics while choosing optimal solutions. From an algorithm perspective, scalability of the proposed algorithm to large planning regions needs further investigation. Either a meta-heuristic method can be investigated or explore a hierarchical approach. For example, an aggregate analysis can first identify the required density of charging stations for different regions/neighborhoods and detailed charging network planning can then be carried by the proposed algorithm.

9.2 Efficient Algorithms for Autonomous Electric Vehicle Min-max Routing Problem

We studied the routing problem for a fleet of autonomous electric vehicles. The natural synergy between electric and autonomous vehicles possibly can relieve the limitations regarding access to charging infrastructure, time management, and range anxiety. A fleet of Autonomous Electric Vehicles is considered to be employed by transportation and logistic companies to take advantage of AEVs capabilities. However, the limited battery capacities of AEVs and the scarcity of charging stations are the limitations that have to be considered in the route planning to avoid inefficient routing strategies. We introduced the min-max autonomous electric vehicle routing problem where the maximum distance traveled by any AEV is minimized while considering charging stations for recharging. We propose an efficient mixed-integer programming formulation and computational results are presented for small scale instances using branch and cut procedure. For the large-scale instances, we developed a Genetic Algorithm-based heuristic. The algorithm is consists of construc-

tion, improvement, and post-improvement phases. In each phase, we developed and implemented multiple heuristics to generate high-quality solutions. The results showed that the algorithm is capable of producing high-quality solutions with a short amount of time. In addition, we performed a data-driven simulation study using robot operating system (ROS) to showcase the application of the AEVRP for robots.

Future work could include AEVs with freight capacities and the targets with time window. Another extension could be incorporating uncertainties in the battery consumption rate as well as the location of target locations especially for surveillance applications. From the algorithm perspective, use of decomposition algorithms like column generation method can be investigated.

APPENDIX A

Utility Construction

A study by [116] analyzed the driver charging choices through web-based preference survey. The authors used mixed logit model with various predictor variables. The following predictor variables are considered in the utility function calculations:

- **Power (Pw):** 1.9, 6.6 and 50 KW are the powers that we consider for EVSE level 1, level 2, and level 3 respectively.
- **Dwell Time (DT):** Dwell Time is calculated based on arrival and departure of the EV drivers.
- **Energy Consumption (EC):** Based on the current BEVs in the market, we have considered $0.34 \left(\frac{kW-h}{mi} \right)$ for average energy consumption.
- **Max Range (MR):** We considered 75 mile as an average for BEV's maximum range.
- **Current Range (CR):** Current range will be calculated based on the SOC of BEVs when they arrive at charging stations.
- **Price (Pr):** Based on the current charging price at Michigan, $0.3 \left(\frac{\$}{h} \right)$, $1.5 \left(\frac{\$}{h} \right)$, and $21 \left(\frac{\$}{h} \right)$ are considered as the charging prices for EVSE level 1, level 2, and level 3, respectively.
- **Electricity Price at Home (EPH):** $0.14 \left(\frac{\$}{kW-h} \right)$ is considered as an average for electricity price at home in Michigan.
- **Distance to Home (DH):** More than 50 cities and suburban within the 40-mile distance from midtown of Detroit are considered as origins of EV drivers. Based on

SEMCOG data [1], a distribution is obtained based on the origin's population and traffic flow to estimate the distance to the home of EV drivers from parking locations. Also, we added a fixed distance varying from 0 to 40 miles in 10-mile increments for all the drivers. In this way, additional trips by the drivers are accounted before they head back to their original origin.

Also, to capture the interaction between dwell time, charging power, and SOC and other predictor variables the following derived interaction variables are introduced:

I Range Charged at Station (RCS)

This variable determines the amount of charge (miles) an EV can get during the charging period. RCS is calculated by taking the minimum of the amount of charge that an EV can get by using a specific EVSE during driver's dwell time and the difference between the capacity and the current range of the battery.

$$RCS = \min \left(\frac{Pr(kW) \times DT(h)}{EC \left(\frac{kW-h}{mi} \right)}, (MR(mi) - CR(mi)) \right)$$

II Charging Cost (CC)

In order to calculate the charging cost at each station, we assume that an EV driver will only unplug the vehicle at the end of his/her activity. Hence, charging cost can be calculated by the multiplying the charging cost by the dwell time:

$$CC(\$) = Pr\left(\frac{\$}{h}\right) \times DT(h)$$

III Cost at Home (CH)

The 'Cost at Home' variable is calculated based on the amount of Range to be Charge at Home (RCH), electricity price at home and the energy consumption.

$$CH(\$) = RCH(mi) \times EC\left(\frac{kW-h}{mi}\right) \times EPH\left(\frac{\$}{kW-h}\right)$$

Also, RCH depends on whether the driver will charge EV at charging station and the amount of charge that is consumed during the trip to home. If the EV driver decides to not charge the vehicle at charging station then the range to be charged at home will be calculated as follow:

$$RCH(mi) = \min \left(MR(mi), (MR(mi) - CR(mi) + DH(mi)) \right)$$

However, if the EV driver decides to charge the vehicle at charging station then the amount of charge received in the charging station will be considered in calculating the RCH:

$$RCH(mi) = \min \left(MR(mi), (MR(mi) - CR(mi) + DH(mi) - RCS(mi)) \right)$$

IV Remained Range (RR)

Remained Range represents the amount of charge (without charging) that is remained at the end of the driver's trip. So RR can be calculated as the difference between the current range and the distance to home.

$$RR(mi) = \min(CR(mi), (MR(mi) - CR(mi) + DH(mi) - RCS(mi)))$$

V Enough to Next Charging Opportunity (ENCO)

This variable indicates whether the current range is enough to the next charging opportunity. In our model, it is assumed that charging at home is the only next charging opportunity for the EV drivers. So the ENCO is 1 if the current range is more than the distance to home.

APPENDIX B

Table 11: Computational results of benchmark instances; set Random

Instance	Targets(#)	AEV(#)	F	α	B&C				GAH		
					Obj	Time(s)	Gap(%)	Cuts(#)	Obj	Time(s)	PI(%)
c15-1-F1	10	2	100	0.8	279.7	68	0	101	279.7	22	0
	15	3	100	0.8	279.4	7200	29.3	1206	269	39	2
c15-2-F1	10	2	100	0.8	230.5	19	0	53	230.5	24	0
	15	3	100	0.8	220.1	7200	21.9	261	216	40	5
c15-3-F1	10	2	100	0.8	205.8	22	0	77	205.8	21	0
	15	3	100	0.8	190.7	7200	21.5	158	189	41	3
c15-4-F1	10	2	100	0.8	214.7	21	0	67	214	25	2
	15	3	100	0.8	205.7	7200	14.2	320	202	44	8
c15-5-F1	10	2	100	0.8	217.7	11	0	41	219	44	0
	15	3	100	0.8	191.9	7200	0.006	158	194	31	0
c20-1-F1	10	2	100	0.8	217.2	18	0	31	217.2	20	0
	15	3	100	0.8	214.9	7200	6	211	214.9	34	3
c20-2-F1	10	2	100	0.8	241.5	34	0	73	24.5	21	0
	15	3	100	0.8	211.6	7200	16.8	234	206	33	6
c20-3-F1	10	2	100	0.8	245.9	21	0	87	245.9	18	0
	15	3	100	0.8	212.4	7200	22	417	209	41	2
c20-4-F1	10	2	100	0.8	203	16	0	34	205	17	0
	15	3	100	0.8	180.8	7200	9	85	182	32	3
c20-5-F1	10	2	100	0.8	215	5.2	0	47	215	25	0
	15	3	100	0.8	212.9	7200	0.03	721	212.9	38	6
c25-1-F1	10	2	100	0.8	207.3	11	0	38	207.3	19	0
	15	3	100	0.8	197.1	2175	0	68	197.1	19	4
c25-2-F1	10	2	100	0.8	279.8	184	0	236	28	18	2
	15	3	100	0.8	264.8	7200	29.1	1285	258.6	35	0
c25-3-F1	10	2	100	0.8	236.5	39	0	83	236.5	29	0
	15	3	100	0.8	192.4	7200	11.1	129	192.4	35	5
c25-4-F1	10	2	100	0.8	237.9	35	0	144	237.9	26	0
	15	3	100	0.8	226.5	7200	23.9	1579	220	50	0
c25-5-F1	10	2	100	0.8	193.1	5	0	30	193.1	22	0
	15	3	100	0.8	191.3	7200	7	107	191.3	49	7
c30-1-F1	10	2	100	0.8	225.4	15	0	49	225.4	23	0
	15	3	100	0.8	228.5	7200	2	218	230	40	0
c30-2-F1	10	2	100	0.8	185	13	0	73	185	29	0
	15	3	100	0.8	159.3	423	0	92	159.3	47	5
c30-3-F1	10	2	100	0.8	203.9	11	0	60	203.9	31	0
	15	3	100	0.8	194.1	4009	0	152	194.1	47	3
c30-3-F1	10	2	100	0.8	227.3	11	0	61	227.3	27	0
	15	3	100	0.8	219.8	7200	7	166	221	59	0
c30-4-F1	10	2	100	0.8	227.3	11	0	61	227.3	27	0
	15	3	100	0.8	219.8	7200	7	166	221	59	0
c30-5-F1	10	2	100	0.8	230.4	10	0	50	230.4	13	0
	15	3	100	0.8	190.8	2170	0	138	193	41	6

Table 12: Computational results of benchmark instances; set A

Instance	Targets(#)	AEV(#)	F	α	B&C				GAH		
					Obj	Time(s)	Gap(%)	Cuts(#)	Obj	Time(s)	PI(%)
A-32-k5	10	2	100	0.82	275.6	20	0	53	275.6	23	0
	15	3	100	0.82	237.4	7200	12.8	111	237.4	55	4
A-n33-k5	10	2	100	0.89	237.9	26	0	68	239	28	0
	15	3	100	0.89	187	7200	10	66	185	53	3
A-n33-k6	10	2	100	0.90	151.4	24	0	70	151.4	29	2
	15	3	100	0.90	144	7200	11.3	116	144	58	0
A-n34-k5	10	2	100	0.92	230.3	35	0	49	230.3	75	1
	15	3	100	0.92	191.5	7200	12	94	188	73	2
A-n36-k5	10	2	100	0.88	244.4	17	0	67	244.4	37	3
	15	3	100	0.88	235.7	7200	19.3	323	232	74	4
A-n37-k5	10	2	100	0.81	194.6	7	0	27	194.6	29	0
	15	3	100	0.81	184	7200	9.4	226	184	67	0
A-n37-k6	10	2	100	0.95	234	17	0	83	237	33	0
	15	3	100	0.95	234	7200	12.7	360	234	45	0
A-n38-k5	10	2	100	0.96	213.4	5	0	31	213.4	29	4
	15	3	100	0.96	213.4	7200	18	142	213.2	45	8
A-n39-k5	10	2	100	0.95	197.7	22	0	40	199	35	0
	15	3	100	0.95	195.9	7200	25	177	190	54	6
A-n39-k6	10	2	100	0.88	223.1	24	0	102	225	47	0
	15	3	100	0.88	188	4673	0	161	192	62	0
A-n44-k6	10	2	100	0.95	266.9	24	0	114	266.9	51	0
	15	3	100	0.95	230	1400	0	177	234	71	5
A-n45-k6	10	2	100	0.99	243.3	15	0	55	243.3	37	0
	15	3	100	0.99	228.4	7200	1.7	162	228.4	55	7
A-n45-k7	10	2	100	0.91	236.8	9	0	45	236.8	34	2
	15	3	100	0.91	215.8	7200	1.2	211	220	69	2
A-n48-k7	10	2	100	0.89	262.7	16	0	70	262.7	38	0
	15	3	100	0.89	243.1	7200	20	302	239	81	7
A-n53-k7	10	2	100	0.95	189.9	4	0	32	192	35	0
	15	3	100	0.95	207.6	3438	0	129	211	77	3
A-n54-k7	10	2	100	0.96	246.8	14	0	82	246.8	38	2
	15	3	100	0.96	230.5	7200	20	780	228	44	5
A-n55-k9	10	2	100	0.93	203.2	7	0	47	203.2	39	0
	15	3	100	0.93	195.1	7200	2	205	195.1	51	0
A-n60-k9	10	2	100	0.92	255.5	13	0	55	255.5	47	0
	15	3	100	0.92	246.5	5091	0	270	246.5	92	8

Table 13: Computational results of benchmark instances; set B

Instance	Targets(#)	AEV(#)	F	α	B&C				GAH		
					Obj	Time(s)	Gap(%)	Cuts(#)	Obj	Time(s)	PI(%)
B-n31-k5	10	2	100	0.82	188.8	0	2	35	188.8	22	0
	15	3	100	0.82	236.6	7200	10	69	236.6	71	0
B-n34-k5	10	2	100	0.91	195.9	0	16	19	195.9	23	0
	15	3	100	0.91	195.2	7200	19.3	35	188.2	66	0
B-n35-k5	10	2	100	0.87	282.4	11	0	59	282.4	28	2
	15	3	100	0.87	259.7	7200	17.2	183	259.7	88	5
B-n38-k6	10	2	100	0.85	226.2	6	0	67	228	31	0
	15	3	100	0.85	173.3	241	0	144	173.3	80	5
B-n39-k5	10	2	100	0.88	194.3	6	0	45	194.3	55	0
	15	3	100	0.88	176.4	7200	1.3	87	179	72	2
B-n41-k6	10	2	100	0.95	243.3	8	0	36	243.3	37	0
	15	3	100	0.95	217.4	7200	14.1	163	216.8	72	5
B-n43-k6	10	2	100	0.87	184.4	99	0	49	184.4	67	4
	15	3	100	0.87	174.9	7200	11.8	212	175	89	7
B-n44-k7	10	2	100	0.92	210.9	9	0	34	210.9	29	0
	15	3	100	0.92	206.1	7200	16.5	105	203.8	91	3
B-n45-k5	10	2	100	0.97	190.3	4	0	20	190.3	35	1
	15	3	100	0.97	185.4	7200	11.4	135	183.6	82	3
B-n45-k6	10	2	100	0.99	177	13	0	22	177	47	3
	15	3	100	0.99	176.7	7200	11	135	178.5	88	0
B-n50-k7	10	2	100	0.87	199.9	4	0	37	199.9	23	0
	15	3	100	0.87	172.5	7200	11.7	25	168.2	90	0
B-n50-k8	10	2	100	0.92	284.6	34	0	210	288	32	0
	15	3	100	0.92	247.9	7200	19.9	897	242	72	4
B-n51-k7	10	2	100	0.98	248.2	15	0	31	248.2	26	2
	15	3	100	0.98	239.8	7200	34.6	64	225	68	6
B-n52-k7	10	2	100	0.87	209.1	5	0	20	209.1	31	3
	15	3	100	0.87	211.8	7200	10.7	106	210.6	72	5
B-n56-k7	10	2	100	0.88	197.1	5	0	43	197.1	35	0
	15	3	100	0.88	196.3	7200	16.8	79	194	74	6
B-n57-k7	10	2	100	1	298.4	32	0	119	301	33	3
	15	3	100	1	219.1	7200	4	139	222	63	0
B-n57-k9	10	2	100	0.89	269.2	20	0	61	269.2	44	0
	15	3	100	0.89	251.8	7200	29.1	467	248	69	4

Table 14: Computational results of benchmark instances; set P

Instance	Targets(#)	AEV(#)	F	α	B&C				GAH		
					Obj	Time(s)	Gap(%)	Cuts(#)	Obj	Time(s)	PI(%)
P-n19-k2	18	2	160	0.97	112.7	399	0	15	112.7	33	0
	18	3	160	0.97	89.5	4661	0	33	89.5	56	2
P-n20-k2	19	2	160	0.97	112.7	274	0	56	112.7	41	0
	19	3	160	0.97	90.1	7200	4.6	48	90.1	82	0
P-n21-k2	20	2	160	0.93	112.7	793	0	47	112.7	63	0
	20	3	160	0.93	90.1	7200	7.3	64	90.1	91	2
P-n22-k2	21	2	160	0.96	112.7	422	0	22	112.7	72	0
	21	3	160	0.96	90.9	7200	12.6	109	90.9	88	3
B-n22-k8	21	2	3000	0.94	158.7	0	0	50	158.7	91	2
	21	3	3000	0.94	115.9	7200	7.7	16	115	77	7
P-n40-k5	15	2	140	0.88	124.7	8	0	18	124.7	57	0
	15	3	140	0.88	94.6	675	0	41	96.2	66	6
P-n45-k5	15	2	150	0.92	0 124.7	15	0	9	124.7	44	1
	15	3	150	0.92	94.6	670	0	16	94.6	88	3
P-n50-k7	15	2	150	0.91	1 112.4	6	0	6	112.4	40	4
	15	3	150	0.91	86.9	271	0	21	86.9	53	0
P-n50-k8	15	2	120	0.99	112.4	8	0	19	112.4	58	3
	15	3	120	0.99	86.9	204	0	20	86.9	69	4
P-n50-k10	15	2	100	0.95	118.6	30	0	27	118.6	55	2
	15	3	100	0.95	86.9	602	0	79	86.9	80	5
P-n51-k10	15	2	80	0.97	153.3	4971	0	11	153.3	64	7
	15	3	80	0.97	100.7	80	0	17	102	77	6
P-n55-k7	15	2	170	0.88	112.4	7	0	3	112.4	68	0
	15	3	170	0.88	86.9	254	0	27	86.9	76	0
P-n55-k10	15	2	115	0.91	112.4	10	0	12	112.4	71	2
	15	3	115	0.91	86.9	188	0	58	86.9	81	6
P-n55-k15	15	2	70	0.99	129.4	128	0	20	129.4	58	4
	15	3	70	0.99	109.5	7200	17.3	68	107.2	87	4
P-n60-k10	15	2	120	0.95	112.4	6	0	28	112.4	45	0
	15	3	120	0.95	86.9	708	0	30	86.9	79	2
P-n60-k15	15	2	130	0.94	129.4	349	0	7	129.4	66	1
	15	3	130	0.94	92.4	1614	0	21	92.4	93	5

REFERENCES

- [1] Southeast michigan council of governments (SEMCOG). Available: <http://semcog.org/data-and-maps>. Accessed: Aug 2019.
- [2] N. Ahmadian, G. J. Lim, M. Torabbeigi, and S. J. Kim. Collision-free multi-uav flight scheduling for power network damage assessment. In *2019 International Conference on Unmanned Aircraft Systems (ICUAS)*, pages 794–798. IEEE, 2019.
- [3] M. Ajam, V. Akbari, and F. S. Salman. Minimizing latency in post-disaster road clearance operations. *European Journal of Operational Research*, 277(3):1098–1112, 2019.
- [4] M. Amini and F. Yousefian. An iterative regularized mirror descent method for ill-posed nondifferentiable stochastic optimization. *arXiv preprint arXiv:1901.09506*, 2019.
- [5] A. Ansaripour, A. Mata, S. Nourazari, H. Kumin, et al. Some explicit results for the distribution problem of stochastic linear programming. *Open Journal of Optimization*, 5(04):140, 2016.
- [6] A. Ansaripour and T. B. Trafalis. A robust multicriteria optimization model for city logistic terminal locations. In *IIE Annual Conference. Proceedings*, page 2801. Institute of Industrial and Systems Engineers (IISE), 2013.
- [7] O. Arslan and O. E. Karaşan. A benders decomposition approach for the charging station location problem with plug-in hybrid electric vehicles. *Transportation Research Part B: Methodological*, 93:670–695, 2016.
- [8] P. Augerat, J. M. Belenguer, E. Benavent, A. Corberán, D. Naddef, and G. Rinaldi. *Computational results with a branch and cut code for the capacitated vehicle routing*

- problem*, volume 34. IMAG, 1995.
- [9] I. S. Bayram, G. Michailidis, I. Papapanagiotou, and M. Devetsikiotis. Decentralized control of electric vehicles in a network of fast charging stations. In *2013 IEEE Global Communications Conference (GLOBECOM)*, pages 2785–2790. IEEE, 2013.
- [10] S. Benati and P. Hansen. The maximum capture problem with random utilities: Problem formulation and algorithms. *European Journal of Operational Research*, 143(3):518–530, 2002.
- [11] J. R. Birge. The value of the stochastic solution in stochastic linear programs with fixed recourse. *Mathematical programming*, 24(1):314–325, 1982.
- [12] J. R. Birge and F. Louveaux. *Introduction to stochastic programming*. Springer Science & Business Media, 2011.
- [13] R. P. Brooker and N. Qin. Identification of potential locations of electric vehicle supply equipment. *Journal of Power Sources*, 299:76–84, 2015.
- [14] H. Cai, X. Jia, A. S. Chiu, X. Hu, and M. Xu. Siting public electric vehicle charging stations in beijing using big-data informed travel patterns of the taxi fleet. *Transportation Research Part D: Transport and Environment*, 33:39–46, 2014.
- [15] A. M. Campbell, D. Vandenbussche, and W. Hermann. Routing for relief efforts. *Transportation Science*, 42(2):127–145, 2008.
- [16] J. Carlsson, D. Ge, A. Subramaniam, A. Wu, and Y. Ye. Solving min-max multi-depot vehicle routing problem. *Lectures on global optimization*, 55:31–46, 2009.
- [17] J. Cavadas, G. H. de Almeida Correia, and J. Gouveia. A mip model for locating slow-charging stations for electric vehicles in urban areas accounting for driver

- tours. *Transportation Research Part E: Logistics and Transportation Review*, 75:188–201, 2015.
- [18] T. D. Chen and K. M. Kockelman. Management of a shared autonomous electric vehicle fleet: Implications of pricing schemes. *Transportation Research Record*, 2572(1):37–46, 2016.
- [19] S. H. Chung and C. Kwon. Multi-period planning for electric car charging station locations: A case of korean expressways. *European Journal of Operational Research*, 242(2):677–687, 2015.
- [20] S. Cui, H. Zhao, and C. Zhang. Locating charging stations of various sizes with different numbers of chargers for battery electric vehicles. *Energies*, 11(11):3056, 2018.
- [21] N. Daina, A. Sivakumar, and J. W. Polak. Electric vehicle charging choices: Modelling and implications for smart charging services. *Transportation Research Part C: Emerging Technologies*, 81:36–56, 2017.
- [22] L. Davis. Applying adaptive algorithms to epistatic domains. In *IJCAI*, volume 85, pages 162–164, 1985.
- [23] G. Desaulniers, F. Errico, S. Irnich, and M. Schneider. Exact algorithms for electric vehicle-routing problems with time windows. *Operations Research*, 64(6):1388–1405, 2016.
- [24] E. W. Dijkstra et al. A note on two problems in connexion with graphs. *Numerische mathematik*, 1(1):269–271, 1959.
- [25] S. Erdoğ an and E. Miller-Hooks. A green vehicle routing problem. *Transportation Research Part E: Logistics and Transportation Review*, 48(1):100–114, 2012.

- [26] P. Fan, B. Sainbayar, and S. Ren. Operation analysis of fast charging stations with energy demand control of electric vehicles. *IEEE Transactions on Smart Grid*, 6(4):1819–1826, 2015.
- [27] S. Faridimehr, S. Venkatachalam, and R. B. Chinnam. A stochastic programming approach for electric vehicle charging network design. *IEEE Transactions on Intelligent Transportation Systems*, (99):1–13, 2018.
- [28] S. S. Fazeli, S. Venkatachalam, R. B. Chinnam, and A. Murat. Two-stage stochastic choice modeling approach for electric vehicle charging station network design in urban communities. *IEEE Transactions on Intelligent Transportation Systems*, 2020.
- [29] L. P. Fernandez, T. G. San Román, R. Cossent, C. M. Domingo, and P. Frias. Assessment of the impact of plug-in electric vehicles on distribution networks. *IEEE transactions on power systems*, 26(1):206–213, 2010.
- [30] A. Forsyth, M. Hearst, J. Oakes, and K. Schmitz. Design and destinations: Factors influencing walking and total physical activity. *Urban Studies*, 45(9):1973–1996, 8 2008.
- [31] T. Franke and J. F. Krems. Understanding charging behaviour of electric vehicle users. *Transportation Research Part F: Traffic Psychology and Behaviour*, 21:75–89, 2013.
- [32] J. C. E. Garcia and L. Alfandari. Robust location of new housing developments using a choice model. *Annals of Operations Research*, pages 1–24, 2015.
- [33] M. Gen and R. Cheng. *Genetic Algorithms and Manufacturing Systems Design*. John Wiley & Sons, Inc., 1996.
- [34] L. Gurobi Optimization. Gurobi optimizer reference manual, 2020.

- [35] D. Hall, H. Cui, and N. Lutsey. Electric vehicle capitals of the world: What markets are leading the transition to electric? 2017.
- [36] P. Hansen, N. Mladenović, and J. A. M. Pérez. Variable neighbourhood search: methods and applications. *Annals of Operations Research*, 175(1):367–407, 2010.
- [37] S. Hardman, A. Jenn, G. Tal, J. Aksen, G. Beard, N. Daina, E. Figenbaum, N. Jakobsson, P. Jochem, N. Kinnear, et al. A review of consumer preferences of and interactions with electric vehicle charging infrastructure. *Transportation Research Part D: Transport and Environment*, 62:508–523, 2018.
- [38] F. He, D. Wu, Y. Yin, and Y. Guan. Optimal deployment of public charging stations for plug-in hybrid electric vehicles. *Transportation Research Part B: Methodological*, 47:87–101, 2013.
- [39] F. He, Y. Yin, and J. Zhou. Deploying public charging stations for electric vehicles on urban road networks. *Transportation Research Part C: Emerging Technologies*, 60:227–240, 2015.
- [40] K. Helsgaun. An effective implementation of the lin–kernighan traveling salesman heuristic. *European Journal of Operational Research*, 126(1):106–130, 2000.
- [41] D. Hershberger, D. Gossow, and J. Faust. Rviz, 3d visualization tool for ros. URL: <http://wiki.ros.org/rviz> [cited 06-12-2020].
- [42] M. K. Hidrue, G. R. Parsons, W. Kempton, and M. P. Gardner. Willingness to pay for electric vehicles and their attributes. *Resource and Energy Economics*, 33(3):686–705, 2011.
- [43] G. Hiermann, R. F. Hartl, J. Puchinger, and T. Vidal. Routing a mix of conventional, plug-in hybrid, and electric vehicles. *European Journal of Operational Research*,

- 272(1):235–248, 2019.
- [44] G. Hiermann, J. Puchinger, S. Ropke, and R. F. Hartl. The electric fleet size and mix vehicle routing problem with time windows and recharging stations. *European Journal of Operational Research*, 252(3):995–1018, 2016.
- [45] W. Ho, G. T. Ho, P. Ji, and H. C. Lau. A hybrid genetic algorithm for the multi-depot vehicle routing problem. *Engineering Applications of Artificial Intelligence*, 21(4):548–557, 2008.
- [46] M. Hosseini and S. MirHassani. Refueling-station location problem under uncertainty. *Transportation Research Part E: Logistics and Transportation Review*, 84:101–116, 2015.
- [47] A. A. Juan, J. Goentzel, and T. Bektaş. Routing fleets with multiple driving ranges: Is it possible to use greener fleet configurations? *Applied Soft Computing*, 21:84–94, 2014.
- [48] A. A. Juan, C. A. Mendez, J. Faulin, J. De Armas, and S. E. Grasman. Electric vehicles in logistics and transportation: A survey on emerging environmental, strategic, and operational challenges. *Energies*, 9(2):86, 2016.
- [49] A. C. Kapoutsis, S. A. Chatzichristofis, and E. B. Kosmatopoulos. Darp: divide areas algorithm for optimal multi-robot coverage path planning. *Journal of Intelligent & Robotic Systems*, 86(3-4):663–680, 2017.
- [50] S. Khuller, A. Malekian, and J. Mestre. To fill or not to fill: the gas station problem. In *European Symposium on Algorithms*, pages 534–545. Springer, 2007.
- [51] M. Kiani, B. Eksioglu, T. Isik, A. Thomas, and J. Gilpin. Evaluating appointment postponement in scheduling patients at a diagnostic clinic. *arXiv preprint*

- arXiv:1905.11201*, 2019.
- [52] S. J. Kim, N. Ahmadian, G. J. Lim, and M. Torabbeigi. A rescheduling method of drone flights under insufficient remaining battery duration. In *2018 International Conference on Unmanned Aircraft Systems (ICUAS)*, pages 468–472. IEEE, 2018.
- [53] P. R. kit. Turtlebot. URL: <https://www.turtlebot.com/> [cited 06-12-2020].
- [54] F. Kley, C. Lerch, and D. Dallinger. New business models for electric cars—a holistic approach. *Energy policy*, 39(6):3392–3403, 2011.
- [55] A. J. Kleywegt, A. Shapiro, and T. Homem-de Mello. The sample average approximation method for stochastic discrete optimization. *SIAM Journal on Optimization*, 12(2):479–502, 2002.
- [56] Ç. Koç and I. Karaoglan. The green vehicle routing problem: A heuristic based exact solution approach. *Applied Soft Computing*, 39:154–164, 2016.
- [57] R. Krohn, S. Müller, and K. Haase. Preventive health care facility location planning with quality-conscious clients. Technical report, Working paper, 2016.
- [58] J. Krumm. How people use their vehicles: Statistics from the 2009 national household travel survey. Technical report, SAE Technical Paper, 2012.
- [59] A. Y. Lam, Y.-W. Leung, and X. Chu. Electric vehicle charging station placement: Formulation, complexity, and solutions. *IEEE Transactions on Smart Grid*, 5(6):2846–2856, 2014.
- [60] D. Levy, K. Sundar, and S. Rathinam. Heuristics for routing heterogeneous unmanned vehicles with fuel constraints. *Mathematical Problems in Engineering*, 2014, 2014.

- [61] M. Li, Y. Jia, Z. Shen, and F. He. Improving the electrification rate of the vehicle miles traveled in beijing: A data-driven approach. *Transportation Research Part A: Policy and Practice*, 97:106–120, 2017.
- [62] C. Liu and Z. Lin. How uncertain is the future of electric vehicle market: Results from monte carlo simulations using a nested logit model. *International Journal of Sustainable Transportation*, 11(4):237–247, 2017.
- [63] H. Liu and D. Z. Wang. Locating multiple types of charging facilities for battery electric vehicles. *Transportation Research Part B: Methodological*, 103:30–55, 2017.
- [64] B. Lunz, Z. Yan, J. B. Gerschler, and D. U. Sauer. Influence of plug-in hybrid electric vehicle charging strategies on charging and battery degradation costs. *Energy Policy*, 46:511–519, 2012.
- [65] C. Luo, Y.-F. Huang, and V. Gupta. Placement of ev charging stations—balancing benefits among multiple entities. *IEEE Transactions on Smart Grid*, 8(2):759–768, 2015.
- [66] N. Lutsey, S. Searle, S. Chambliss, and A. Bandivadekar. Assessment of leading electric vehicle promotion activities in united states cities. *International Council on Clean Transportation*, 2015.
- [67] H.-Y. Mak, Y. Rong, and Z.-J. M. Shen. Infrastructure planning for electric vehicles with battery swapping. *Management Science*, 59(7):1557–1575, 2013.
- [68] W.-K. Mak, D. P. Morton, and R. K. Wood. Monte carlo bounding techniques for determining solution quality in stochastic programs. *Operations Research Letters*, 24(1):47–56, 1999.

- [69] S. G. Manyam, D. W. Casbeer, and K. Sundar. Path planning for cooperative routing of air-ground vehicles. In *2016 American Control Conference (ACC)*, pages 4630–4635. IEEE, 2016.
- [70] C. Marmaras, E. Xydas, and L. Cipcigan. Simulation of electric vehicle driver behaviour in road transport and electric power networks. *Transportation Research Part C: Emerging Technologies*, 80:239–256, 2017.
- [71] G. P. McCormick. Computability of global solutions to factorable nonconvex programs: Part i—convex underestimating problems. *Mathematical programming*, 10(1):147–175, 1976.
- [72] S. Melkote and M. S. Daskin. Capacitated facility location/network design problems. *European journal of operational research*, 129(3):481–495, 2001.
- [73] S. MirHassani and R. Ebrazi. A flexible reformulation of the refueling station location problem. *Transportation Science*, 47(4):617–628, 2012.
- [74] A. Molavi, J. Shi, Y. Wu, and G. J. Lim. Enabling smart ports through the integration of microgrids: A two-stage stochastic programming approach. *Applied Energy*, 258:114022, 2020.
- [75] M. Najarian and G. J. Lim. Optimizing infrastructure resilience under budgetary constraint. *Reliability Engineering & System Safety*, 198:106801, 2020.
- [76] H. Nazaripouya, B. Wang, and D. Black. Electric vehicles and climate change: Additional contribution and improved economic justification. *IEEE Electrification Magazine*, 7(2):33–39, 2019.
- [77] M. Nicholas, D. Hall, and N. Lutsey. Quantifying the electric vehicle charging infrastructure gap across us markets. 2019.

- [78] J.-S. Oh, V. Kwigizile, and A. Feizi. Sustainable and smart-growth city ranking: Multifaceted transportation performance measures in smart cities. *Communities*, 9:30–2019, 2019.
- [79] J.-S. Oh, V. Kwigizile, R. Van Houten, A. Feizi, M. Mastali, et al. Effects of safe bicycle passing laws on drivers' behavior and bicyclists' safety. Technical report, Western Michigan University, 2018.
- [80] N. C. Onat, M. Kucukvar, and S. Afshar. Eco-efficiency of electric vehicles in the united states: A life cycle assessment based principal component analysis. *Journal of Cleaner Production*, 212:515–526, 2019.
- [81] A. Ozdemir et al. Distributed storage capacity modelling of ev parking lots. In *2015 9th International Conference on Electrical and Electronics Engineering (ELECO)*, pages 359–363. IEEE, 2015.
- [82] F. Pan, R. Bent, A. Berscheid, and D. Izraelevitz. Locating phev exchange stations in v2g. *arXiv preprint arXiv:1006.0473*, 2010.
- [83] M. E. Posner and C.-T. Wu. Linear max-min programming. *Mathematical Programming*, 20(1):166–172, 1981.
- [84] R. Riemann, D. Z. Wang, and F. Busch. Optimal location of wireless charging facilities for electric vehicles: flow-capturing location model with stochastic user equilibrium. *Transportation Research Part C: Emerging Technologies*, 58:1–12, 2015.
- [85] ROS. Robot operating system. URL: <https://www.ros.org/> [cited 06-12-2020].
- [86] ROS. Ros kinetic kame. URL: <http://wiki.ros.org/kinetic> [cited 06-12-2020].
- [87] P. Sadeghi-Barzani, A. Rajabi-Ghahnavieh, and H. Kazemi-Karegar. Optimal fast charging station placing and sizing. *Applied Energy*, 125:289–299, 2014.

- [88] M. Schneider, A. Stenger, and D. Goeke. The electric vehicle-routing problem with time windows and recharging stations. *Transportation Science*, 48(4):500–520, 2014.
- [89] Z. Shahmoradi and T. Ünlüyurt. Failure detection for series systems when tests are unreliable. *Computers & Industrial Engineering*, 118:309–318, 2018.
- [90] N. Shahraki, H. Cai, M. Turkay, and M. Xu. Optimal locations of electric public charging stations using real world vehicle travel patterns. *Transportation Research Part D: Transport and Environment*, 41:165–176, 2015.
- [91] C. J. Sheppard, A. Harris, and A. R. Gopal. Cost-effective siting of electric vehicle charging infrastructure with agent-based modeling. *IEEE Transactions on Transportation Electrification*, 2(2):174–189, 2016.
- [92] P. Slowik and N. Lutsey. The continued transition to electric vehicles in us cities, 2018.
- [93] M. Smith and J. Castellano. Costs associated with non-residential electric vehicle supply equipment: Factors to consider in the implementation of electric vehicle charging stations. Technical report, 2015.
- [94] S. Solaymani. Co2 emissions patterns in 7 top carbon emitter economies: The case of transport sector. *Energy*, 168:989–1001, 2019.
- [95] X.-H. Sun, T. Yamamoto, and T. Morikawa. Charge timing choice behavior of battery electric vehicle users. *Transportation Research Part D: Transport and Environment*, 37:97–107, 2015.
- [96] K. Sundar and S. Rathinam. Algorithms for routing an unmanned aerial vehicle in the presence of refueling depots. *IEEE Transactions on Automation Science and*

- Engineering*, 11(1):287–294, 2013.
- [97] K. Sundar, S. Venkatachalam, and S. G. Manyam. Path planning for multiple heterogeneous unmanned vehicles with uncertain service times. In *2017 International Conference on Unmanned Aircraft Systems (ICUAS)*, pages 480–487. IEEE, 2017.
- [98] K. Sundar, S. Venkatachalam, and S. Rathinam. An exact algorithm for a fuel-constrained autonomous vehicle path planning problem. *arXiv preprint arXiv:1604.08464*, 2016.
- [99] A. Tafreshian and N. Masoud. Trip-based graph partitioning in dynamic ridesharing. *Transportation Research Part C: Emerging Technologies*, 114:532–553, 2020.
- [100] A. Tafreshian, N. Masoud, and Y. Yin. Ride-matching for peer-to-peer ridesharing: A review and future directions.
- [101] H. Tahami, A. Mirzazadeh, A. Arshadi-khamseh, and A. Gholami-Qadikolaei. A periodic review integrated inventory model for buyer’s unidentified protection interval demand distribution. *Cogent Engineering*, 3(1):1206689, 2016.
- [102] H. Tahami, A. Mirzazadeh, and A. Gholami-Qadikolaei. Simultaneous control on lead time elements and ordering cost for an inflationary inventory-production model with mixture of normal distributions ltd under finite capacity. *RAIRO-Operations Research*, 53(4):1357–1384, 2019.
- [103] M. Tavana, K. Khalili-Damghani, D. Di Caprio, and Z. Oveisi. An evolutionary computation approach to solving repairable multi-state multi-objective redundancy allocation problems. *Neural Computing and Applications*, 30(1):127–139, 2018.
- [104] M. Torabbeigi, G. J. Lim, and S. J. Kim. Drone delivery scheduling optimization considering payload-induced battery consumption rates. *Journal of Intelligent &*

- Robotic Systems*, pages 1–17, 2019.
- [105] M. Torabbeigi, G. J. Lim, and S. J. Kim. Drone delivery scheduling optimization considering payload-induced battery consumption rates. *Journal of Intelligent & Robotic Systems*, 97(3):471–487, 2020.
- [106] K. E. Train. *Discrete choice methods with simulation*. Cambridge university press, 2009.
- [107] T. Trigg, P. Telleen, R. Boyd, F. Cuenot, D. D’Ambrosio, R. Gaghen, J. Gagné, A. Hardcastle, D. Houssin, A. Jones, et al. Global ev outlook: understanding the electric vehicle landscape to 2020. *Int. Energy Agency*, pages 1–40, 2013.
- [108] W. Tushar, C. Yuen, S. Huang, D. B. Smith, and H. V. Poor. Cost minimization of charging stations with photovoltaics: An approach with ev classification. *IEEE Transactions on Intelligent Transportation Systems*, 17(1):156–169, 2015.
- [109] C. Upchurch, M. Kuby, and S. Lim. A model for location of capacitated alternative-fuel stations. *Geographical Analysis*, 41(1):85–106, 2009.
- [110] S. Venkatachalam, M. Bansal, J. M. Smereka, and J. Lee. Two-stage stochastic programming approach for path planning problems under travel time and availability uncertainties. *arXiv preprint arXiv:1910.04251*, 2019.
- [111] S. Vergis and B. Chen. Comparison of plug-in electric vehicle adoption in the united states: A state by state approach. *Research in Transportation Economics*, 52:56–64, 2015.
- [112] F. Y. Vincent, A. P. Redi, Y. A. Hidayat, and O. J. Wibowo. A simulated annealing heuristic for the hybrid vehicle routing problem. *Applied Soft Computing*, 53:119–132, 2017.

- [113] G. Wang, Z. Xu, F. Wen, and K. P. Wong. Traffic-constrained multiobjective planning of electric-vehicle charging stations. *IEEE Transactions on Power Delivery*, 28(4):2363–2372, 2013.
- [114] X. Wang, C. Yuen, N. U. Hassan, N. An, and W. Wu. Electric vehicle charging station placement for urban public bus systems. *IEEE Transactions on Intelligent Transportation Systems*, 18(1):128–139, 2016.
- [115] Y.-W. Wang and C.-C. Lin. Locating multiple types of recharging stations for battery-powered electric vehicle transport. *Transportation Research Part E: Logistics and Transportation Review*, 58:76–87, 2013.
- [116] Y. Wen, D. MacKenzie, and D. R. Keith. Modeling the charging choices of battery electric vehicle drivers by using stated preference data. *Transportation Research Record: Journal of the Transportation Research Board*, (2572):47–55, 2016.
- [117] R. Wolbertus, M. Kroesen, R. van den Hoed, and C. G. Chorus. Policy effects on charging behaviour of electric vehicle owners and on purchase intentions of prospective owners: Natural and stated choice experiments. *Transportation Research Part D: Transport and Environment*, 62:283–297, 2018.
- [118] L. Wright and L. Fulton. Climate change mitigation and transport in developing nations. *Transport Reviews*, 25(6):691–717, 2005.
- [119] J. Wu, H. Liao, J.-W. Wang, and T. Chen. The role of environmental concern in the public acceptance of autonomous electric vehicles: A survey from china. *Transportation Research Part F: Traffic Psychology and Behaviour*, 60:37–46, 2019.
- [120] Y. Wu, J. Shi, G. Lim, L. Fan, and A. Molavi. Optimal management of transactive distribution electricity markets with co-optimized bidirectional energy and ancillary

- service exchanges. *IEEE Transactions on Smart Grid*, 2020.
- [121] X. Xi, R. Sioshansi, and V. Marano. Simulation–optimization model for location of a public electric vehicle charging infrastructure. *Transportation Research Part D: Transport and Environment*, 22:60–69, 2013.
- [122] Y. Xiong, J. Gan, B. An, C. Miao, and A. L. Bazzan. Optimal electric vehicle fast charging station placement based on game theoretical framework. *IEEE Transactions on Intelligent Transportation Systems*, 19(8):2493–2504, 2017.
- [123] H. Xu, S. Miao, C. Zhang, and D. Shi. Optimal placement of charging infrastructures for large-scale integration of pure electric vehicles into grid. *International Journal of Electrical Power & Energy Systems*, 53:159–165, 2013.
- [124] M. Xu, Q. Meng, K. Liu, and T. Yamamoto. Joint charging mode and location choice model for battery electric vehicle users. *Transportation Research Part B: Methodological*, 103:68–86, 2017.
- [125] Y. Yang and A. V. Diez-Roux. Walking distance by trip purpose and population subgroups. *American journal of preventive medicine*, 43(1):11–19, 2012.
- [126] W. Yao, J. Zhao, F. Wen, Z. Dong, Y. Xue, Y. Xu, and K. Meng. A multi-objective collaborative planning strategy for integrated power distribution and electric vehicle charging systems. *IEEE Transactions on Power Systems*, 29(4):1811–1821, 2014.
- [127] Z. Yi, J. Smart, and M. Shirk. Energy impact evaluation for eco-routing and charging of autonomous electric vehicle fleet: Ambient temperature consideration. *Transportation Research Part C: Emerging Technologies*, 89:344–363, 2018.
- [128] P. You, S. H. Low, W. Tushar, G. Geng, C. Yuen, Z. Yang, and Y. Sun. Scheduling of ev battery swapping—part i: Centralized solution. *IEEE Transactions on Control of*

- Network Systems*, 5(4):1887–1897, 2017.
- [129] P.-S. You and Y.-C. Hsieh. A hybrid heuristic approach to the problem of the location of vehicle charging stations. *Computers & Industrial Engineering*, 70:195–204, 2014.
- [130] R. Yu, W. Zhong, S. Xie, C. Yuen, S. Gjessing, and Y. Zhang. Balancing power demand through ev mobility in vehicle-to-grid mobile energy networks. *IEEE Transactions on Industrial Informatics*, 12(1):79–90, 2015.
- [131] S. J. Zaloga. *Unmanned aerial vehicles: robotic air warfare 1917–2007*. Bloomsbury Publishing, 2011.
- [132] H. Zhang, Z. Hu, Z. Xu, and Y. Song. An integrated planning framework for different types of pev charging facilities in urban area. *IEEE Transactions on Smart Grid*, 7(5):2273–2284, 2015.
- [133] H. Zhang, C. J. Sheppard, T. E. Lipman, and S. J. Moura. Joint fleet sizing and charging system planning for autonomous electric vehicles. *IEEE Transactions on Intelligent Transportation Systems*, 2019.
- [134] S. Zhang, Y. Gajpal, and S. Appadoo. A meta-heuristic for capacitated green vehicle routing problem. *Annals of Operations Research*, 269(1-2):753–771, 2018.
- [135] M. Zhong, J. Hunt, and X. Lu. Studying differences of household weekday and weekend activities: a duration perspective. *Transportation Research Record: Journal of the Transportation Research Board*, (2054):28–36, 2008.
- [136] Z. Zhu, Z. Gao, J. Zheng, and H. Du. Charging station planning for plug-in electric vehicles. *Journal of Systems Science and Systems Engineering*, 27(1):24–45, 2018.
- [137] S. Zoepf, D. MacKenzie, D. Keith, and W. Chernicoff. Charging choices and fuel displacement in a large-scale demonstration of plug-in hybrid electric vehicles. *Trans-*

portation Research Record: Journal of the Transportation Research Board, (2385):1–10, 2013.

ABSTRACT**STOCHASTIC PROGRAMMING MODELS FOR ELECTRIC VEHICLES' OPERATION:
NETWORK DESIGN AND ROUTING STRATEGIES**

by

SEYED SAJJAD FAZELI**August 2020****Advisor:** Dr. Saravanan Venkatachalam**Major:** Industrial Engineering**Degree:** Doctor of Philosophy

Logistic and transportation (L&T) activities become a significant contributor to social and economic advances throughout the modern world. Road L&T activities are responsible for a large percentage of CO₂ emissions, with more than 24% of the total emission, which is mostly caused by fossil fuel vehicles. Researchers, governments, and automotive companies put extensive effort to incorporate new solutions and innovations into the L&T system. As a result, Electric Vehicles (EVs) are introduced and universally accepted as one of the solutions to environmental issues. Subsequently, L&T companies are encouraged to adopt fleets of EVs. Integrating the EVs into the logistic and transportation systems introduces new challenges from strategic, planning, and operational perspectives. At the strategic level, one of the main challenges to be addressed to expand the EV charging infrastructures is the location of charging stations. Due to the longer charging time in EVs compared to the conventional vehicles, the parking locations can be considered as the candidate locations for installing charging stations. Another essential factor that should be considered in designing the Electric Vehicle Charging Station (EVCS) network is the size

or capacity of charging stations. EV drivers' arrival times in a community vary depending on various factors such as the purpose of the trip, time of the day, and day of the week. So, the capacity of stations and the number of chargers significantly affect the accessibility and utilization of charging stations. Also, the EVCSs can be equipped by distinct types of chargers, which are different in terms of installation cost, charging time, and charging price. City planners and EVCS owners can make low-risk and high-utilization investment decisions by considering EV users charging pattern and their willingness to pay for different charger types. At the operational level, managing a fleet of electric vehicles can offer several incentives to the L&T companies. EVs can be equipped with autonomous driving technologies to facilitate online decision making, on-board computation, and connectivity. Energy-efficient routing decisions for a fleet of autonomous electric vehicles (AEV) can significantly improve the asset utilization and vehicles' battery life. However, employing AEVs also comes with new challenges. Two of the main operational challenges for AEVs in transport applications is their limited range and the availability of charging stations. Effective routing strategies for an AEV fleet require solving the vehicle routing problem (VRP) while considering additional constraints related to the limited range and number of charging stations. In this dissertation, we develop models and algorithms to address the challenges in integrating the EVs into the logistic and transportation systems.

AUTOBIOGRAPHICAL STATEMENT

Sajjad received the B.S. degree from Iran University Science and Technology in 2011. He got ranked 17 in the Iran national Master entrance exam in the field of industrial and system engineering. He received M.S. degree from Sharif University of Technology, Tehran, Iran, in 2015, all in industrial engineering. He started his Ph.D. at Wayne state university in January 2016. He has been a graduate teaching assistant for four years and five different courses. His current research interests include stochastic programming, large scale optimization, and intelligent transportation systems.